Determining the Role of Scavenger Receptor Class B Type I as a Source of Cholesterol for *de novo* Androgen Synthesis in Castration-resistant Prostate Cancer

by

Ankur Midha

B.Sc. (Pharm), The University of British Columbia, 2010

A THESIS SUBMITTED IN PARTIAL FULFILLMENT OF

THE REQUIREMENTS FOR THE DEGREE OF

MASTER OF SCIENCE

in

THE FACULTY OF GRADUATE AND POSTDOCTORAL STUDIES

(Pharmaceutical Sciences)

THE UNIVERSITY OF BRITISH COLUMBIA

(Vancouver)

August 2015

Abstract

Existing therapies for castration-resistant prostate cancer (CRPC) extend life and provide clinical benefit; however, patients develop therapeutic resistance. Persistent androgen signaling in CRPC is maintained in part by intratumoral steroidogenesis from the precursor cholesterol. The high density lipoprotein-cholesterol (HDL) receptor, scavenger receptor class B type I (SR-BI), is upregulated in CRPC models *in vitro* and *in vivo*. This thesis tests the hypothesis that depriving CRPC cells of HDL as a cholesterol source by silencing SR-BI will diminish *de novo* steroidogenesis and resultant androgen receptor-mediated signaling necessary for CRPC viability.

The effects of SR-BI silencing were studied using CRPC C4-2 cells transfected with either Stealth RNAi duplexes targeting SR-BI (SRBI-KD) or Lo GC Negative Control (NC) duplexes. Cells cultured in androgen-depleted conditions for varying times post-transfection were assessed for SR-BI expression, prostate specific antigen (PSA) expression by chemiluminescence, cholesterol levels by fluorometry, and steroid levels by liquid-chromatography-mass spectrometry. HDL-uptake was measured by flow cytometry of the fluorescent cholesterol mimetic 1,1′-dioctadecyl-3,3,3′,3′-tetramethylindocarbocyanine perchlorate (DiI-HDL). Cell cycle state was assessed by flow cytometry of propidium iodide DNA staining, while cell cycle markers were assessed by immunoblotting. Adaptive stress responses were assessed by immunoblotting for autophagy markers, as well by flow cytometry for senescence associated beta-galactosidase (SA-β-gal) using a fluorogenic substrate, 5-dodecanoylaminofluorescein di-β-D-galactopyranoside.

SRBI-KD treatment reduced SR-BI levels by ~57% by 2 days and ~86% by 4 days post-transfection. This correlated with reduced DiI-HDL-uptake by 22%, reduced cellular testosterone

levels two-fold, and reduced PSA secretion by 39% compared to NC cells. These changes were accompanied by reduced proliferation, G_1S cell cycle arrest, and a small, but measurable increase in cell death at 4 to 6 days post-transfection. Cell stress was evidenced by enhanced autophagy activity and induced stress marker expression while senescence was evidenced by increased SA-β-gal activity.

These studies indicate that SR-BI silencing reduced DiI-HDL uptake which reduced cellular androgen content and androgen signaling, resulting in induction of an adaptive stress response characterized by cell cycle arrest, autophagy, senescence, and eventually death of these CRPC cells. The data presented herein provide support for SR-BI as a cholesterol source for androgen synthesis in CRPC cells.

Preface

At the time of writing, none of the work presented in this thesis has been published. The research presented herein is a collaborative effort of researchers at the Vancouver Prostate Centre and Faculty of Pharmaceutical Sciences at the University of British Columbia in Vancouver, Canada as well as the College of Pharmacy and Nutrition at the University of Saskatchewan in Saskatoon, Canada. My advisors and principle investigators Dr. Michael Cox and Dr. Kishor Wasan identified and designed the research program. I completed all aspects of experimentation including designing experiments, performing all the work described in this thesis, and data analysis, with the exceptions noted below. I performed most of the western blotting analysis presented herein; however, some were performed by Miss Jacquiline Tan and Miss Shaghayegh Nouruzi, both trained and supervised by Dr. Mitali Pandey. Densitometry analysis for these particular blots was performed by Dr. Mitali Pandey. Additionally, one set of western blotting was performed by Dr. Yubin Guo. In all these cases, I performed the cell culture work, collected and prepared samples for analysis which were subsequently analyzed by those mentioned. Fluorescence microscopy was performed by Mr. Jonathan Frew; I performed the cell culture work and fixed the cells for analysis. Mr. Frew performed all aspects of cell staining and imaging, along with analysis of nuclear size. He then provided me with images and nuclear size data. LC-MS analysis was performed by Mr. Hans Adomat in the laboratory of Dr. Emma Guns. I performed the cell culture work and sample preparation for analysis. Mr. Adomat performed all aspects of LC-MS including running the samples and data analysis. He then provided me with LC-MS data. Statistical consultation was provided by Dr. Robert Bell of the Vancouver Prostate Centre. All work in this thesis was conducted according to the guidelines of the University Biosafety Committee covered by certificate number B14-0111.

Table of Contents

Abstract ii

Preface iv

Table of Contents v

List of Tables ix

List of Figures x

List of Abbreviations xi

Acknowledgements xiii

Chapter 1: Literature review, hypothesis, and specific aims 1

1.1 Prostate cancer 1

1.1.1 Epidemiology 1

1.2 Development and function of the prostate 2

1.3 Prostate cancer 3

1.3.1 Development 3

1.3.1.1 Androgens 5

1.3.1.1.1 Androgen synthesis 5

1.3.1.1.2 Androgen receptor 6

1.3.2 Diagnosis 8

1.3.3 Classifications of prostate cancer 9

1.3.3.1 Tumor-node-metastasis classification and staging 9

1.3.3.2 Gleason Grading 9

1.3.4 Prognosis 9

1.3.5 Treatment, adaptations, and progression to CRPC 11

1.3.5.1 Localized therapies 11
1.3.5.2 Systemic therapies 11
1.3.5.2.1 AR axis-targeted therapy 11
1.3.5.2.2 Cytotoxic chemotherapy 13
1.3.5.2.3 Bone-targeted therapies 14
1.3.5.2.4 Immune therapies 15
1.4 Cellular responses to therapy and progression to CRPC 16
1.4.1 Cell death 17
1.4.1.1 Apoptosis 17
1.4.1.2 Necrosis 19
1.4.2 Adaptive stress responses 20
1.4.2.1 Autophagy 20
1.4.2.2 Senescence 22
1.4.3 Progression to CRPC 23
1.4.3.1 AR hypersensitivity 23
1.4.3.2 AR ligand independence 24
1.4.3.3 *De novo* steroidogenesis 25
1.4.4 Cholesterol in PCa 26
1.4.4.1 Cellular cholesterol homeostasis 26
1.4.4.2 Sources of cellular cholesterol 27
1.4.4.2.1 LDLR 28
1.4.4.2.2 SR-BI 29
1.4.4.3 SR-BI in CRPC 31

1.5 Experimental models 32
1.5.1 LNCaP cell line 32
1.5.2 LNCaP xenograft mouse 32
1.5.3 C4-2 cell line 33
1.6 Scope of thesis 33
1.6.1 Hypothesis 33
1.6.2 Rationale and specific aims 33
Chapter 2: Materials and methods 35
2.1 Materials and reagents 35
2.2 Cell culture 35
2.3 RNA-interference transfection protocol 35
2.4 Whole cell lysate preparation 36
2.5 Western blotting 37
HDL-cholesterol uptake assay 38
2.6 Cholesterol quantification 39
2.7 Steroid analysis by liquid chromatography-mass spectrometry 40
2.8 PSA quantification 41
2.9 Cell viability assay 41
2.10 Flow cytometry based cell cycle analysis 41
2.11 Bright field and fluorescence microscopy 42
2.12 Detection of senescence-associated beta-galactosidase activity 43
2.13 Statistical Analyses 44
Chapter 3: Results 45

3.1 Knockdown of SR-BI protein expression by C4-2 cells is suppressed by siRNA treatment 45
3.2 HDL-lipid uptake by C4-2 CRPC cells is impaired by knockdown and small molecule inhibition of SR-BI 48
3.3 Androgen signaling in C4-2 cells is suppressed by knockdown of SR-BI 50
3.4 Knockdown of SR-BI reduces viability of C4-2 cells by inducing cell cycle arrest 54
3.5 Knockdown of SR-BI induces adaptive stress responses in C4-2 cells 61
3.6 Silencing SR-BI expression is associated with the emergence of senescent features .. 63
Chapter 4: Discussion 68
4.1 Limitations and future directions 85
4.2 Summary of findings..... 87
References 89

List of Tables

Table 2.1: Antibody specifications for primary antibodies used in western blotting 38

List of Figures

Figure 1.1: Steroidogenesis pathway. 7

Figure 3.1: SR-BI protein expression is suppressed by siRNA treatment. 46

Figure 3.2: SR-BI protein expression is suppressed by siRNA treatment. 47

Figure 3.3: HDL-lipid uptake is impaired by knockdown and small molecule inhibition of SR-BI. 49

Figure 3.4: Total cellular cholesterol concentrations remain unchanged despite knockdown of SR-BI. 50

Figure 3.5: Androgen levels are suppressed by knockdown of SR-BI. 52

Figure 3.6: Secreted PSA is reduced by knockdown of SR-BI. 53

Figure 3.7: Knockdown of SR-BI reduces viability of C4-2 cells. 54

Figure 3.8: Knockdown of SR-BI induces cell cycle arrest. 57

Figure 3.9: Knockdown of SR-BI induced growth arrest is correlated with activation of p53 and pRB tumor suppressor pathways. 60

Figure 3.10: Knockdown of SR-BI induces autophagy activity and stimulates CLU expression. 62

Figure 3.11: Knockdown of SR-BI is associated with a senescence-like morphological transformation. 65

Figure 3.12: Activity of SA-βgal is enhanced by knockdown of SR-BI. 67

List of Abbreviations

ABC	ATP-binding cassette
ACTH	Adrenocorticotropin hormone
ADT	Androgen deprivation therapy
Akt	RAC-alpha serine/threonine-protein kinase
APC	Antigen presenting cell
Apo	Apolipoprotein
AR	Androgen receptor
AR-V	Androgen receptor splice variants
Atg	Autophagy-related protein
BCA	Bicinchoninic acid
BLT	Blocker of lipid transport
BSA	Bovine serum albumin
C_{12}FDG	5-dodecanoylaminofluorescein di-β-D-galactopyranoside
CDK	Cyclin-dependent kinase
CE	Cholesteryl ester
CLU	Clusterin
CQ	Chloroquine
CRPC	Castration-resistant prostate cancer
CSS	Charcoal stripped fetal bovine serum
CYP	Cytochrome P450
DDR	DNA damage response
DiI	1,1′-dioctadecyl-3,3,3′,3′-tetramethylindocarbocyanine perchlorate
DMSO	Dimethyl sulfoxide
DOX	Doxorubicin
DRE	Digital rectal exam
DHT	Dihydrotestosterone
EPC	Endothelial progenitor cell
ER	Endoplasmic reticulum
ERG	E26 transformation-specific related gene
ETS	E26 transformation-specific
FACS	Fluorescence activated cell sorting
FBS	Fetal bovine serum
FITC	Fluorescein isothiocyanate
FSC	Forward scatter
GM-CSF	Granulocyte-macrophage colony-stimulating factor
HDL	High density lipoprotein
HMGCR	3-methyl-3-glutaryl CoA reductase
HSL	Hormone sensitive lipase
LC3	Microtubule-associated protein light chain 3
LC-MS	Liquid chromatography-mass spectrometry
LDB	Ligand binding domain
LDH	Lactate dehydrogenase
LDL	Low density lipoprotein

LH	Luteinizing hormone
LXR	Liver X receptor
LHRH	Luteinizing hormone-releasing hormone
MAPK	Mitogen-activated protein kinase
MDM2	Mouse double minute 2 homolog
MOMP	Mitochondrial outer membrane permeability
mTOR	Mammalian target of rapamycin
MTS	3-(4,5-dimethylthiazol-2-yl)-5-(3-carboxymethoxyphenyl)-2- (4-sulfophenyl)-2H-tetrazolium
MYC	Myelocytomatosis
NC	Negative control siRNA transfected cells
NF-κB	Nuclear factor-κB
NKX3.1	Homeobox protein 3 type 1
NT	Untreated
PAP	Prostatic acid phosphatase
PARP	Poly (ADP) ribose polymerase
PCa	Prostate cancer
PE	Phycoerythrin
PI	Propidium iodide
PI3K	Phosphatidylinositol 3-kinase
PPAR	Peroxisome proliferator-activator receptor
pRB	Retinoblastoma protein
PSA	Prostate-specific antigen
PTEN	Phosphatase and tensin homolog
RANK	Receptor activator of Nuclear factor-κB
RANKL	Receptor activator of Nuclear factor-κB ligand
RIPA	Radioimmunoprecipitation assay
SA-βgal	Senescence-associated beta-galactosidase
SASP	Senescence-associated secretory phenotype
shRNA	Short-hairpin RNA
SCAP	Sterol regulatory element binding protein cleavage activating protein
SR-BI	Scavenger receptor class B type I
SRBI-KD	SR-BI siRNa transfected cells
SREBP	Sterol regulatory element binding protein
SRD5A	Steroid-5α reductases
StAR	Steroidogenic acute regulatory protein
TMPRRS2	Transmembrane protease, serine 2
TNF	Tumor necrosis factor
TNM	Tumor-node-metastasis
TRAMP	Transgenic adenocarcinoma of the mouse prostate
UGE	urogenital sinus epithelium
UGM	urogenital sinus mesenchyme
UGS	urogenital sinus
VLDL	Very low density lipoprotein
WGA	Wheat germ agglutinin

Acknowledgements

I would like to express my sincere appreciation to all of the individuals who have supported me throughout my academic training. First, I would like to thank my supervisors Dr. Michael Cox and Dr. Kishor Wasan. Dr. Cox, your wealth of knowledge and rigorous standards inspired me to push myself to continually improve. Dr. Wasan, your enthusiasm and love for academic science gave me my start in this field and informed my professional path. Together, you have instilled in me the skills and passion to pursue research and for this I am immensely grateful. I would like to thank my advisory committee: Dr. Stelvio Bandiera, Dr. Jiri Frohlich, and Dr. Judy Wong. You have kept me focused and guided my way through this degree. You have also challenged me to be my best and make the most of this opportunity. I am indebted to you for all of your help. I would also like to thank Dr. Stephen Lee and Dr. Carlos Leon, my undergraduate supervisors. Dr. Lee, your extensive knowledge and attention to detail have driven me to learn as much as I possibly can. You also encouraged me to develop conscientious work habits. Dr. Leon, you taught me all the fundamental laboratory skills that I have relied on throughout this degree and you did so with the utmost patience, without which I surely would not have repeatedly returned to the lab. Additionally I would like to thank everyone I had the good fortune to work with in the Cox and Wasan labs over the years, for their guidance and comradery. Finally I would like to thank all of my fellow trainees as well as the faculty and staff at the Faculty of Pharmaceutical Sciences and the Vancouver Prostate Centre. You have provided company, support, and encouragement through all the highs and lows that grad school has to offer. Without all of you, this would not have been such a positive and fruitful learning experience.

Chapter 1: Literature review, hypothesis, and specific aims

1.1 Prostate cancer

With the exception of cutaneous cancers, prostate cancer (PCa) is the most frequently diagnosed cancer and third leading cause of cancer-deaths in North American men (1). In Canada, 1 in 8 males are anticipated to be diagnosed with PCa in their lifetimes, with approximately 24,000 new cases expected in 2015, accounting for roughly 24% of new cancers diagnosed in males. In the same time, 1 in 27 males will die of PCa accounting for approximately 4,100 deaths, or 10% of male cancer deaths (2). The median age at diagnosis is 68 years (3); with the aging baby boomer population, the incidence of PCa and consequentially its logistic and economic strain on the health care system are expected to increase substantially in the foreseeable future (1,4).

1.1.1 Epidemiology

Though our understanding of the causes of PCa is fairly poor, various risk factors have been identified, including: age, ethnicity, family history, genetic predisposition, and dietary factors (5–7). PCa is most commonly diagnosed in men above the age of 50 years and estimates based upon autopsy findings indicate more than 75% of men older than 85 years have histologic PCa. The highest rates are amongst African-Americans living in the United States whereas the lowest rates are found predominantly in Asia, though with increasing longevity, and cultural and life-style changes, PCa is emerging as a serious problem in Asian and other developing countries.

A positive correlation for familial clustering and risk of PCa exists, indicating that heritable factors contribute to disease incidence (8,9). Having one first-degree relative with PCa doubles the risk of developing disease while having two or more first-degree relatives increases

the risk as much as 11-fold, making hereditary susceptibility a strong risk factor. Genomic studies of germline variants and DNA germline mutations have identified several potential susceptibility genes, reviewed elsewhere (10–13).

Dietary correlations in PCa include animal, soy, and tomato products as well as fat consumption. Epidemiological evidence is suggestive of a correlation between red-meat consumption and development of PCa. Meats cooked at high temperatures including charred meats have been identified as potential sources of carcinogens. However, conflicting evidence exists and further study is needed (14,15). Positive associations have been found between fat consumption, and in particular saturated fat consumption, and PCa (16,17). Men who consumed higher levels of fat in Japan, where fat intake is relatively lower than Western countries, had an increased risk of developing aggressive disease (14). Reducing dietary fat has also been shown to reduce tumor growth in animal models of PCa (18). In contrast, soy and tomato products are thought to reduce the risk for developing PCa (5,6). Although dietary factors are associated with PCa risk, there is no evidence for dietary interventions in the prevention or eradication of disease.

1.2 Development and function of the prostate

The prostate is an exocrine gland in the male reproductive system located inferior to the urinary bladder, surrounding the proximal urethra (19,20). The developed prostate is divided into three regions of different embryologic origin: the central zone, the transition zone, and the peripheral zone; the peripheral zone is the most frequent site of PCa occurrence. Structurally, the prostate consists of an epithelial ductal system supported by smooth muscle stroma. Constant, reciprocal interaction between these tissues guides the development, maintenance, and function of the prostate.

The prostate is of endodermal origin and develops from the urogenital sinus (UGS), consisting of UGS mesenchyme (UGM) and UGS epithelium (UGE) (21,22). Commencing *in utero* and throughout development, testicular androgens stimulate the androgen receptor (AR) in UGM tissue, guiding UGE growth, branching, and differentiation into mature glandular secretory epithelium. The AR is a nuclear hormone receptor which activates a myriad of genes including proteins and various microRNAs (23,24). Developing UGE in turn promotes UGM differentiation into stromal fibroblasts and smooth muscle tissue. In addition to androgens, growth factor and developmental signaling by factors such as fibroblast growth factor and sonic hedgehog are also essential to normal prostatic development.

The adult prostate is a compact gland; the shape, size, and mass are approximately similar to a walnut (22). The chief function of this gland is to contribute alkaline secretions to seminal fluid whose components promote successful fertilization following ejaculation from the male reproductive tract (25,26). Semen consists of spermatozoa originating from the testis, seminal fluid from the seminal vesicles, as well as various proteins secreted from the prostate in the form of membrane-bound secretory vesicles called prostasomes. Secretory products of the prostate have an array of functions, including: enhancing sperm motility and promoting fertilization by liquefying semen, neutralizing the acidic environment of the vaginal tract, providing sperm with calcium ions, and modulating immunity in the female reproductive system.

1.3 Prostate cancer

1.3.1 Development

Cancers arise from malignant transformation via acquisition of mutations allowing cells to grow uncontrollably; despite the contributions of non-genetic factors, cancer is a genetic disease and tumorigenesis is largely attributed to gene mutations (27). Tumor initiation is

thought to be a multi-step process, characterized by numerous genetic alterations which progressively imbibe cells with the ability to overcome the many inherent barriers to cancer development. Conceptually, tumorigenesis can be understood as the acquisition of biological capabilities as summarized by Hanahan and Weinberg: sustained proliferative signaling, evasion of growth suppressors, resisting cell death, enabling replicative immortality, inducing angiogenesis, tissue invasion and metastasis, avoiding immune destruction, promoting inflammation, and deregulating cellular energetics (28,29).

In PCa, normal epithelial cells become cancerous through deregulated oncogenes and tumor suppressors (30–33). Dominant oncogenes include E26 transformation-specific (ETS) family members ETS-related gene (ERG) and ETS variant 1, the oncogenic transcription factor myelocomatosis (MYC), as well as the AR which is continuously activated. Over expression of ETS transcription factors is caused by translocation events resulting in the fusions between their 3'-ends with the 5'end of the androgen regulated gene encoding transmembrane protease, serine 2 (TMPRSS2), which is on its own overexpressed in PCa cells, as is the resultant fusion product. Meanwhile, the tumor suppressor phosphatase and tensin homolog (PTEN), an antagonist of pro-proliferative phosphatidylinositol 3-kinase (PI3K) signaling through RAC-alpha serine/threonine-protein kinase (Akt), is commonly hypermethylated, mutated, and deleted in PCa. Additionally affected tumor suppressors include the homeobox protein NKX-3.1, the cell cycle regulator retinoblastoma protein (pRB), the cell cycle inhibitor p27, the cell cycle checkpoint protein p53, among others. The result of these various mutations is promotion of proliferation, cell cycle progression, and evasion of cell death.

Though the clinical presentation of the aforementioned genomic abnormalities vary greatly between patients (34), the vast majority of PCa cases depend heavily on sustained

androgen signaling mediated by the AR. Despite the clinical availability of numerous tools to inhibit AR signaling, PCa cells develop mechanisms to avert therapeutic interventions (34,35). Awarded the Nobel Prize for Physiology or Medicine in 1966, Charles Huggins first described the role of androgens in prostate function by treating dogs with castration or estrogen administration leading to prostate atrophy, reversible by re-administering androgens. With his colleague, Clarence Hodges, he later demonstrated the benefits of androgen deprivation in metastatic PCa patients (36,37). These pioneering studies showed marked PCa tumor regression by inhibition of androgen synthesis and demonstrated prostate cell reliance on androgens, forming the basis of PCa biology that continues to this day.

1.3.1.1 Androgens

Steroid hormones are essential components of the endocrine system with involvement in a multitude of physiologic functions including: inflammation & immunity, salt & water balance, sexual development & function, and metabolic homeostasis (38,39). The male sex hormones – androgens – primarily testosterone and dihydrotestosterone (DHT) are the key hormonal regulators of prostate growth, development and physiological function (19,20). They elicit various biological effects by activating the AR and are crucial for male reproductive development and physiology in addition to being key drivers for PCa progression (23).

1.3.1.1.1 Androgen synthesis

Testosterone, produced in the testes, is converted to DHT, an androgen approximately five-fold more potent than testosterone, in prostate cells by the steroid 5α-reductases (SRD5A). Androgen production is governed by the hypothalamic-pituitary-adrenal-gonadotropic axis. Briefly, the hypothalamus releases luteinizing hormone-releasing hormone (LHRH), stimulating the pituitary to release luteinizing hormone (LH) and adrenocorticotropin hormone (ACTH). LH

stimulates Leydig cells in the testes to produce testosterone while ACTH stimulates cells of the adrenal cortex to release dehydroepiandrosterone, which undergoes conversion to testosterone in prostate cells. Testosterone is carried in the circulation primarily by albumin and sex hormone binding globulin. LHRH and testosterone exhibit negative feedback regulation at the levels of the hypothalamus and pituitary (40,41).

Biosynthesis of testosterone and DHT is achieved in multiple ways, as outlined in Figure 1.1. Synthesis begins in the mitochondria with the essential precursor cholesterol, which is first shuttled into the mitochondrial matrix by steroidogenic acute regulatory protein (StAR) for eventual formation of DHT through multiple enzymatic pathways. Enzymes of particular importance include members of the cytochrome P450 (CYP) superfamily and CYP17A1 in particular, hydroxyl dehydrogenases , aldo-keto reductases and SRD5As which finally convert testosterone to DHT (40–42).

1.3.1.1.2 Androgen receptor

In general, the AR shares structural similarity with other steroid receptors with an N-terminal domain, a DNA-binding domain, a hinge region, and the C-terminal domain which contains the ligand binding domain (LBD), as well as transactivation domains.

Ligand binding to the AR, which is usually bound to molecular chaperones such as heat-shock proteins in the cytoplasm, leads to dissociation of the chaperones, exposure of a nuclear localization signal and receptor phosphorylation (43–45). This is followed by homodimerization of two AR-ligand complexes and subsequent translocation to the nucleus to bind androgen response elements and co-regulatory proteins resulting in changes in gene transcription of various target genes, including prostate specific antigen (PSA). Additionally, AR acts in the cytoplasm or at the cell membrane to modulate signaling events (46).

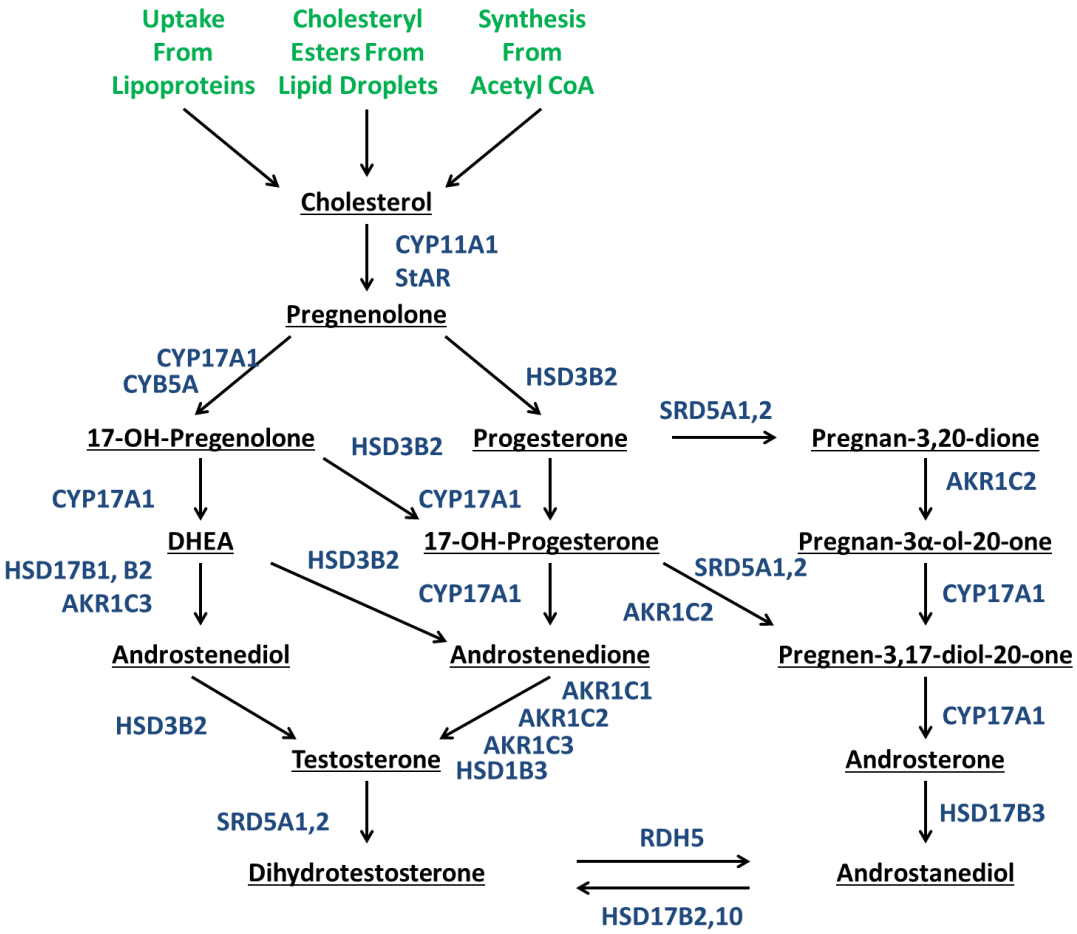

Figure 1.1: Steroidogenesis pathway.
The mitochondrial steroidogenesis pathway whereby cholesterol is converted to testosterone and DHT. Steroids are portrayed in black and enzymes are portrayed in blue. Reversibility of enzymatic reactions is indicated by the direction of arrows. Figure modified from (47).

AR activation is associated with the regulation of numerous downstream gene targets (48). Over 4,000 genes are thought to be regulated by varying concentrations of androgen. Many of these changes include regulators of cell cycle checkpoints, as well as factors involved in cell survival and programmed cell death signaling, often resulting in enhanced proliferation and survival of PCa cells. Furthermore, the expression of proteins involved in the homeostasis of lipids and steroids is also affected by androgen signaling (49,50).

1.3.2 Diagnosis

PCa is frequently asymptomatic at diagnosis and even when the patient has symptoms, they are vague and nonspecific, requiring differential diagnostics to rule out other urogenital maladies (51). Screening for PCa includes the digital rectal exam (DRE), measurement of serum PSA level, and transrectal ultrasound-guided biopsy. Abnormal DRE and/or PSA findings would prompt follow up with a biopsy for histopathological verification of PCa (51).

A DRE is performed to determine whether the prostate is enlarged or presents with abnormal nodules that are often indicative of PCa foci (52). Because a DRE primarily addresses the dorsal prostate, it can miss a substantial portion of PCas, is poorly reproducible and subjective, with high inter-examiner variability, especially as a screening tool for detection of low-grade PCa (53).

PSA is a serine protease of the tissue kallikrein protease family, produced by prostate epithelial tissue and secreted into the lumen in response to AR activation. The physiologic function of PSA is cleavage of semenogelin I and II, effectively liquefying seminal fluid to allow greater motility of sperm. As PSA is secreted directly into the lumen, serum levels are usually low. Serum PSA can be elevated in response to PCa, benign prostatic hypertrophy, prostatitis, and in response to prostate biopsy or any insult that compromises the architecture of the prostate stroma; hence, PSA findings are not specific for PCa. Nevertheless, PSA is a valuable biomarker used in detection, prognosis, and monitoring of treatment response and disease recurrence in PCa. While clinically it is used primarily to monitor changes in cancer cell growth, experimentally PSA can also be used as an indirect measure of AR activation (54,55).

1.3.3 Classifications of prostate cancer

1.3.3.1 Tumor-node-metastasis classification and staging

The tumor-node-metastasis (TNM) staging system is widely used in clinical oncology to standardize cancer classification. The system describes the anatomical involvement of cancer by indicating the presence of the tumor at the primary site (T), presence or absence of cancer in regional lymph nodes (N), and the presence or absence of metastatic lesions beyond regional lymph nodes (M). T is subdivided T1 to T4 to describe increasing size of the primary lesion while N and M consist of either 0 or 1 indicating the absence or presence of lesions in these regions. T1 and T2 describe organ confined tumors while T3 and T4 describe extraprostatic spread of disease (51,56,57).

1.3.3.2 Gleason Grading

Published in *Cancer Chemotherapy Reports* in 1966, the Gleason scoring system was developed by Donald Gleason in an attempt to standardize PCa grading. Grading is based on hematoxylin and eosin staining and histologic identification of Gleason patterns ranging from cancerous tissue resembling normal prostate (Pattern 1) to tissue lacking differentiation and recognizable glands (Pattern 5). The scores of the most common and second-most common patterns are then added together and the Gleason score is a sum of these two grades (58,59).

1.3.4 Prognosis

The prognosis of PCa varies with a multitude of factors, including: clinical stage of disease, Gleason score, PSA levels, prior exposure and response to therapeutic interventions, and age (60). Favorable prognostic factors include local disease (stage T1 and T2), Gleason score < 7, serum PSA < 10 ng/mL, and lack of prior therapeutic intervention. Less favorable prognostic factors include metastatic disease (stages T3 and T4), Gleason score > 7, serum PSA > 20

ng/mL, and prior exposure to hormonal therapy. Age is more difficult to predict as younger patients tend to have more aggressive disease while older patients usually present with other illnesses. 5-year relative survival for patients in Canada is 96%; however, for patients with widely disseminated stage IV disease, 5-year relative survival is 31%.

Some molecular prognostic markers include the following genetic changes associated with poor survival: *PTEN* loss, *TMPRSS2-ERG* fusion, *P53* mutations, overexpression of *MYC,* as well as alterations in the gene products of *RB,* B-cell CLL/Lymphoma 2 (*BCL2),* cathepsin D *(CTSD),* and e-cadherin (*CDH1).* Decreased expression of p27 is associated with increased risk of disease recurrence (61,62). Inclusion of these and other markers into the diagnostic and prognostic spectrum are under development to better risk-stratify patients.

The majority of patients with low-risk disease can defer treatment, and instead be monitored by active surveillance, involving regular PSA and DRE testing and occasional repeat biopsies (63). As a result of surveillance, patients are at a decreased risk for over-treatment and associated adverse effects. Selective delayed intervention has seen a cancer specific mortality at 10 – 15 years of just 3%. Though clinically localized disease is potentially curable, 20 – 40% of men will experience recurrence within ten years of treatment, as determined by rising PSA levels (64–66). Among patients with evidence of recurrent disease, approximately 30% will develop metastases, with bone being the first site of metastatic lesions in most patients. Metastasis-free survival can range from 1 to 10 years depending on individual risk factors. Median time to death for men with confirmed metastatic disease is 5 years; given enough time, all patients with metastatic disease will inevitably progress to the lethal CRPC. For patients with confirmed metastatic CRPC, survival time is less than 2 years.

1.3.5 Treatment, adaptations, and progression to CRPC

1.3.5.1 Localized therapies

Localized disease is potentially curable and selection of an appropriate treatment scheme depends upon various prognostic factors, including: Gleason score, clinical stage, PSA level and life expectancy. Determined by the balance of life expectancy, disease burden and treatment risk, active surveillance can be recommended for some patients. Lower risk cases of localized disease can be potentially cured with radical prostatectomy, surgical removal of the prostate and surrounding tissue, and radiation (3,54). Radical prostatectomy is associated with 15-year progression-free survival rates as high as 88% in patients with low to intermediate-risk disease (67). 15-year PCa-specific mortality is reduced from 20% in untreated patients to 7% in patients treated with prostatectomy (68). Meanwhile, radiation therapy is associated with 10-year progression-free survival rates as high as 90% in the same cohort (69).

1.3.5.2 Systemic therapies

Given the poor prognosis associated with metastatic disease, and in particular metastatic CRPC (65,66), various systemic therapies have been developed with varying success. Despite considerable progress including symptomatic improvement and survival benefits, CRPC remains incurable.

1.3.5.2.1 AR axis-targeted therapy

Androgen deprivation therapy (ADT), which aims to reduce androgen-mediated signaling, is the mainstay of therapy in confirmed metastatic disease (70–72). In addition to metastatic PCa, ADT can also be used to treat patients with rising PSA after local therapy and as an adjunctive therapy in patients receiving radiation therapy as well as to palliate symptoms in advanced disease. Castrate testosterone levels can be achieved surgically through bilateral

orchiectomy, or chemically using a variety of agents including LHRH agonists and antagonists which act to suppress androgen synthesis by negatively regulating the hypothalamic-pituitary-adrenal-gonadotropic axis (71,72). LHRH modulators act in a reversible fashion, are noninvasive, and enable minimizing the adverse effects associated with ADT, making them the preferred method of suppressing androgen synthesis. LHRH antagonists are preferred over agonists due to their rapid action and lack of testosterone flare associated with LHRH agonist activity. They can be administered continuously or intermittently to minimize adverse effects and improve tolerability. While ADT extends patient lifespan by an average of 18 months (73), it is not curative and is associated with disease recurrence and progression to CRPC.

Androgen signaling can also be suppressed using AR antagonists (70–72,74), also known as antiandrogens, which act as competitive inhibitors of the LBD. These drugs act to block AR activation and nuclear translocation, but suffer from markedly lower affinity for the AR than its preferred ligand, DHT. They can be used alone or in combination with LHRH analogues to confer an additional survival advantage (< 5%) compared to LHRH analogues alone, though combination therapy is limited by toxicity. Enzalutamide, a second generation AR antagonist, has demonstrated up to eight-fold higher binding affinity for the AR as compared to older agents such as bicalutamide (75). The AFFIRM trial in patients who progressed on first-line therapy (docetaxel, discussed in section 1.5.3.2.2) demonstrated effective attainment of castrate testosterone levels as well as a 37% reduction in mortality risk compared to placebo, leading to early termination of the study so patients in the placebo arm could be offered treatment with this new agent (76). Overall survival was extended by 5 months in the enzalutamide arm, as was time to PSA progression. The PREVAIL trial demonstrated a 21% mortality risk reduction, and extended progression-free survival compared to placebo in metastatic CRPC patients treated with

enzalutamide (77). These studies demonstrated marked clinical benefit and have established enzalutamide as an effective therapy for advanced disease.

Androgen synthesis can be targeted directly by inhibition of CYP enzymes (71,78,79). CYP17A1 catalyzes two enzymatic reactions in the androgen synthesis pathway (Figure 1.1). Its activity can be blocked by two agents. The first, ketoconazole, is a nonspecific CYP inhibitor which also inhibits the activity of a key xenobiotic metabolizing enzyme, CYP3A4. The second, abiraterone, is an analogue of pregnenolone which specifically and irreversibly inhibits CYP17A1, thereby reducing androgen synthesis, while increasing progesterone levels. Prior to the development of abiraterone, ketoconazole enjoyed some use in CRPC management; however, its use is limited due to its nonspecific action and potential for drug-drug interactions with agents metabolized by CYP3A4. The specificity of abiraterone renders it a significantly more potent androgen synthesis inhibitor. In docetaxel treated CRPC patients, the COU-AA-301 trial demonstrated a median overall survival advantage and time to PSA progression of approximately 4 months in patients treated with abiraterone compared to the placebo arm (80). As with enzalutamide, abiraterone has also shown improved overall survival and progression-free survival compared to placebo in therapy-naïve CRPC patients (81).

1.3.5.2.2 Cytotoxic chemotherapy

In 2004, two landmark trials – TAX 327 and SWOG 99-16 – demonstrated a survival benefit with docetaxel (78,82–84). A survival advantage of approximately 3 months made the combination of docetaxel and prednisone the mainstay of CRPC therapy. Docetaxel and other taxanes are cytotoxic chemotherapeutic agents which act by binding and stabilizing microtubule filaments, physically preventing cell division, ultimately leading to mitotic arrest and cell death (66). Cabazitaxel is a newer semisynthetic taxane approved in 2010. The TROPIC trial of

docetaxel treated CRPC patients demonstrated a survival benefit of approximately 2.5 months for patients treated with cabazitaxel compared to those treated with mitoxantrone (85,86). This and other studies demonstrated that cabazitaxel retains anticancer activity after resistance has developed against docetaxel. While increasing the options available to clinicians, taxane treatments present the challenge of tolerability relative to agents targeting the AR-axis (87,88).

1.3.5.2.3 Bone-targeted therapies

The most common site for metastatic lesions in PCa is bone, particularly the ribs, spine, and pelvis (89). The high frequency of bone metastases, manifesting as severe pain, fracture, nerve compression, and myelosuppression, increases disease burden and substantially impacts patient quality of life. The bone microenvironment likely promotes colonization and growth of PCa cells by paracrine signaling; therefore, multiple bone-targeting therapies have been developed.

Bone physiology and bone metastasis pathophysiology are governed by the interaction between a variety of cell types, including: osteoblasts, osteoclasts, osteocytes, and PCa cells (89–91). Osteoclast survival, differentiation, and activity are regulated by receptor activator of nuclear factor kappa-B ligand (RANKL) signaling via its receptor, RANK. RANK-RANKL signaling is also activated in PCa cells and is implicated in bone colonization. Osteoclasts can be targeted by bisphosphonates and the human monoclonal antibody against RANKL, denosumab. The bisphosphonate zoledronic acid effectively inhibits bone resorption in PCa patients with bone metastases, reducing skeletal-related events including bone pain by 26% compared to placebo. Denosumab administration is also associated with impaired bone resorption and decreased skeletal-related events in CRPC. Osteoclast-targeting therapies are indicated in a

supportive manner for symptomatic improvement as no survival advantages have been demonstrated thus far.

Bone-targeted radiopharmaceuticals exhibit cytotoxic effects on PCa cells in bone metastases by delivering focal radiation by β–particle emission (89). ^{89}Sr was the first radiopharmaceutical developed for CRPC, demonstrating pain relief and improved quality of life in the absence of survival benefits. This formed the basis for further radiopharmaceutical development and ^{89}Sr was followed by ^{153}Sm. Despite symptomatic benefits, ^{89}Sr and ^{153}Sm are limited by haematologic toxicity and are not indicated in CRPC. In contrast, the α-paritcle emitter ^{223}Ra has demonstrated minimal myelotoxicity in addition to an overall survival benefit of approximately 3 months compared to placebo in the ALSYMPCA trial (78,92). As such, ^{223}Ra is recommended in patients with pain due to bone metastases, though not in the presence of visceral metastases (93).

1.3.5.2.4 Immune therapies

The immune system can recognize antigens on cancer cells resulting in an antitumor immune response (94,95). The ability of cancer cells to modulate immune cells contributes to their growth and survival and is an important acquired capability. Cancer cells must be able to proliferate in chronically inflamed environments, evade recognition by the immune system, and suppress immune reactivity to give rise to tumors. Immune cells can be actively trained and stimulated to attack cancer cells, an emerging approach in PCa (96,97). Sipuleucel-T is an *ex vivo* processed vaccine against CPRC cells: a patient's peripheral blood mononuclear cells including, antigen-presenting cells (APCs) (dendritic cells, macrophages, and B cells), are collected by leukapheresis and cultured. In culture, they are treated with granulocyte-macrophage colony-stimulating factor (GM-CSF) fused to a prostatic antigen, prostatic acid

phosphatase (PAP), as well as other immune stimulating factors. The APCs, which process and display PAP fragments on their surface, are then infused back into the patient along with T-cells, natural killer cells and B cells ultimately leading to an immune response against PAP-expressing cells. Multiple trials have demonstrated survival benefits of Sipuleucel-T compared to placebo, thus its indication for metastatic CRPC (78).

Additional immunotherapies are under investigation, including anti-cancer vaccines and immune-checkpoint inhibitors (96). PSA-TRICOM is a poxvirus-based vaccine that uses poxvirus as a vehicle to transmit information to immune cells. They include genes for PSA as well as T-cell stimulating factors that trigger an immune response to PCa cells. GVAX is a whole-cell vaccine consisting of GM-CSF secreting PC-3 and LNCaP cell lines. While vaccines are designed to stimulate immune cells to attack cancer cells, immune-checkpoint inhibitors modulate immunoregulatory signaling to prolong immune cell activation. Antibodies against the immune-checkpoint regulators cytotoxic T-lymphocyte associated protein 4 and programmed cell death protein 1 are under investigation for PCa as well as other cancers.

1.4 Cellular responses to therapy and progression to CRPC

The varying clinical outcomes associated with PCa treatments are largely the result of differential cellular responses to therapy. The aim of anti-cancer treatments is to reduce cancer cell proliferation, preferably by inducing death of cancer cells, while sparing non-cancerous cells. Tumor regression follows treatment induced cell death; however, the application of such selective pressures can induce adaptive stress responses which promote cancer cell survival, treatment-resistance, disease recurrence, and progression (30,98).

1.4.1 Cell death

1.4.1.1 Apoptosis

Programmed cell death is an evolutionarily conserved process fundamental for the development and homeostasis of multicellular organisms (99). Apoptosis, also known as type I cell death, is the best understood form of programmed cell death, initiation and execution of which is regulated by the caspases, a family of cysteine proteases. Initiator caspases (caspase-2, -8, -9, and -10) commence the apoptotic program in response to upstream signals, while effector caspases (caspase-3, -6, and -7) guide cellular degradation (100). Caspases can be activated by a multitude of signals, executing programmed cell death through various targets: regulators of apoptosis such as pro-apoptotic kinases, structural proteins such as fodrin and gelsolin leading to disruption of actin filaments and cytoskeletal degradation, DNA repair proteins such as poly(ADP-ribose) polymerase (PARP), and cell cycle regulators such as p21 and p27 (101). Classical outcomes of apoptotic cell death include chromatin condensation, DNA fragmentation, shedding of apoptotic bodies, and display of phagocytosis markers, leading to clearance of apoptotic bodies (102). As such, cleavage products of PARP and caspase-3, as well as assessment of DNA content serve as common markers for apoptosis.

The intrinsic apoptosis pathway is governed by mitochondrial proteins and relies on mitochondrial outer membrane permeabilization (MOMP) and release of pro-apoptotic proteins such as cytochrome c (99,100). The Bcl family of proteins regulates MOMP and includes anti-apoptotic proteins (Bcl-2, Bcl-xL, MCl-1), pro-apoptotic proteins (Bax, Bak), and stress-sensing proteins (Bid, Bim, Bad, Noxa). Stress-sensing proteins either activate the anti-apoptotic proteins or inhibit the pro-apoptotic proteins. Cytochrome c forms the apoptosome complex with other proteins including Apaf-1 and caspase-9, thereby initiating apoptosis. Bcl-2 proteins are also

involved in apoptotic death in response to endoplasmic reticulum (ER) stress. ER stress eventually results in calcium release into the cytosol, ultimately leading to activation of the intrinsic pathway. MOMP can also be triggered by lysosomal permeabilization.

The extrinsic pathway involves activation of cell surface receptors (99,100). A multi-protein complex called the death-inducing signaling complex is formed upon ligand binding to death receptors followed by recruitment of adaptor proteins and caspase-8, which is then catalytically activated. Caspase-8 can then activate the effector caspase-3 directly or can activate the intrinsic apoptosis pathway via interaction with Bid.

Apoptosis is a favorable response to many PCa therapies. Radiation therapy causing DNA breaks and oxidative stress activates the intrinsic apoptosis cascade (103). Cells react to DNA damage by cleavage activation of PARP, a DNA repair protein whose action is inactivated by caspases (101). Microtubule stabilization by taxane treatments has been linked to downstream phosphorylation and inhibition of Bcl-2, promoting an apoptotic response (104). Cells adapt to taxane therapy and treatment resistance can emerge by overexpression of efflux pumps such as P-glycoprotein, an established cause of therapeutic resistance to multiple chemotherapeutics, including docetaxel (105). Antagonism of androgen signaling by any of the aforementioned mechanisms is well documented to promote growth arrest and apoptosis in PCa cells (106,107), while apoptotic tumor regression is thought to be the consequence of bilateral orchiectomy (108). Mirroring the clinical situation, castration of mice bearing xenograft PCa tumors leads to tumor regression and decreased serum PSA levels; however, after a delay, PSA levels rise and the tumor re-emerges in a castrate-resistant state (109,110,110). This regrowth is understood to be an adaptation to castrate androgen levels resulting in resumed tumor proliferation. Additional anti-apoptotic adaptations include changes to apoptotic proteins where overexpression of Bcl-2 is

linked to treatment resistance, as well as induction of protective chaperones, and activation/modulation of growth factor mediated survival signaling (103,111).

1.4.1.2 Necrosis

Necrotic cells are characterized by swelling of organelles including the ER and mitochondria, plasma membrane rupture, and cell lysis (102,112). In contrast to apoptosis, the nucleus usually remains intact. Necrosis, also known as type III cell death, is thought of as an inflammatory process; selective release of pro-inflammatory factors, such as high mobility group box 1 and hepatoma-derived growth factor, are sensed by and activate a protein complex called the inflammasome, resulting in release of pro-inflammatory cytokines. Cell damage leading to mitochondrial ATP release also contributes to activation of the inflammasome.

Unlike the coordinated nature of death associated with apoptosis, necrosis was thought to be an accidental process in response to stress (102,112); however, emerging evidence indicates that many forms of necrosis are also tightly regulated. A classic example of a necrotic response is activation by tumor necrosis factor (TNF) signaling, mediated by receptor-interacting protein kinases among others, leading to activation of nuclear factor-κB (NF-κB), which can inhibit apoptosis by stimulating expression of the anti-apoptotic Bcl-xL, ultimately leading to reactive oxygen species (ROS) formation, osmotic swelling, and necrotic death (113). In this context, necrosis can serve as an alternative death mechanism when apoptosis is inhibited. Several regulated necrosis pathways have been proposed, including: necroptosis, ferroptosis, oxytosis, and ETosis, among others. Whereas an apoptotic response results in shedding and phagocytosis of apoptotic bodies, leaving surrounding tissue largely unharmed, the outcome of necrosis signaling is cell death invoking tissue damage and an inflammatory response. Similar to apoptosis, coordinated necrosis also follows similar mechanistic steps: stress/trigger activates an

initiating mechanism which through several mediators activates factors which execute necrotic cell death (112).

Established necrotic conditions include hypoxyia, ROS formation, and as a response to microbial and viral infections (101). Other necrosis-inducing factors include treatment with DNA alkylating agents, Ca^{2+}, H_2O_2, activation by cell surface receptor signaling, and loss of cellular ATP, for example by the energy intensive activity of PARP in the absence of caspase inhibition present during apoptosis (101,112,114). Necrosis likely occurs in tumor tissue due to the pro-necrotic hypoxic and inflammatory microenvironment, and in response to therapeutic intervention. TNF levels correlate with PCa disease progression, though its roles appear both tumor suppressive and tumor promoting (115). While TNF is cytotoxic to PCa cells in some conditions, exposure to low levels of TNF may lead to androgen hypersensitivity thereby enhancing androgen signaling (116–118), exemplifying the diverse outcomes associated with treatment-induced necrosis.

1.4.2 Adaptive stress responses

1.4.2.1 Autophagy

Autophagy is a mechanism by which cellular components such as proteins and whole organelles are removed and degraded while their components are recycled and reused (98,100,102). Autophagy occurs at a basal level, ubiquitously throughout the body for the maintenance of homeostasis, but can also be induced by various stresses including starvation and in response to anti-cancer therapy. Autophagy can protect against infections as well as tumor formation; cells with deficient autophagy activity are more susceptible to genomic damage and instability. Excessive autophagy can promote cell death, known as type II cell death, in a

mechanism distinct from apoptosis and necrosis. Unlike apoptosis, autophagic cell death is thought to be independent of caspase activation.

Autophagy is regulated by the autophagy-related genes (Atg) (98,100,102). Many upstream signaling pathways regulate autophagy activity, typically through mammalian target of rapamycin (mTOR), an inhibitor of autophagy, though mTOR-independent pathways have also been found. Autophagy-inducing signals result in the formation of autophagic vesicles known as autophagosomes which ultimately fuse with lysosomes to form autolysosomes. Atg 12 and Atg 8, also known as microtubule-associated protein light chain 3 (LC3), are activated by Atg7. This leads to Atg-dependent conjugation with Atg 5 and phosphatidylethanolamine respectively. These conjugates are required for autophagosome formation. Unconjugated LC3 is known as LC3-I, while conjugated LC3 is known as LC3-II. LC3-II remains associated with autophagosomes and is eventually digested by autolysosomes. Autophagy can be monitored by monitoring autophagic flux via the conversion of LC3-I to LC3-II by immunoblotting (119).

Clusterin (CLU) is a multifunctional stress-activated chaperone with a key role in protein homeostasis (98,103). CLU suppresses protein aggregates and mediates ER stress and the unfolded protein response by inhibiting protein aggregation during stress caused by multiple factors, including hormonal, radiation, and chemotherapy in cancer (120,121). Autophagy inducing-stress has been shown to induce CLU expression (98), both of which have been identified as responses to cancer therapy and subsequent treatment resistance, including to androgen deprivation in PCa (122–124). Emerging evidence indicates a direct role of CLU in autophagy activation by interaction of LC3, facilitating lipidation and conversion of LC3-I to LC3-II. Ultimately, these stress responses contribute to inhibition of PCa cell apoptosis and promote tumor cell survival (98).

1.4.2.2 Senescence

Cellular senescence is a stable and long-term loss of proliferative capacity in the presence of continued metabolic activity (125). The proliferative potential of explanted cells in primary culture was observed to change over time. Freshly harvested cells proliferated slowly, presumably while adapting to their new environment, followed by rapid proliferation which gradually slowed to a halt, suggesting finite replicative capacity (126,127). Gradual attrition of telomeres by incomplete replication of lagging strands by DNA polymerase causes them to shorten to a critical length, triggering a DNA damage response (DDR), amplification of which activates checkpoint kinases 1 and 2. Activation of cell cycle proteins follows, including p53, leading to proliferative arrest (128,129). Cells then attempt to repair their damaged DNA, unless the damage is too extensive. Cells then either undergo apoptosis or senescence, though the triggers responsible for this cell fate decision are not entirely clear. In addition to p53, the cyclin-dependent kinase inhibitor p16 and its downstream signaling partner, the tumor suppressor RB, are also activated in senescence and contribute to growth arrest (130,131).

Though several markers exist for identification, not all senescent cells express every associated marker (125,132). Further, there is no marker specific to the senescence state. Despite this, a senescent phenotype can be defined by key characteristics: irreversible growth arrest, large flat morphology, expression of senescence-associated β-galactosidase (SA-βgal), nuclear foci in the case of DDR-induced senescence, activated tumor suppressor signaling, and emergence of a senescence-associated secretory phenotype (SASP).

Senescent arrest can be induced by a variety of mechanisms in addition to telomere shortening; oxidative stress, oncogenic rat sarcoma (RAS) signaling, and tumor suppressor (PTEN) loss can result in senescence, suggesting an inherent tumor suppressor role of

senescence (125). When cancer is already established, senescence can be induced by anti-cancer agents such as doxorubicin and cyclophosphamide (133).

1.4.3 Progression to CRPC

Cancer cells respond to the selective pressures of anti-cancer therapies by several mechanisms, resulting in the emergence of a treatment-resistant phenotype. Metastatic PCa treated with ADT results in marked tumor regression and symptomatic improvement, but as detailed above, these treatment benefits are temporary and inevitably, the disease recurs as the incurable castration-resistant form known as CRPC (43,71,134). While several contributing factors have been proposed such as enhanced oncogenic signaling and tumor suppressor deletion, disease progression is largely dependent on re-activation of AR signaling by numerous means including receptor hypersensitivity, ligand independence, and *de novo* steroidogenesis.

1.4.3.1 AR hypersensitivity

CRPC cells can acquire the ability to thrive in androgen deprived conditions by diverse mechanisms such as increasing expression of the AR, point mutations leading to amino acid substitutions, and de-regulation of AR co-regulators (30,43). Amplification of the AR gene was demonstrated in approximately 30% of CRPC tumor samples relative to paired untreated primary tumors, allowing proliferation despite castrate androgen levels (135,136). Gene expression analysis during ADT has also revealed enhanced AR gene transcription in patients treated with goserelin and flutamide (137). Negative regulation of the hypothalamic-pituitary-adrenal-gonadotropic axis by LHRH analogues markedly increases transcription of the AR gene, applying pressure on the AR gene rendering it susceptible to DNA breakage and chromosomal rearrangement, ultimately leading to gene amplification (30). Increased AR sensitivity can also be accomplished by mutations to the LBD (43). One such gain-of-function mutation resulting

from the substitution of alanine for threonine at amino acid 877 (T877A) allows AR activation by metabolites of DHT in addition to non-androgen ligands including progestins, estrogens, glucocorticoids, as well as the AR antagonist flutamide. This mutation was shown to promote PCa cell growth and survival and may be a response to selective pressure by AR antagonist therapy (138). Additionally, as abiraterone increases progesterone levels, its use has been shown to select for cells expressing T877A ARs (139). Another mutation of interest resulting from substitution of leucine for histidine at position 702 renders the AR insensitive to androgens but sensitive to glucocorticoids, complicating use of agents such as abiraterone that require co-administration of prednisone (140,141). Finally, modulation of AR co-regulators in the form of amplification of co-activators or suppression of co-repressors may also promote AR hypersensitivity, suggested by the overexpression of two co-activators in some tumors samples and PCa cell lines (142).

1.4.3.2 AR ligand independence

Signaling by growth factors, such as insulin-like growth-factor 1, keratinocyte growth factor, and epidermal growth factor can activate the AR in the absence of androgen (143). Activation of the AR appears to require the presence of an LBD, as demonstrated by the ability of bicalutamide to block its activation by signaling cascades. Growth factor signaling activates signaling by mitogen-activated protein kinases (MAPK) as well as by PI3K, both of which may phosphorylate and activate the AR (144–146). The clinical importance of AR activation by these pathways is unclear, as is the therapeutic potential of targeting these signaling cascades (43).

While in most cases, PCa cells depend upon ligand-activated AR signaling for growth and survival, high transcriptional pressure on the AR gene can also produce variant ARs (AR-Vs) by faulty splicing (30). These AR-Vs are truncated and lack a LBD and therefore do not

require ligand-activation, are constitutively active in the nucleus, and are not subject to antagonism by anti-androgen drugs. AR-V expression is distinct from full length AR and their presence is thought to confer resistance to AR antagonists and androgen synthesis inhibitors. However, their functional significance is not well characterized and full length AR is still believed to be the primary mechanism by which PCa cells continue AR signaling (147).

1.4.3.3 *De novo* steroidogenesis

Serum total testosterone levels in normal adult human males range between 3 – 10 ng/mL, while castrate levels as low as < 0.2 ng/mL and < 0.5 ng/mL can be reached by surgical and chemical castration, respectively (148). Despite our best efforts to block androgen synthesis, androgens continue to be detectable in the prostates of PCa patients post-castration (149). In fact, intratumoral testosterone levels in CRPC patients are similar to prostate tissue levels in patients with benign prostatic hypertrophy, while DHT and androgen precursors are also present in amounts sufficient for AR activation (150). Potential androgen sources include adrenal precursors and androgens synthesized intratumorally. Adrenalectomy paired with ADT was not shown to inhibit PCa progression, suggesting that even if adrenal precursors continue to provide androgens to CRPC cells, an alternative source likely exists. (151) Gene expression analysis of CRPC bone metastases confirmed expression of transcripts for various enzymes involved in testosterone synthesis, demonstrating the ability of CRPC cells to convert adrenal precursors to testosterone and DHT (152,153). Furthermore, using the LNCaP xenograft model, intratumoral androgens were shown to increase during progression to CRPC. CRPC tumor cells cultured from these same animals were able to convert the cholesterol precursor acetic acid into steroids, including DHT, demonstrating the ability of CRPC cells to produce their own androgens *de novo* from cholesterol (47).

1.4.4 Cholesterol in PCa

In addition to serving as a precursor for steroid hormones, cholesterol modulates the functions of membrane proteins including G protein-coupled receptors, participates in endosomal trafficking, and regulates membrane fluidity and permeability (154). Though contentious, various lines of evidence indicate that men with elevated serum cholesterol levels have an increased risk for development of aggressive forms of PCa; meanwhile, several studies suggest inhibition of cholesterol synthesis by statins, inhibitors of 3-hydroxy-3-methylglutaryl-coenzyme A reductase (HMGCR), reduce this risk (155). Upregulation of the mevalonate cholesterol synthesis pathway, in addition to other aberrations, facilitates the cellular accumulation of cholesterol, thereby contributing to the lipogenic phenotype, characterized by enhanced synthesis of fatty acids and cholesterol (156). Cellular cholesterol is unevenly distributed across the endomembrane system; < 1% of total cellular cholesterol is found in the ER while approximately 90% is found at the plasma membrane, accounting for up to 25 – 30% of plasma membrane lipid content (157). Despite containing the smallest proportion of cellular cholesterol, the ER is the primary site of cholesterol homeostasis due to the presence of sterol sensors and enzymes involved in cholesterol synthesis (154).

1.4.4.1 Cellular cholesterol homeostasis

Intracellular cholesterol levels are tightly regulated by nuclear receptor transcriptional regulators (158). Briefly, sterol depletion in the ER is monitored by a multi-protein sterol sensing system which activates sterol regulatory element binding proteins (SREBPs). Interestingly, SREBPs are also activated by androgen stimulation (159). SREBPs function to increase cholesterol levels by increasing transcription of HMGCR and low density lipoprotein receptor (LDLR) (154). Conversely, liver X receptors (LXRs) are activated by high cholesterol levels,

increase cholesterol efflux, and reduce cholesterol uptake by targeted degradation of LDLR. Cholesterol efflux is achieved mainly by members of the ATP-binding cassette (ABC) protein family, including ABCA1, ABCG1, and the heterodimeric ABCG5/G8. ABCA1 and ABCG1 efflux cholesterol to high density lipoproteins (HDL) in the circulation, while ABCG5&G8 are involved in cholesterol elimination from the liver and intestine into the intestinal lumen (160).

Free cholesterol and fatty acids are esterified to cholesteryl esters (CE) in the ER by acyl CoA:cholesterol acyltranserases for storage in lipid droplets (154). These CEs can be cleaved to produce free cholesterol by hormone-sensitive lipase (HSL) which is expressed in steroidogenic tissue and activated upon phosphorylation by several kinases in response to hormones such as catecholamines and ACTH (161). When activated, HSL acts on HDL-derived CEs which can then be delivered to the mitochondria by StAR for steroidogenesis (162,163).

1.4.4.2 Sources of cellular cholesterol

Cells obtain cholesterol either by synthesis through the multistep, enzymatic conversion of acetate or by uptake from extracellular sources (154,164). The rate-limiting step of cholesterol synthesis is the conversion of HMG-CoA to mevalonic acid by HMGCR (154,164). Cholesterol synthesis is controlled by SREBP-2 , which is usually complexed to SREBP cleavage-activating protein (SCAP) in the ER, anchored by insulin-induced gene-1 (165,166). Above a certain threshold, oxysterol metabolites of cholesterol disallow this complex to transport to the Golgi via transport vesicles. Decreased oxysterol levels result in release of SCAP-SREBP and transport to the Golgi for processing by proteolytic cleavage to produce the soluble SREBP transcription factor, which subsequently translocates to the nucleus to activate transcription of numerous target genes, including HMGCR (167–170). High sterol levels lead to ubiquitination and

degradation of HMGCR (171). Interestingly, cholesterol synthesis can be stimulated by androgen treatment *in vitro* in PCa cell lines (172).

Extracellular cholesterol is transported through the circulation in the form of lipoproteins consisting of a hydrophobic core composed of triglycerides and CEs and an outer surface containing a phospholipid monolayer, free cholesterol, and apolipoproteins (Apo) (173). Lipoproteins are named according to their density, ranging from lowest to highest density: chylomicrons, very low density lipoproteins (VLDL), low density lipoproteins (LDL), and high density lipoproteins (HDL). They vary not only with regards to density, but also apolipoprotein and lipid composition (154,173). Cellular cholesterol uptake from lipoproteins involves lipoprotein receptors; of particular interest to steroidogenesis are the LDL receptor (LDLR) and scavenger receptor class B type I (SR-BI) which has been identified as a receptor for HDL (174).

1.4.4.2.1 LDLR

Cholesterol is transported to peripheral tissues primarily by LDL particles which account for up to 80% of circulating cholesterol in humans. LDL particles are produced in the liver and consist mainly of cholesterol and CEs and contain ApoB-100, which is recognized by cell surface LDLR (173). LDLR binding by LDL particles facilitates endocytosis of the LDL-LDLR complex and subsequent processing in the endosomal-lysosomal system, where triglycerides and CE are hydrolyzed by lysosomal acid lipase, releasing free cholesterol and free fatty acids, followed by return of LDLR to the cell surface (175). As with HMGCR, LDLR transcription is also activated by SREBPs, as described above. When sterol levels are high, LXR facilitates the degradation of LDLR by stimulating expression of inducible degrader of LDLR, resulting in LDLR ubiquitination and lysosomal degradation (176).

In PCa patients, LDL levels increase post-castration, though the cancer-specific clinical significance of this is unclear (177). Results from *in vitro* studies indicate differing effects on proliferation of PCa cells lines, without a clear or consistent result identified (178,179). Studies have shown that LDLR expression is upregulated in CRPC (180), likely due to dysregulated SREBP (181–183), implying it may be an important source of cholesterol for PCa cells. LDL particles have been shown to stimulate steroid production in steroidogenic tissues (184–186); however, a study in mice showed that knocking out LDLR did not affect adrenal steroid production (187), implying a different source of cholesterol is preferred for steroidogenesis. With the exception of steroidogenesis in the luteal cells of the ovaries where LDL appears to be the preferred source of cholesterol, most lines of evidence indicate HDL is the primary source of substrate for steroid synthesis in rodents, where most study of steroidogenesis has taken place (188). In humans, normal LDLR function does not appear to be necessary for normal adrenal function, as suggested by plasma cortisol responses to ACTH administration in LDLR deficient homozygous familial hypercholesterolemia patients (189). Abetalipoproteinemic patients also exhibit normal adrenal function despite little ApoB-100 and an absence of LDL (190). Furthermore, HDL is the preferred provider of cholesterol for steroid production in rats (191). Taken together, HDL is a likely source of cholesterol for steroidogenesis in humans.

1.4.4.2.2 SR-BI

Produced by the liver and intestine as discoidal, lipid-poor precursors, HDLs are remodeled by enzymes in the plasma where they acquire lipids from cells and other lipoproteins, gradually maturing into spherical HDL particles contain CEs and various apolipoproteins: apoA-I, apoA-II, apoC, apoD, and apoE (173). HDLs serve as a mechanism of removing free cholesterol from peripheral tissues, which is then converted to CEs by the HDL-associated

enzyme, lecithin:cholesterol acyltransferase. These CEs are delivered to steroidogenic tissues, to be used by cells of the adrenals, testes, ovaries, and breasts (188,192). Unlike the endocytosis-mediated cholesterol uptake pathway used by LDLR (175), HDL does not appear to require entry into the cell to deliver its components. Instead, HDL binding to the cell surface results in free cholesterol flux from the cell surface to the HDL particle in exchange for CEs (193). This form of lipid transfer is termed selective lipid uptake and is the preferred method by which rodent steroidogenic tissues acquire cholesterol (188). In 1996, Monty Krieger's group identified SR-BI as the receptor for HDLs (174), and later demonstrated that selective lipid uptake is protein-mediated, requiring interaction between SR-BI and apolipoproteins (193), and that this action can be blocked with small molecule inhibitors (194).

SR-BI, encoded by the *SCARB1* gene, is expressed primarily as a highly glycosylated, cell surface receptor (195,196). Most of the 509-amino acid sequence takes the form of an extracellular loop domain, anchored to the plasma membrane by both the N and C termini which have short cytroplasmic extensions of 10 and 40 amino acids respectively (192,197). The C-terminal tail is implicated in SR-BI-mediated signal transduction through MAPK/ERK and PI3K/Akt signal pathways, studied primary in endothelial cells (198–200). SR-BI is expressed ubiquitously, with particular enrichment in hepatic and steroidogenic tissues such as the adrenal glands, ovaries, and Leydig cells of the testes (188,192). Notably, SR-BI protein has also been detected in adult human prostate tissue by immunoblot (201). Adrenal expression can be induced by administration of ACTH while administration of the glucocorticoid dexamethasone suppresses SR-BI protein levels, demonstrating hormonal control of SR-BI expression and an important link to the hypothalamic-pituitary-adrenal-gonadotropic axis (195,196). Consistent with increased SR-BI protein levels, ACTH stimulation is also associated with substantial

increases in selective lipid uptake from HDL (202,203). SR-BI expression is regulated by a variety of dietary, hormonal, and metabolic factors, including: SREBP-1, steroidogenic factor-1, farsenoid X receptor, LXR, liver receptor homolog 1, PPARγ, and HNF4α (158,188,192,201). Interestingly, sex differences in expression indicate higher *SCARB1* transcript levels in males than in females, suggesting a tighter link between SR-BI and androgen homeostasis (204,205). The diversity of regulating factors implies a multi-functional role for SR-BI in physiology, with clear importance in steroid hormone production and associated cholesterol homeostasis.

1.4.4.3 SR-BI in CRPC

Several lines of evidence suggest that SR-BI may be an essential player in PCa disease progression to CRPC. In addition to its presence in normal adult human prostate tissue, SR-BI mRNA and protein have been detected in the following PCa cell lines: PC3, LNCaP, and DU145 (179,206). Additionally, *SCARB1* transcripts were detected in human prostate biopsy samples in untreated PCa patients as well as those treated with ADT (179). A study in the transgenic adenocarcinoma of the mouse prostate (TRAMP) model demonstrated that mice fed a diet high in fat and cholesterol had accelerated tumor growth, reduced plasma cholesterol levels, increased angiogenesis, and increased tumoral SR-BI expression compared with mice fed a control chow diet (207). More interestingly, colleagues found increased SR-BI protein expression in CRPC tumors compared to tumors harvested pre-castration and immediately following castration (nadir) in the LNCaP xenograft mouse model (180). This increase in expression occurred alongside increases in serum PSA and intratumoral testosterone concentrations. While LDLR protein levels also appeared to increase in CRPC tumors relative to pre-castration and nadir tumors, this change was not statistically significant. More recently, SR-BI protein expression was found to be approximately two-fold higher in the castration-resistant, LNCaP lineage

derived C4-2 cell line, relative to LNCaP cells (208). Furthermore, knockdown of SR-BI by siRNA treatment resulted in decreased PSA secretion and cell viability compared to control transfected cells. Reduced viability could not be reversed by supplementation with exogenous HDL, implying that knockdown of SR-BI effectively reduced the cell's capacity to derive lipids from HDL particles, though this was not tested. Together, these various observations implicate SR-BI in PCa recurrence and progression to castrate-resistant disease.

1.5 Experimental models

1.5.1 LNCaP cell line

The LNCaP cell line is among one of the oldest and most widely used cell lines in PCa research. Originally isolated by needle biopsy from a lymph node metastatic lesion of a 50-year-old Caucasian male, LNCaP cells are androgen sensitive and respond to androgen deprivation. AR is expressed, PSA is produced, and xenograft tumors are formed when injected into mice. The T877A AR mutation is found in this cell type. Various sublines have been developed, one of which is the C4-2 line (209).

1.5.2 LNCaP xenograft mouse

The LNCaP xenograft mouse model has been developed by inoculating athymic mice with LNCaP cells subcutaneously and grown until a preset tumor volume. The mice are then castrated and the tumors grown for several more weeks. The remaining cancer cells are castration-resistant. Serum PSA and tumor volume can be followed to track PCa progression from androgen-dependent at the outset, to nadir immediately post-castration, and then finally to castration-resistance (183,210). This model has been employed extensively by our group and others to study cholesterol homeostasis as a potential therapeutic opportunity in CRPC (47,163,172,180,211).

1.5.3 C4-2 cell line

The C4-2 cell line is a chimeric cell line produced by coinoculating LNCaP cells with human osteosarcoma MS cell line into host mice and collecting the resultant tumors 4 weeks post-castration, producing the C4 cell line. The C4 cells were then coinoculated with MS cells in castrated host mice and collecting the resultant tumors to produce the C4-2 line. These cells are an *in vitro* model of CRPC which express AR, produce PSA, and grow faster than their parental LNCaP cell line (209). This cell line was used previously by our group to study the role of SR-BI in castrate-resistance and was therefore chosen as the model system for this study (208).

1.6 Scope of thesis

1.6.1 Hypothesis

SR-BI contributes cholesterol as a substrate for *de novo* androgen synthesis within castration-resistant prostate cancer cells.

1.6.2 Rationale and specific aims

Currently, CRPC is lethal and existing therapies are not curative. While many emerging therapies target androgen signaling, which continues to be an essential component of CRPC and a valid target, therapeutic resistance continues to limit clinical success. Therefore, it is pertinent to target this signaling pathway upstream of existing treatment modalities. Accordingly, cholesterol metabolism is under intense investigation to identify novel therapeutic targets. In particular, cholesterol uptake via SR-BI may contribute to castration-resistance by providing a necessary precursor for androgen synthesis. Loss of SR-BI reduces cell viability as well as androgen signaling, as measured by secreted PSA; however, the mechanisms underlying these observations remain unidentified and need to be further explored in order to better characterize SR-BI as a potential novel therapeutic target in castration-resistant disease.

The stated hypothesis will be tested by completing these specific aims:

1. Determine the effect of silencing SR-BI on HDL uptake in C4-2 cells.

2. Determine the effect of silencing SR-BI on the cell cycle profile in C4-2 cells.

Chapter 2: Materials and methods

2.1 Materials and reagents

Blocker of Lipid Transport-1 (BLT), bovine serum albumin (BSA), chloroquine diphosphate crystalline (CQ), dimethyl sulfoxide (DMSO), LY 294,002 hydrochloride (LY), nonyl phenoxypolyethylenyl ethanol (NP-40), phenylmethylsulonyl fluoride (PMSF), 0.01% poly-L-lysine, propidium iodide, rapamycin from Streptomyces, sodium dodecyl sulfate (SDS), Tween 20, and Triton X-100 were purchased from Sigma-Aldrich (St. Louis, MO). Human high density lipoproteins and DiI labelled high density lipoproteins were purchased from Alfa Aesar (Ward Hill, MA). MG-132 was purchased from EMD Millipore (Billerica, MA). RNAse A was purchased from Life Technologies (Burlington, Ontario). All other general laboratory chemicals were purchased from Fisher Scientific (Waltham, MA).

2.2 Cell culture

The human CRPC C4-2 cell line was generously provided by Dr. Paul Rennie (The Vancouver Prostate Centre, Vancouver Coastal Health Research Institute, Vancouver, BC). Cells were maintained in phenol red-free Roswell Park Memorial Institute (RPMI) 1640 media (Life Technologies) supplemented with 5% fetal bovine serum (FBS, Life Technologies) and penicillin-streptomycin (100 U/mL-100 µg/mL, Life Technologies) at 37°C in a humidified, 5% CO_2 environment.

2.3 RNA-interference transfection protocol

Cells were seeded in RPMI-1640 with 5% FBS at a density of 2.5×10^4 cells per well in 6-well plates for transfection using a modified method developed previously (208). 48 hours after seeding, the media was changed to Opti-MEM I reduced serum media (Life Technologies). Cells were transfected for 5 hours with 10 nM final concentrations of either Stealth RNAi

duplexes targeting SR-BI (SRBI-KD, Oligo ID HSS101571: AUAAUCCGAACUUGUCCUUGAAGGG, Cat. No. 1299001) or Lo GC Negative Control duplexes (NC, Cat. No. 12935-110) with 2.0 x 10^3 µM Lipofectamine RNAiMAX transfection reagent all purchased from Life Technologies. Cells were then allowed to recover overnight in Opti-MEM I. The next day, cells were washed with PBS and media was changed to RPMI-1640 with 5% charcoal-dextran stripped FBS (CSS, Life Technologies) or 1% FBS, depending on the experiment, for the remainder of the experiment to mimic androgen-depleted conditions (212).

2.4 Whole cell lysate preparation

Cells were washed with ice cold PBS before being lysed with ice cold modified radioimmunoprecipitation assay (RIPA) buffer (50 mM Tris-HCl pH 7.4, 1% NP-40, 0.25% sodium deoxycholate, 150 mM NaCl, 0.1% SDS) supplemented with Roche protease and phosphatase inhibitors (Sigma-Aldrich). Cells in RIPA buffer were recovered from the plate using a cell scraper, placed into 1.5 mL microcentrifuge tubes, and homogenized by passing through a 25-guage needle at least 5 times. The samples were then centrifuged at 14,000 rpm for 20 minutes at 4°C and the supernatant was recovered. Protein concentrations of cell lysates were measured using the Pierce BCA Protein Assay (Fisher) according to manufacturer's instructions. The bicinchoninic acid (BCA) based colorimetric protein quantification method uses the reduction of Cu^{2+} to Cu^{1+} forming a purple-colored, water-soluble complex with BCA, which can be detected by absorbance at 562 nm. The assay determines protein concentrations using a standard curve generated by serial dilution of BSA over the working range of 0 – 2000 µg/mL.

2.5 Western blotting

Whole cell lysate protein samples were subjected to SDS-polyacrylamide gel electrophoresis (SDS-PAGE) using 8 or 15% gels as previously described (208); 15% gels were used to resolve proteins < 30 kDa in size while 8% gels were used to resolve all other proteins analyzed. After gel electrophoresis, proteins were transferred to nitrocellulose membranes (Bio-Rad, Hercules, CA). After transfer, membranes were blocked with 3% BSA in Odyssey Blocking Buffer (LI-COR, Lincoln, NE) for 1 hour at room temperature or overnight at 4 °C. Membranes were then incubated with primary antibodies overnight at 4 °C, washed 3 times for 10 minutes each with tris-buffered saline wash buffer with 0.1% Tween 20, pH 7.4 (TBS-T) and incubated with secondary antibodies for 1 hour at room temperature. Antibody specifications for primary antibodies used are summarized in Table 2.1. Membranes were then washed 3 more times for 10 minutes each in TBS-T before being scanned on an Odyssey CLx infrared imaging system using Odyssey software version 3.0 (LI-COR). Band density was analyzed using ImageJ version 1.47 software (National Institutes of Health, Bethesda, MD). Background correction was done using the software's inbuilt rolling ball method, setting the rolling ball size at half the resolution of the corresponding images. A rectangular box was defined with dimensions approximately equal to one third the width of each lane and the length tightly fitting the height of the band. Band densities were quantified by obtaining integrals of optical density profiles for each band (213–215).

Table 2.1: Antibody specifications for primary antibodies used in western blotting

Antigen	Host	Clonality	Dilution	Source
Beta-actin	rabbit	polyclonal	1:3000	Sigma-Aldrich (A5060)
Cleaved Caspase 3	rabbit	polyclonal	1:1000	Cell Signaling (9661)
Clusterin	goat	polyclonal	1:1000	Santa Cruz (sc-6419)
LC3B	rabbit	polyclonal	1:1000	Cell Signaling (2775)
p21	rabbit	monoclonal	1:200	Cell Signaling (2947)
p53	mouse	monoclonal	1:1000	EMD Millipore (OP03)
PARP	rabbit	monoclonal	1:1000	Cell Signaling (9532)
phospho-RB (807/811)	rabbit	polyclonal	1:1000	Cell Signaling (9308)
phospho-RB (780)	rabbit	polyclonal	1:1000	Cell Signaling (9307)
SR-BI	rabbit	monoclonal	1:1000	Abcam (ab52629)

HDL-cholesterol uptake assay

Uptake of HDL-derived cholesterol was approximated by cellular uptake of the fluorescent lipid 1,1′-dioctadecyl-3,3,3′,3′-tetramethylindocarbocyanine perchlorate (DiI, excitation max: 549 nm, emission max: 565 nm) from labelled HDL particles (DiI-HDL) using an assay adapted and modified from previously published methods (216–219). Cells were cultured and treated as described in sections 2.2 and 2.3. On the day of the assay, cells were washed twice with PBS prior to incubation in assay medium (RPMI 1640 + 5% CSS, 0.5% BSA) containing DiI-HDL (10 µg HDL protein per mL) for two hours at 37 °C. Cells were then washed twice with ice-cold PBS and harvested by trypsinization, followed by centrifugation at 400 x g for 5 minutes. Cells were then washed once with ice-cold PBS to remove trypsin and serum before being suspended in 500 µL of ice-cold PBS and immediately subjected to FACS analysis on a BD LSR II flow cytometer. 75 µL aliquots were taken from each sample, replicates were pooled together then pelleted by centrifugation, resuspended in RIPA buffer for lysate preparation and western blot analysis to confirm successful knockdown of SR-BI protein

expression as described in sections 2.4 and 2.5. A 488 nm laser line was used for excitation, while fluorescence was detected using the PE channel (excitation max: 496, 564 nm; emission: 578 nm). Debris was gated out based on forward (FSC) and side scatter characteristics according to standard gating protocols (220). Median fluorescent intensity data were analyzed using BD FACSDiva software (Beckman, Dickinson & Company). Untreated cells and cells treated for one hour with 10 µM of the SR-BI inhibitor BLT-1 were used as controls for normal cellular SR-BI activity and antagonized SR-BI activity, respectively. DiI uptake in the presence of 50-fold excess unlabeled HDL was assessed for all sample conditions to determine nonspecific uptake and this value was subtracted from total uptake (absence of unlabeled HDL) to determine uptake attributable to SR-BI protein. Representative histograms for figures were produced using Flow Jo software version 7.6.1 (Flow Jo Enterprise).

2.6 Cholesterol quantification

Cellular cholesterol content was assessed using the fluorogenic hydrogen peroxide (H_2O_2) probe, 10-acetyl-3,7-dihydroxyphenoxazine (Amplex Red) Cholesterol Assay (Life Technologies). Cells were cultured and treated as described in sections 2.2 and 2.3 and whole cell lysates (prior to clarification by centrifugation) were collected as detailed in section 2.4 and used for cholesterol quantification. Cell lysates were diluted 1:50 in serum-free RPMI 1640 media and the assay was performed according to manufacturer's instructions. The assay uses an enzyme-coupled reaction to detect cholesteryl esters and free cholesterol. First, cholesteryl esters are hydrolyzed by cholesterol esterase into cholesterol before oxidation by cholesterol oxidase, producing H_2O_2 which is reacted 1:1 with Amplex® Red reagent in the presence of horseradish peroxidase to produce the fluorescent resorufin (excitation 560-560 nm, emission 590 nm) which can be detected in a fluorescence microplate reader (221). The assay determines cholesterol

concentrations using a standard curve generated by serial dilution of provided cholesterol standards over the working range of 0 – 8 µg/mL.

2.7 Steroid analysis by liquid chromatography-mass spectrometry

Cellular testosterone and dihydrotestosterone (DHT) levels were quantified by tandem liquid chromatography-mass spectrometry (LC/MS) as described previously (211,222). Cells were cultured and treated by adapting the protocols described in sections 2.2 and 2.3 for use in 75 cm^2 cell culture flasks to obtain cell pellets of at least 100 mg mass. 250,000 cells were seeded into each of 5 flasks per treatment group. Cells were harvested in a pre-weighed 15 mL centrifugation tube by trypsinization followed by centrifugation at 500 x g for 5 minutes. Cells were washed once by centrifugation with ice-cold PBS then resuspended in 4.25 mL of PBS. 250 µL of this suspension was pelleted by centrifugation and resuspended in RIPA buffer for lysate preparation and western blot analysis to confirm knockdown of SR-BI protein expression as described in sections 2.4 and 2.5. The remaining suspension was pelleted by centrifugation, weighed on a scale to record cell pellet mass, and stored at -80 °C until analysis.

Internal standards (deuterated testosterone/DHT; C/D/N isotopes) were added to cell pellets and steroids were extracted with 60/40 hexane/ethyl acetate. Extracts were dried under vacuum and reconstituted in 50 mM hydroxylamine prior to analysis on a Waters Acquity UPLC Separations Module coupled to a Waters Quattro Premier XE Mass Spectrometer. Chromatographic separations were performed using a C18 column and an acetonitrile/water mobile phase gradient. MS data were collected in positive ionization multiple reaction monitoring mode. Data were processed with QuanLynx software (Waters, Mississauga, Ontario).

2.8 PSA quantification

PSA secreted into media was quantified using an electrochemiluminescent immunoassay on a Cobas e 411 analyzer (Roche Diagnostics, Indianapolis, IN). Cells were cultured and treated as described in sections 2.2 and 2.3 and media samples were collected in 1.5 mL microcentrifuge tubes and stored at -80 °C until analysis. Samples were diluted 1:1 with serum-free RPMI 1640 media and analyzed according to manufacturer's instructions. This assay is fully automated and validated for clinical use, determining PSA concentrations over the working range of 0 – 100 ng/mL (223).

2.9 Cell viability assay

Cell viability was determined using the CellTiter 96 AQ_{ueous} One Solution Cell Proliferation Assay (Promega, Madison, WI), performed according to manufacturer's instructions at 6 days post-transfection to confirm previous findings (208). This assay is a tetrazolium reduction assay that uses 3-(4,5-dimethylthiazol-2-yl)-5-(3-carboxymethoxyphenyl)-2- (4-sulfophenyl)-2H-tetrazolium (MTS) to generate a water-soluble, colored formazan product whose absorbance at 490 nm is taken to be directly proportional to the number of viable cells as reduction of MTS involves a reaction with NADH or NADPH, providing a measure of mitochondrial respiration (224).

2.10 Flow cytometry based cell cycle analysis

Cell cycle status was determined using the propidium iodide (PI) flow cytometric method (225–228). This method employs PI (excitation max: 315 nm, emission max: 617 nm) to stain and assess DNA content, providing a precise measure of the cell cycle profile of a given sample by quantifying the number of events vs. PI fluorescence staining intensity(226,228). Cells were cultured and treated as described in sections 2.2 and 2.3 before being subjected to this assay.

Supernatant was collected and set aside in 15 mL centrifuge tubes. Cells were washed twice with ice-cold PBS, harvested by trypsinization and pooled with corresponding supernatant samples in centrifuge tubes, followed by centrifugation at 400 x g for 5 minutes. Cells were then washed once with ice-cold PBS to remove trypsin and serum before being resuspended and fixed in ice-cold 70% ethanol. Samples were stored at -20 °C until analysis. On the day of analysis, samples were washed twice with ice-cold PBS by centrifugation before being resuspended in DNA staining buffer (2% FBS, 25 µg/mL PI, 0.1 mg/mL RNAse A, 0.1% Triton X-100, PBS) for one hour in the dark at room temperature. Immediately after staining, samples were subjected to fluorescence activated cell sorting (FACS) analysis on a Beckman-Dickinson (BD) LSR II flow cytometer (Beckman, Dickinson & Company, Mississauga, Ontario). A 488 nm laser line was used for excitation, while fluorescence was detected using the phycoerythrin (PE) channel (excitation max: 496, 564 nm; emission max: 578 nm). Debris was gated out as described in section 2.6. Data in the form of histograms representing event counts vs. PE area were obtained and analyzed using BD FACSDiva software (Beckman, Dickinson & Company). Interval gates were drawn to separate cell cycle phase fractions based on DNA content according to established methods (227). Representative histograms for figures were produced using Flow Jo software version 7.6.1 (Flow Jo Enterprise, Ashland, OR).

2.11 Bright field and fluorescence microscopy

Cell morphology was examined by immunocytochemistry following standard procedures. Cells were cultured on coverslips (Fisher) in 6-well plates and treated as described in sections 2.2 and 2.3 and allowed to grow until four days post-transfection. Bright field images of cells were obtained using an EVOS FL Cell Imaging System microscope (Advanced Microscopy Group, Life Technologies). Cells were then washed twice with PBS followed by fixation in 10%

buffered formalin (Fisher) for 15 minutes at 37 °C. Cells were then washed twice more with PBS and blocked in background sniper blocking reagent (Biocare Medical, Concord, CA) for 30 minutes at room temperature, followed by another three washes in PBS. Wheat germ agglutinin (WGA) labeling was used to highlight membranous cellular organelles using WGA from *Triticum vulgaris* conjugated to Alexa Fluor 647 (WGA-647, Life Technologies) diluted 1:100 (final concentration 10 μg/mL) in PBS. Cells were incubated for one hour at room temperature, protected from light. After three washing steps, coverslips were mounted and counterstained with VECTASHIELD antifade mounting medium with DAPI (Vector Laboratories, Burlington, ON) for 20 minutes at room temperature.

2.12 Detection of senescence-associated beta-galactosidase activity

Activity of senescence-associated beta-galactosidase (SA-βgal), a biomarker of senescent cells, was detected using 5-dodecanoylaminofluorescein di-β-D-galactopyranoside (C_{12}FDG, Invitrogen), a fluorogenic substrate for the SA-βgal enzyme (excitation max: 490 nm, emission max: 514 nm). The assay was adapted from previously published methods (229,230). Cells were cultured and treated as described in sections 2.2 and 2.3 and allowed to grow until four days post-transfection. On the day of the assay, cells were washed with PBS, treated with 100 μM chloroquine for two hours, then incubated with 33 μM C_{12}FDG for one hour at 37 °C, also in the presence of chloroquine. Cells were then harvested by trypsinization as described in section 2.6, re-suspended in 500 μL of ice-cold PBS and immediately subjected to FACS analysis on a BD LSR II flow cytometer. 75 μL aliquots were taken from each sample, replicates were pooled together then pelleted by centrifugation and resuspended in RIPA buffer for lysate preparation and western blot analysis to confirm successful knockdown of SR-BI protein expression as described in sections 2.4 and 2.5. A 488 nm laser line was used for excitation, while fluorescence

was detected using the fluorescein isothiocyanate (FITC) channel (excitation max: 494 nm, 519 nm). Debris was gated out based on forward and side scatter characteristics as described in section 2.6. Median fluorescent intensity data and forward scatter parameters were analyzed using BD FACSDiva software (Beckman, Dickinson & Company). Representative histograms for figures were produced using Flow Jo software version 7.6.1 (Flow Jo Enterprise).

2.13 Statistical Analyses

Statistical analyses on all data were performed using GraphPad Prism software version 6 (GraphPad, La Jolla, CA). Paired t-tests were used to determine differences between NC and SRBI-KD in matched data sets for SA-βgal and DiI-HDL uptake assays. Student's t-tests were used to determine differences between NC and SRBI-KD treated cells. Means of the data sets were considered to be statistically significantly different if $p < 0.05$.

Chapter 3: Results

3.1 Knockdown of SR-BI protein expression by C4-2 cells is suppressed by siRNA treatment

SR-BI protein levels were found to be increased in both CRPC cells (208) and in LNCaP-derived CRPC tumors (220) relative to their androgen-sensitive counterparts, suggesting a possible role in PCa disease progression to castration-resistance. To investigate the contribution of SR-BI to the castration-resistant phenotype, a siRNA protocol was developed by colleagues to knockdown its expression in the classical LNCaP cell line, and in a castration-resistant lineage-derived C4-2 cell line. They assessed protein levels at 1, 3, and 6 days post-transfection and reported a greater than 80% suppression of SR-B protein expression with their siRNA method (208).

In order to confirm previous findings and adapt the model for study under more relevant steroid-deprived conditions, C4-2 cells were maintained in low-serum (1% FBS) conditions and treated with either control siRNA (NC) or siRNA targeting SR-BI (SRBI-KD) as described in sections 2.2 and 2.3 to generate cell lysate samples which were then subjected to western blot analysis and subsequently analyzed by densitometry as described in section 2.4 to assess the extent of SR-BI silencing. Optical density values for SR-BI were normalized to those obtained for β-actin which was used as a loading control. SR-BI protein expression was significantly reduced at various time points by siRNA treatment, and the extent of knockdown increased over time and suppression was maintained for at least 6 days (Figure 3.1). At 1 day post-transfection, SR-BI protein levels were reduced by approximately 37% in SRBI-KD cells relative to NC (Figure 3.1A). At 3 days post-transfection, approximately 71% reduction was achieved (Figure 3.1B), while at 6-days post transfection, approximately 89% reduction was achieved (Figure

3.1C). These results were similar to those seen previously; Twiddy *et al.* reported greater than 80% and greater than 90% reduction in SR-BI protein levels at 3 and 6 days post-transfection in cells cultured in low FBS conditions (1% FBS), respectively (208).

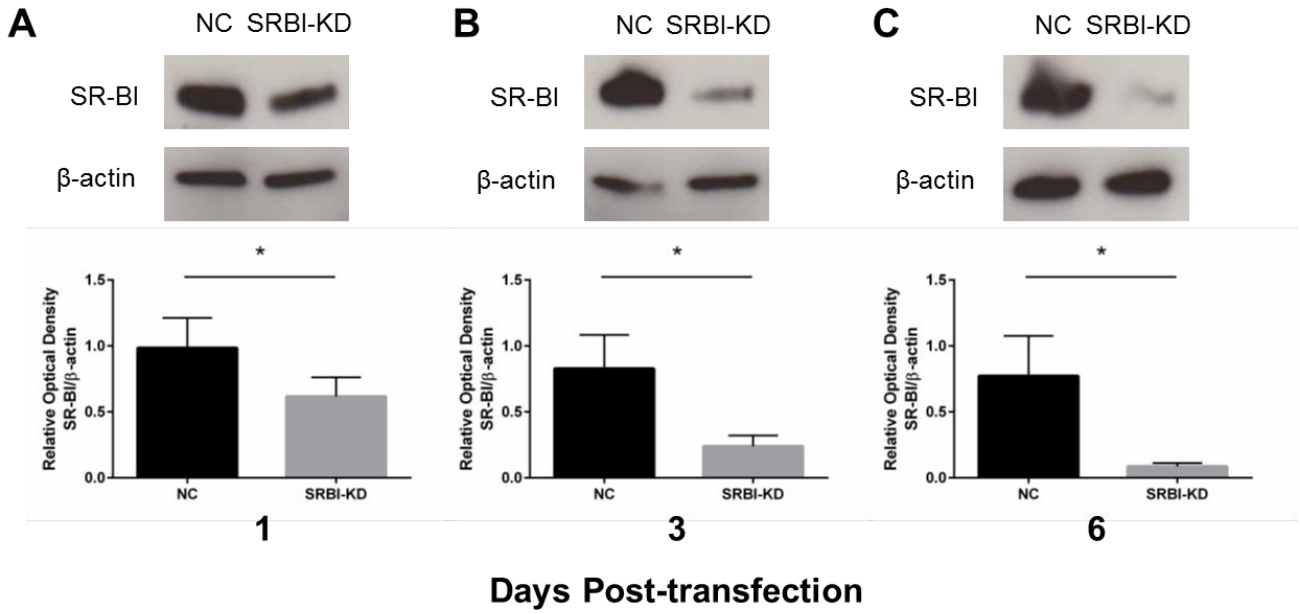

Figure 3.1: SR-BI protein expression is suppressed by siRNA treatment.
C4-2 cells were cultured in 1% FBS for up to 6 days following transfection with either control siRNA (NC) or siRNA targeting SR-BI (SRBI-KD) and whole cell lysates were collected for western blots as described in sections 2.4 and 2.5. In all blots, SR-BI was probed to assess siRNA silencing while β-actin was used as a loading control. Densitometry analysis was completed using ImageJ software as described in section 2.5. Representative western blots and histograms for cells collected at (**A**) 1, (**B**) 3, and (**C**) 6 days post-transfection. Columns represent mean relative optical densities obtained for SR-BI normalized to β-actin from four independent experiments ± SEM, *$p < 0.05$ by student's t-test.

Having validated the previous model, we sought to determine transfection efficiency at time points not reported by Twiddy *et al.* In order to make the method more amenable to shorter experiments, we assessed SR-BI protein levels at 2 and 4 days post-transfection. The results further demonstrated that beginning 1 day post-transfection, SR-BI protein levels steadily decline in the timeline that we assessed them. At 2 days post-transfection, SR-BI protein expression was suppressed by approximately 57% in SRBI-KD cells relative to NC (Figure 3.2A). This demonstrates a steady decline from ~37% suppression 1 day after transfection and ~71%

suppression 3 days after transfection. By 4 days post-transfection, approximately 86% SR-BI protein expression was achieved in SRBI-KD cells relative to NC (Figure 3.2B). Based on these results, maximal knockdown of SR-BI is achieved at 4 days post-transfection, making this a suitable time point for further study. These results confirm the appropriateness of using siRNA-treated C4-2 cells to study the contribution of SR-BI to CRPC cell survival in androgen-deplete conditions. Furthermore, these results confirm that siRNA treatment against SR-BI exhibits persistent suppression of SR-BI protein levels for up to 6 days in C4-2 cells.

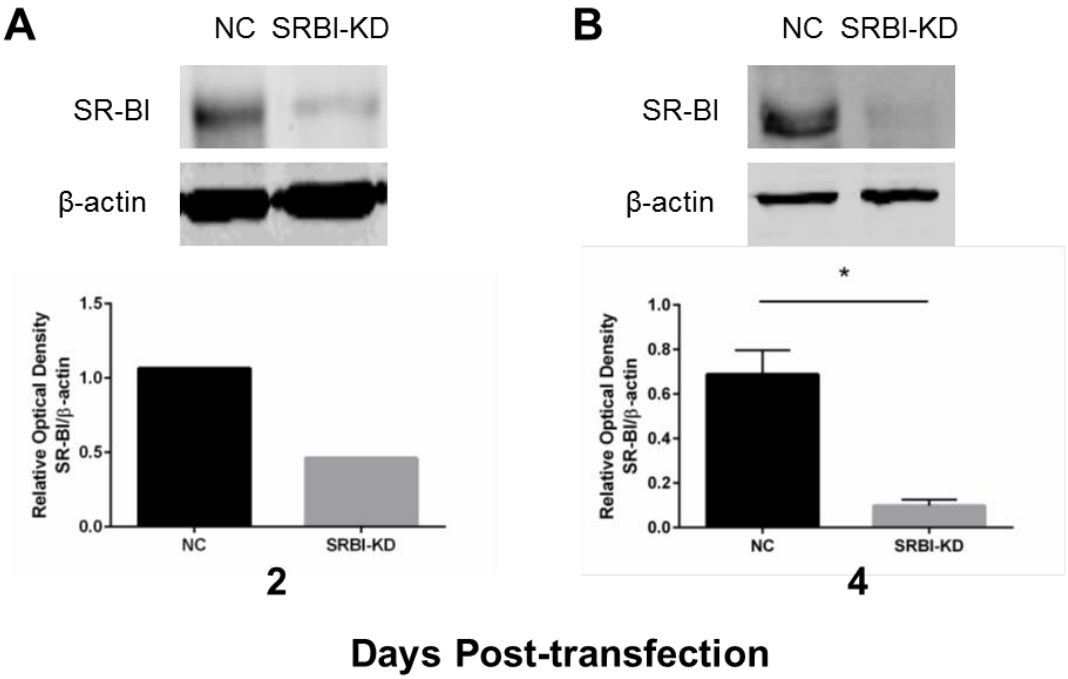

Figure 3.2: SR-BI protein expression is suppressed by siRNA treatment.
C4-2 cells were cultured in CSS for up to 4 days following transfection with either control siRNA (NC) or siRNA targeting SR-BI (SRBI-KD) and whole cell lysates were collected for western blots as described in sections 2.4 and 2.5. In all blots, SR-BI was probed to assess siRNA silencing while β-actin was used as a loading control. Densitometry analysis was completed using ImageJ software as described in section 2.5. (**A**) Representative western blots and histograms for cells collected 2 days post-transfection. Columns represent mean relative optical densities obtained for SR-BI normalized to β-actin from two independent experiments. (**B**) Representative western blots and histograms for cells collected 4 days post-transfection. Columns represent mean relative optical densities obtained for SR-BI normalized to β-actin from four independent experiments ± SEM, *$p < 0.05$ by student's t-test.

3.2 HDL-lipid uptake by C4-2 CRPC cells is impaired by knockdown and small molecule inhibition of SR-BI

In order to maintain AR signaling in castrate conditions, C4-2 cells are thought to rely in part on their ability to produce androgens from the precursor cholesterol. Lipoproteins, in particular HDLs, are an essential source of cholesterol for steroidogenic tissues (192,231–233). Having demonstrated a substantial and persistent suppression of SR-BI protein expression using siRNA constructs, it was imperative to determine the physiologic consequence of targeting a key cholesterol uptake mechanism. Additionally, the impact of siRNA-mediated SR-BI suppression on cholesterol uptake was compared to pharmacologic inhibition using the small molecule inhibitor of SR-BI, BLT-1 (194). Given comparable uptake characteristics between DiI and radiolabeled cholesteryl esters associated with HDL (194,216,217), uptake of DiI from DiI-HDL particles was used to assess whether knockdown of SR-BI effectively reduced cellular uptake of lipids from HDL lipoproteins.

C4-2 cells maintained in androgen-deprived culture for 4 days post-transfection were incubated with DiI-HDL and then analyzed by FACS as described in section 2.6. Knockdown of SR-BI protein expression was confirmed by western blotting analysis as described in section 2.5 using aliquots of samples subjected to FACS analysis (Figure 3.3A). For comparison, untransfected cells were either left untreated (NT) or treated with BLT and subjected to the same analysis. Knockdown of SR-BI resulted in a mean reduction in DiI uptake of 22.5% compared to control transfected cells (Figure 3.3B) while treatment with BLT-1 reduced DiI uptake by 25.6% relative to the NT control (Figure 3.3C).

As cholesterol plays a variety of roles in cellular physiology, numerous control mechanisms exist to regulate cellular cholesterol homeostasis (154,164,234). To assess whether

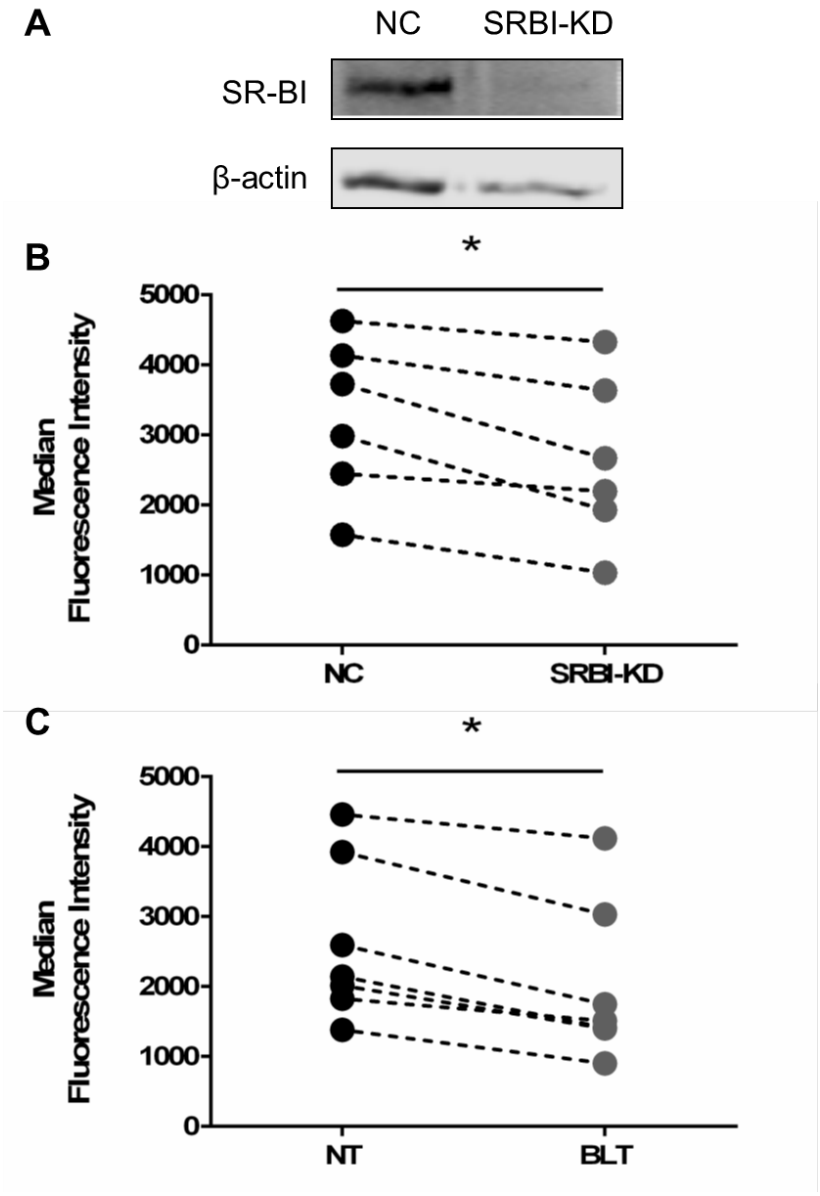

Figure 3.3: HDL-lipid uptake is impaired by knockdown and small molecule inhibition of SR-BI.
HDL-lipid uptake was determined by incubating cells with DiI-HDL (10 µg protein/mL) for 2 hours followed by FACS analysis as described in section 2.6. (**A**) Whole cell lysates were prepared and subjected to western blot analysis as described in sections 2.4 and 2.5. SR-BI was probed to assess siRNA silencing while β-actin was used as a loading control. (**B**) C4-2 cells were cultured in CSS for 4 days following transfection with either control siRNA (NC, black dots) or siRNA targeting SR-BI (SRBI-KD, grey dots) prior to assay. (**C**) Untransfected C4-2 cells were preincubated with (BLT, grey dots) or without (NT, black dots) the SR-BI inhibitor BLT-1 (10 µM) for 1 h prior to assay. SR-BI specific DiI uptake was determined by subtracting nonspecific uptake from total uptake as described in section 2.6. Data points represent means of median fluorescent intensities from each of six (**B**) and seven (**C**) independent experiments, dashed lines connect data points from each experiment, respectively, *$p < 0.05$ by paired t-test for respective matched data sets.

silencing SR-BI impacted total cellular cholesterol content, cholesterol in whole cell lysates was measured using a fluorometric assay as described in section 2.7 (Figure 3.4). Consistent with previous findings (208), cholesterol levels were indistinguishable when SR-BI was silenced and when it was not (32.1 and 30.3 µg cholesterol per µg protein respectively). Thus, while antagonizing SR-BI can effectively reduce the pool of cholesterol acquired from HDL particles, this does not change total cellular cholesterol levels.

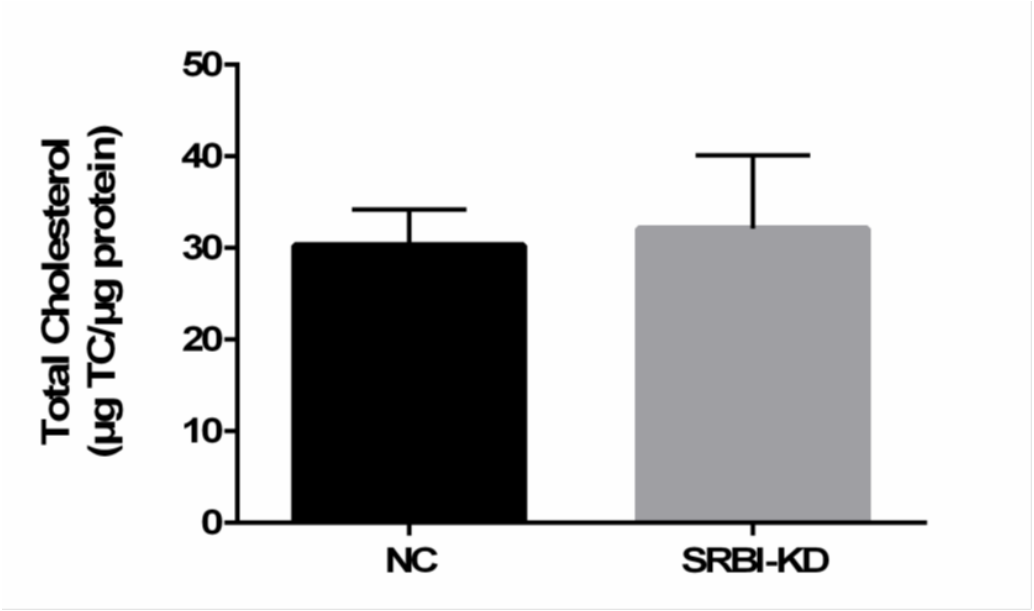

Figure 3.4: Total cellular cholesterol concentrations remain unchanged despite knockdown of SR-BI.
C4-2 cells were cultured in 1% FBS for 6 days following transfection with either control siRNA (NC) or siRNA targeting SR-BI (SRBI-KD). Total cellular cholesterol of whole cell lysates was quantified using a fluorometric assay as described in section 2.7. Columns represent mean total cellular cholesterol (µg) normalized to protein content of corresponding cell lysates (µg) from four independent experiments ± SEM, $p > 0.05$ by Student's t-test.

3.3 Androgen signaling in C4-2 cells is suppressed by knockdown of SR-BI

If AR transcriptional activity of C4-2 cells is sustained by *de novo* steroidogenesis (30,43), their ability to synthesize androgens would depend on a metabolically available pool of cholesterol as a synthetic precursor. This pool of cholesterol can be provided by synthesis from the precursor acetate, scavenged from membrane-sequestered pools, or by uptake from

extracellular sources (164). Our group has previously documented that pharmacologic inhibition of the rate-limiting step in cholesterol biosynthesis, the conversion of HMG-CoA to mevalonic acid, by the HMGCR inhibitor simvastatin, suppresses expression of the AR target gene, PSA, and cellular androgen levels (211,235). Furthermore, targeting uptake from extracellular sources by siRNA-mediated suppression of SR-BI also reduces PSA secretion (208). In order to determine whether the comparable suppression of HDL uptake by SR-BI siRNA treatment and BLT treatment impacted AR activity, we quantified cellular levels of the androgens testosterone and DHT in C4-2 cell lysates harvested from cells maintained in RPMI 1640 medium with 1% FBS for 6 days post-transfection. Using an LC/MS method described in section 2.8, steroid concentrations were normalized to the mass of the corresponding cell pellets to control for differences due to cell number. Knockdown of SR-BI, confirmed by western blotting as described in section 2.4 (Figure 3.5A), resulted in a 2-fold reduction in levels of both androgens relative to control. Testosterone concentration (Figure 3.5B) in the SRBI-KD group was 0.20 ng/mL/mg cell pellet compared to 0.43 ng/mL/mg cell pellet for NC. Similarly, DHT concentration (Figure 3.5C) was also lower in the SRBI-KD group compared to NC (0.41 and 0.94 ng/mL/mg cell pellet respectively). Due to the high cost of transfection reagents, this experiment was conducted only once. The LC/MS assay in use was first developed to measure androgen concentrations in animal tissues (211,222). While not a limiting factors in animal studies, the requirement for a minimum sample mass of 100 mg required the use of cost-inhibiting amounts of transfection reagent to produce each sample. Though the lack of replicates is indeed a limitation of these findings, it should be noted that the androgen concentrations reported reflect the mean concentrations of many millions of cells; a rough approximation indicated that upwards of 35 million cells would be required to produce a single cell pellet of

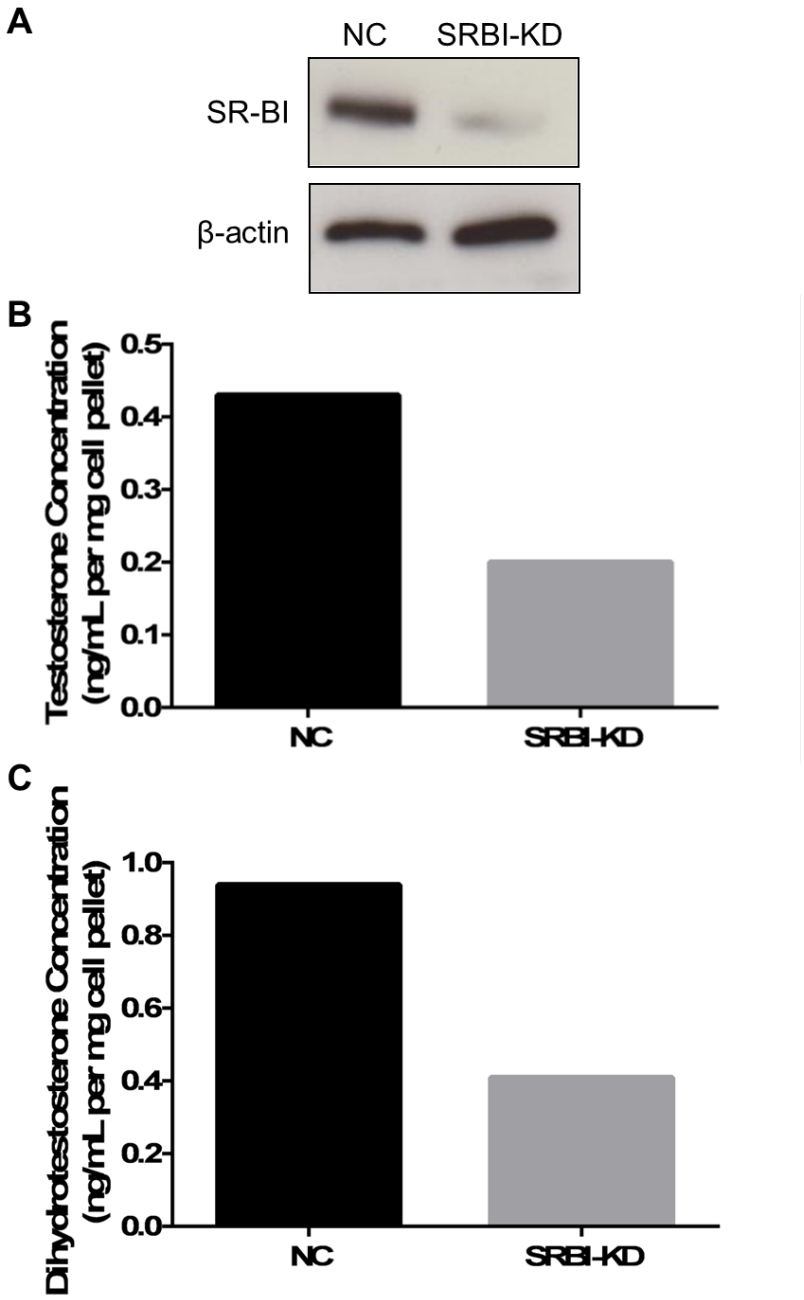

Figure 3.5: Androgen levels are suppressed by knockdown of SR-BI.
C4-2 cells were cultured in 1% FBS for 6 days following transfection with either control siRNA (NC) or siRNA targeting SR-BI (SRBI-KD). (**A**) Whole cell lysates were prepared and subjected to western blot analysis as described in sections 2.4 and 2.5. SR-BI was probed to assess siRNA silencing while β-actin was used as a loading control. (**B&C**) Androgen concentrations in cell pellets were measured by an LC/MS method as described in section 2.8. Columns represent concentration of testosterone (**B**) or dihydrotestosterone (**C**) in cell lysates (ng/mL) normalized to protein content (mg) from one experiment.

adequate mass for use with the LC/MS assay. Hence, the results presented herein indicate that antagonizing SR-BI can effectively reduce cellular androgen levels.

PSA secreted into media from C4-2 cells was quantified to assess the downstream consequences of reduced androgen concentrations on AR activation. C4-2 cells were cultured and treated as described in sections 2.2 and 2.3 and PSA content of media was measured using an electrochemiluminescent method as described in section 2.9. PSA concentrations were then normalized to protein content of corresponding cell lysates to account for differences due to cell number. Consistent with previous work (208), secreted PSA was significantly reduced in SRBI-KD (20.9 ng/mL/µg protein) relative to NC (34.5 ng/mL/µg protein) cells by 39.3% (Figure 3.6). These results suggest that decreased cellular androgen levels associated with knockdown of SR-BI may result in reduced AR activation as suggested by reduced levels of secreted PSA.

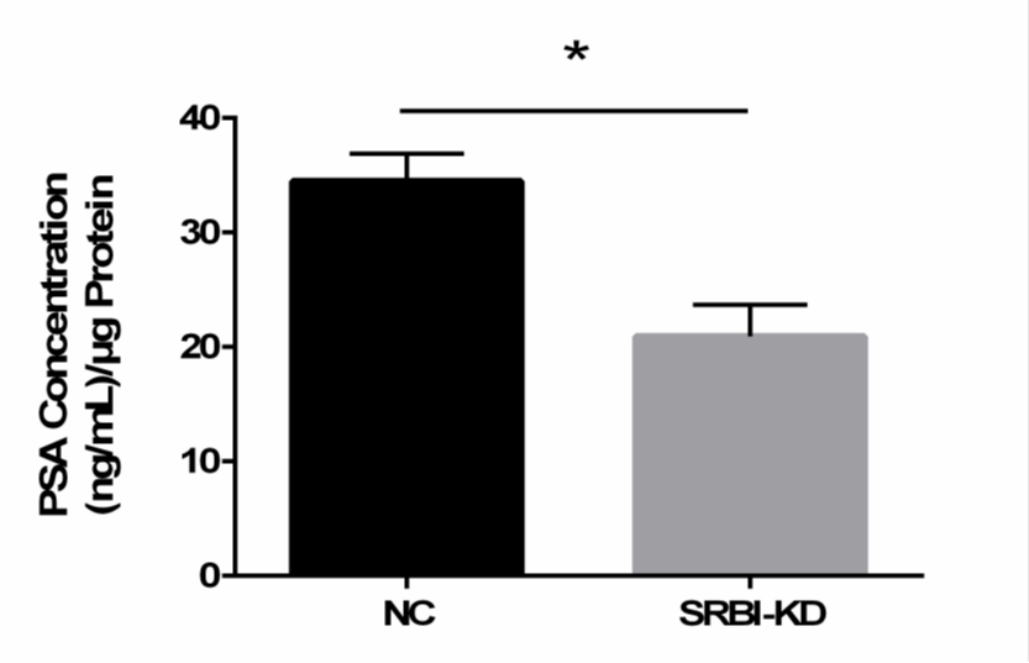

Figure 3.6: Secreted PSA is reduced by knockdown of SR-BI.
C4 -2 cells were cultured in 1% FBS for 6 days following transfection with either control siRNA (NC) or siRNA targeting SR-BI (SRBI-KD). Concentrations of PSA secreted into media were measured on a Cobas e 411 analyzer by an electrochemiluminescent method as described in section 2.9. Columns represent mean concentrations of PSA (ng/mL) in media samples normalized to protein content of corresponding cell lysates (µg) from four independent experiments ± SEM, *$p < 0.05$ by Student's t-test.

3.4 Knockdown of SR-BI reduces viability of C4-2 cells by inducing cell cycle arrest

Previous work has shown reduced "viability" of C4-2 cells cultured in low FBS conditions after knockdown of SR-BI (208). Twiddy *et al.* reported a 22% reduction in viability using the MTS assay. In order to confirm these findings, cell viability was assessed in C4-2 cells 6 days following transfection using an MTS assay as described in section 2.10. Absorbance measurements at 490 nm were taken to be proportionate to the number of viable cells; treatment of C4-2 cells with siRNA targeting SR-BI reduced mean absorbance by approximately 21% relative to control transfected cells (Figure 3.7) indicating reduced cell proliferation and confirming previous findings.

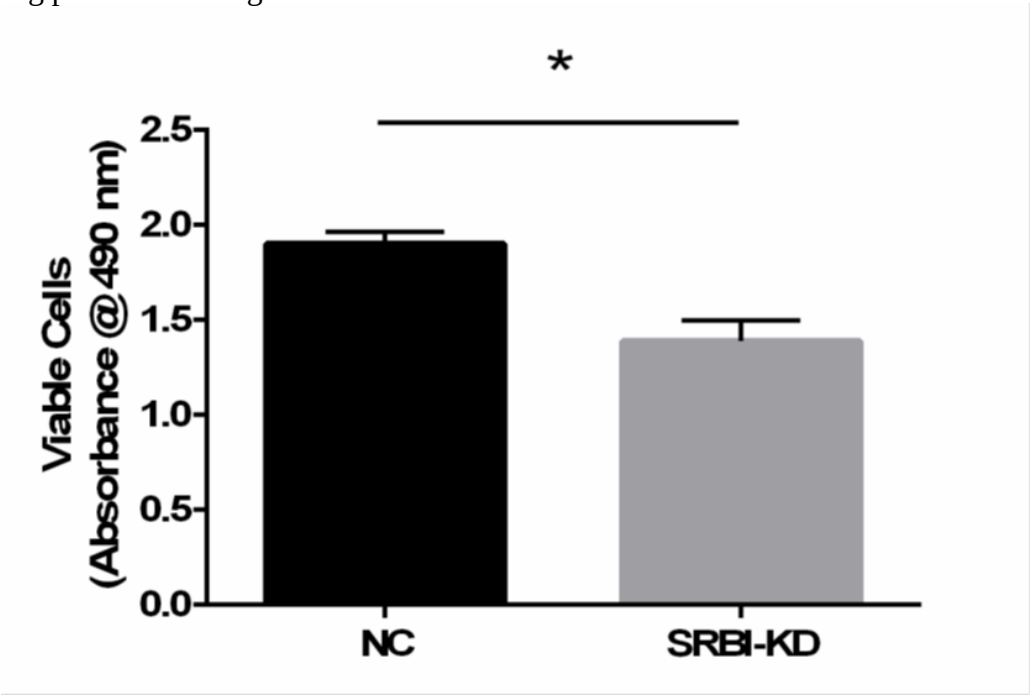

Figure 3.7: Knockdown of SR-BI reduces viability of C4-2 cells.
C4-2 cells were cultured in 1% FBS for 6 days following transfection with either control siRNA (NC) or siRNA targeting SR-BI (SRBI-KD). Cell viability was determined using the MTS assay as described in section 2.10. Columns represent mean absorbance measured at 490 nm from three independent experiments ± SEM, *$p < 0.05$ by student's t-test.

While this provides evidence that antagonizing SR-BI can reduce cell proliferation, an underlying mechanism responsible for these results remains to be uncovered. It is well

demonstrated that androgen deprivation results in cell cycle arrest and apoptosis (106,107); therefore, the cell cycle profiles of C4-2 cells were assessed following transfection. Using a propidium iodide DNA staining method followed by FACS analysis as described in section 2.11, cell cycle profiles for C4-2 cells cultured and treated as described in sections 2.2 and 2.3 were analyzed. As SR-BI siRNA treatment of C4-2 cells was demonstrated to maximally suppress SR-BI protein expression by 4 days post-transfection, and reduced viability was at 6 days post-transfection, cell cycle profiles were assessed at 2 and 4 days post-transfection with the aim of detecting earlier signs of reduced viability. Representative histograms (Figure 3.8A, top) illustrate cell cycle arrest in SRBI-KD cells relative to NC at 2 days post-transfection, a larger G_0-G1 peak (~50K PI-intensity) coupled with a noticeable suppression of the S-phase (~50K < S-phase < ~100K) and G_2M (~100K) populations in SRBI-KD cells relative to NC are indicative of an arrest at the G_1-S checkpoint. This is confirmed by quantification of PI-area as cell cycle phase fractions (Figure 3.8B). A greater proportion of SRBI-KD cells accumulated in the G_0-G_1 phase compared to NC (70.2% SRBI-KD vs. 59.9% NC) while fewer SRBI-KD cells transitioned through S-phase (1.43% SRBI-KD vs. 7.6% NC) to G_2M (19.8% SRBI-KD vs. 23.7% NC). When analyzed as a ratio of cells with 2N DNA content (G_0-G_1 population) to cells with > 2N DNA (S+G_2M populations), growth arrest is clearly demonstrated in SRBI-KD cells compared to NC (3.3 SRBI-KD vs. 1.9 NC, $p < 0.05$). A comparison of the Sub G_0 fraction indicated that there was no apparent increase in apoptotic cell death in the SRBI-KD group compared to NC (9.7% SRBI-KD vs. 8.5% NC).

Representative histograms (Figure 3.8A, bottom) of C4-2 cells 4 days following transfection showed continued suppression of the S-phase and G_2M populations in the SRBI-KD group compared to NC, based on the smaller peaks, while the G_0-G_1 accumulation seen at 2 days

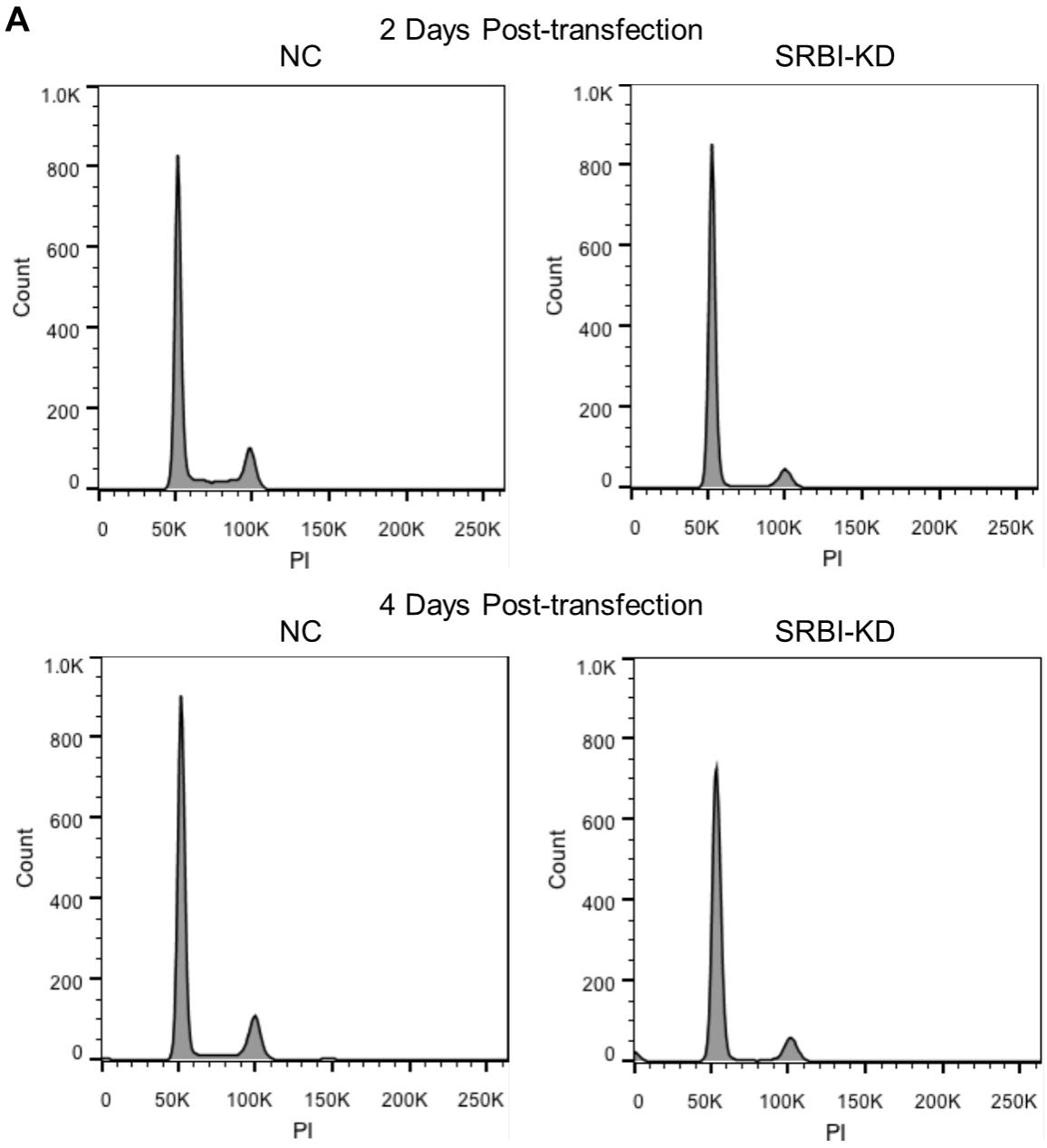
A
2 Days Post-transfection
NC
SRBI-KD
1.0K
800
600
400
200
0
Count
0
50K
100K
150K
200K
250K
PI
4 Days Post-transfection
NC
SRBI-KD

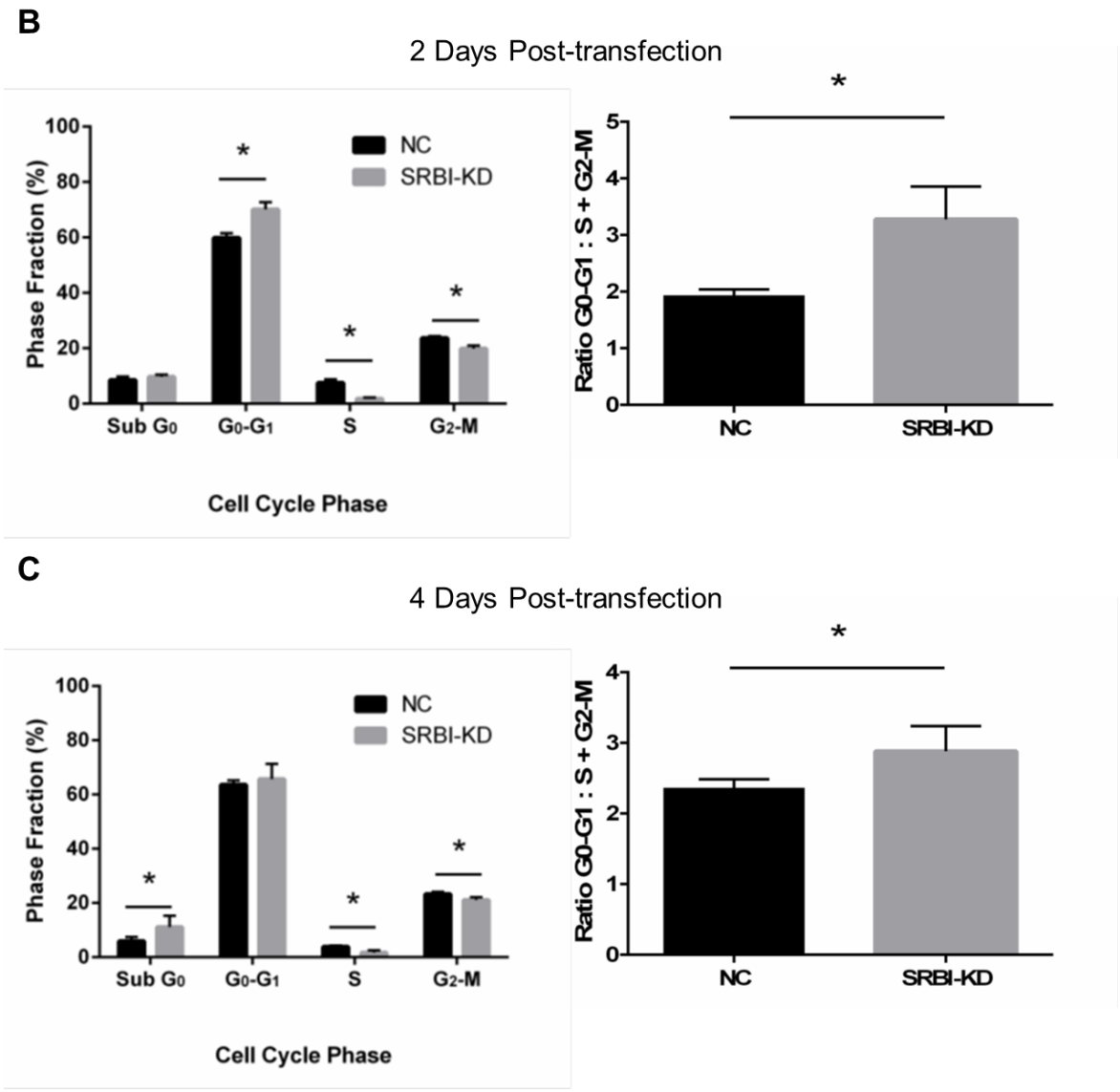

Figure 3.8: Knockdown of SR-BI induces cell cycle arrest.
C4-2 cells were cultured in CSS for up to 4 days following transfection with either control siRNA (NC) or siRNA targeting SR-BI (SRBI-KD) and subjected to flow cytometry based cell cycle analysis as described in section 2.11. (**A**) Representative historgrams of propidium iodide (PI) stained DNA as event counts vs. PI area in NC and SRBI-KD treated cells, 2 and 4 days post-transfection. (**B&C**) Cell cycle phase fractions (left) were calculated based on PI fluorescence intensities of corresponding histogram peaks. Columns represent mean fraction (%) of cells in indicated cell cycle phase from six independent experiments ± SEM, *$p < 0.05$ by student's t-test. The ratio of cells with 2N DNA content to cells with > 2N DNA content (G_0-G_1 : S + G_2M) was calculated as an index of cell cycle arrest. Columns represent mean ratios calculated 2 (**B**) and 4 (**C**) days post-transfection from six independent experiments ± SEM, *$p < 0.05$ by student's t-test.

post-transfection in the SRBI-KD group decreased to the point of being indistinguishable from that of the NC G_0-G_1 population. Similarly, when examined as cell phase fractions (Figure 3.8C), SRBI-KD cells exhibit reduced capacity to transition into S-phase (1.7% SRBI-KD vs. 3.9% NC) to G_2M (21.1% SRBI-KD vs. 23.3% NC). Meanwhile, the respective G_0-G_1 populations were indistinguishable (65.7% SRBI-KD vs. 63.6% NC). Mitotic arrest was still apparent in SRBI-KD cells compared to NC as determined by the index of arrest (2.9 SRBI-KD vs. 2.4 NC). A comparison of the Sub-G_0 phase fraction indicated an increase in apoptotic cell death in SRBI-KD treated cells compared to NC (11.1% vs. 5.9%). The results of cell cycle analysis are indicative of a G_1-S arrest soon after knockdown of SR-BI, and that cells unable to progress through the cell cycle begin to undergo apoptotic cell death.

Having demonstrated evidence of growth arrest underlying reduced proliferation previously seen by MTS assay, we sought to further elucidate the pathways responsible for these results. Cell cycle arrest can be accomplished by activation of tumor suppressor pathways. The p53 tumor suppressor is well established as a mediator of growth arrest and apoptosis (236); cells of the LNCaP lineage express wild-type p53 (209), making this a potential mechanism responsible for the observed growth arrest. Protein levels of p53 can rise in response to numerous stressors and its accumulation is linked to arrest at G_1 and G_2 as well as apoptosis, depending on the circumstances. It can execute its function by inducing expression of the cyclin-dependent kinase inhibitor, p21 (236). Another tumor suppressor expressed in LNCaP and its derivatives is pRB (209). pRB is a nuclear phosphoprotein regulated by cycle-dependent changes in its phosphorylation status; its activity is inhibited by phosphorylation. It regulates progression through G_1-S thereby restricting proliferation when activated (237). In response to various stress signals, protein levels of the tumor suppressor p16 increase, and p16 inhibits the cyclin-

dependent kinases that phosphorylate and inhibit pRB (238). Hence, p53, p21, pRB, and p16 all serve as markers for cell cycle arrest.

In order to determine which, if any, of the aforementioned tumor suppressor pathways might be responsible for the growth arrest evidenced by cell cycle analysis, C4-2 cells were cultured and treated as described in sections 2.2 and 2.3 and lysates were prepared and subjected to western blotting as described in sections 2.4 and 2.5. All blots were probed for SR-BI to ensure transfection efficiency while β-actin was used as a loading control. Additionally, blots were probed for p53, p21, and pRB. SRBI-KD cells exhibited an accumulation of p53 and p21 relative to NC cells (Figure 3.8B). Furthermore, SRBI-KD was correlated with pRB hypophosphorylation at two distinct phosphorylation sites, serine 780 and serine 807/ 811 (Figure 3.8C). Collectively, these results indicate that both p53 and pRB tumor suppressor pathways are activated in response to knockdown of SR-BI, and that activation of these pathways leads to cell cycle arrest.

An increase in the Sub-G_0 population coupled with an accumulation of p53 indicate that knocking down SR-BI in C4-2 cells cultured in androgen-deprived conditions may result in apoptosis, mediated by p53. To determine if the increase in cell death at 4 days post-transfection (Figure 3.8C) was due to apoptosis, we blotted for evidence of PARP cleavage and caspase-3 cleavage. The PI3K inhibitor LY294002 was used as a positive control for apoptosis. Western blots for PARP and caspase 3 cleavage revealed no difference between SRBI-KD and NC cells (Figure 3.9D). Neither group showed any sign of cleavage products, while the LY treated cells showed a clear indication of both PARP and caspase-3 cleavage. While these results suggest a lack of evidence for apoptosis, it cannot be ruled out that apoptosis is indeed occurring but we failed to capture this due to limits of assay detection. Further study is required; however, these

results suggest that the decreased proliferation seen previously in SR-BI silenced C4-2 cells is due to induction of growth arrest followed by a delayed stochastic rate of cells undergoing apoptosis.

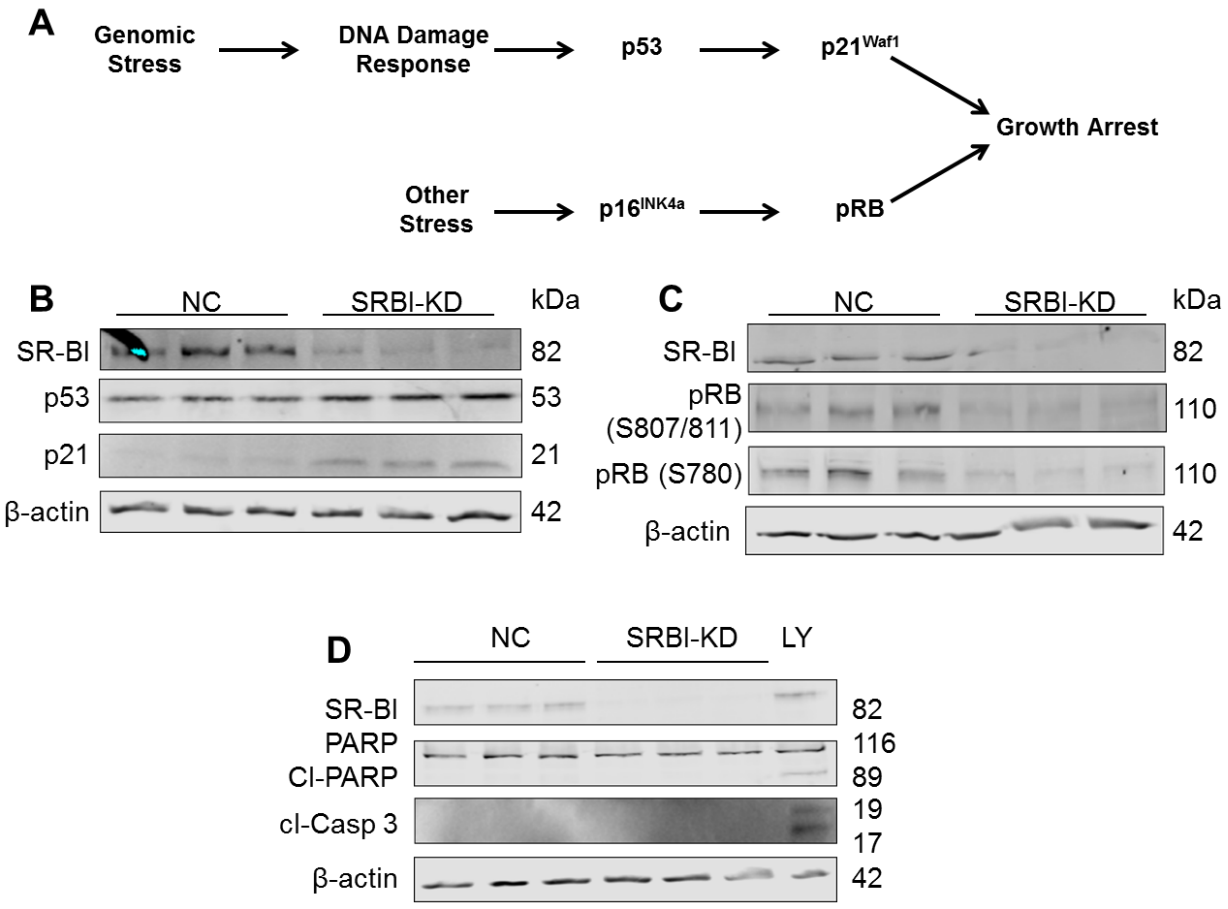

Figure 3.9: Knockdown of SR-BI induced growth arrest is correlated with activation of p53 and pRB tumor suppressor pathways.
C4-2 cells were cultured in CSS for 4 days following transfection with either control siRNA (NC) or siRNA targeting SR-BI (SRBI-KD). Cell lysates were prepared and subjected to western blot analysis as described in sections 2.4 and 2.5. In all blots, SR-BI was probed to assess siRNA silencing while β-actin was used as a loading control. (**A**) Regulation of senescent growth arrest. Cell stress causing genomic damage activates the DNA damage response thereby activating the p53 tumor suppressor which causes growth arrest by inducing the cell cycle inhibitor p21. Other forms of stress induce p16 expression which activates the pRB tumor suppressor which silences proliferative genes leading to growth arrest. (**B**) Western blot analysis of p53-p21 tumor suppressor pathway. Blot shown is representative of 2 independent experiments. (**C**) Western blot analysis of p16-pRB tumor suppressor pathway. Blot shown is representative of 2 independent experiments. (**D**) Western blot analysis of apoptotic markers, cleaved PARP and caspase 3. Untransfected C4-2 cells treated overnight with the phosphatidylinositol 3 kinase inhibitor, LY 294002 (50 μM, LY) were used as a positive control. Blot shown is representative of 2 independent experiments.

3.5 Knockdown of SR-BI induces adaptive stress responses in C4-2 cells

Cancer cells evolve and adapt in response to the stresses of aberrant growth, altered microenvironmental cues, and therapeutic intervention by numerous mechanisms (30,98). Protective stress responses can include autophagy and the upregulation of chaperones. Autophagy is a process by which cells maintain the integrity of cellular components such as proteins and whole organelles. While it occurs at a basal rate in all cells, autophagic flux can be induced in response to various cancer therapies and starvation (98,100,102). During stress, chaperones such as CLU maintain appropriate protein conformations, prevent protein aggregation, and protect cells from apoptosis while promoting survival. Furthermore, CLU has been shown to assist lipidation of LC3-I to LC3-II, thereby promoting autophagic flux by enhancing stability of autolysosomes (98). The result of CLU upregulation and enhanced autophagy activity is resistance to various treatments, including ADT (122–124). As targeting cholesterol homeostasis appears to reduce AR activation (208,211,235), it is possible that in response to loss of SR-BI, CRPC cells activate protective stress responses to survive androgen depletion.

To determine if knocking down SR-BI resulted in adaptive stress responses, C4-2 cells were cultured and treated as described in sections 2.2 and 2.3 and lysates were prepared and subjected to western blotting as described in sections 2.4 and 2.5. All blots were probed for SR-BI to ensure transfection efficiency while β-actin was used as a loading control. Additionally, blots were probed for LC3-I and LC3-II to determine if autophagy activity was enhanced in response to SR-BI suppression. Autophagy activity was determined in the presence of chloroquine in order to inhibit LC3-II degradation by the autolysosome (119). Treatment of cells with the proteasome inhibitor MG132 was used as a positive control for autophagy. LC3-II

protein levels were increased when SR-BI protein expression was suppressed (Figure 3.10A). While NC cells produced LC3-II, the amount was noticeably higher in SRBI-KD cells, indicating upregulated autophagy activity. Next, to evaluate whether enhanced autophagy activity was indicative of a broader stress response, blots were probed for CLU. SR-BI knockdown resulted in increased protein levels of the 70 kDa precursor CLU, as well as a marked increase in the 40 kDa mature CLU, relative to NC. Together, these results indicate that knocking down SR-BI induces cytoprotective stress responses characterized by enhanced autophagic flux and induction of CLU and present evidence of a link between SR-BI silencing-mediated growth arrest and induction of an adaptive stress response.

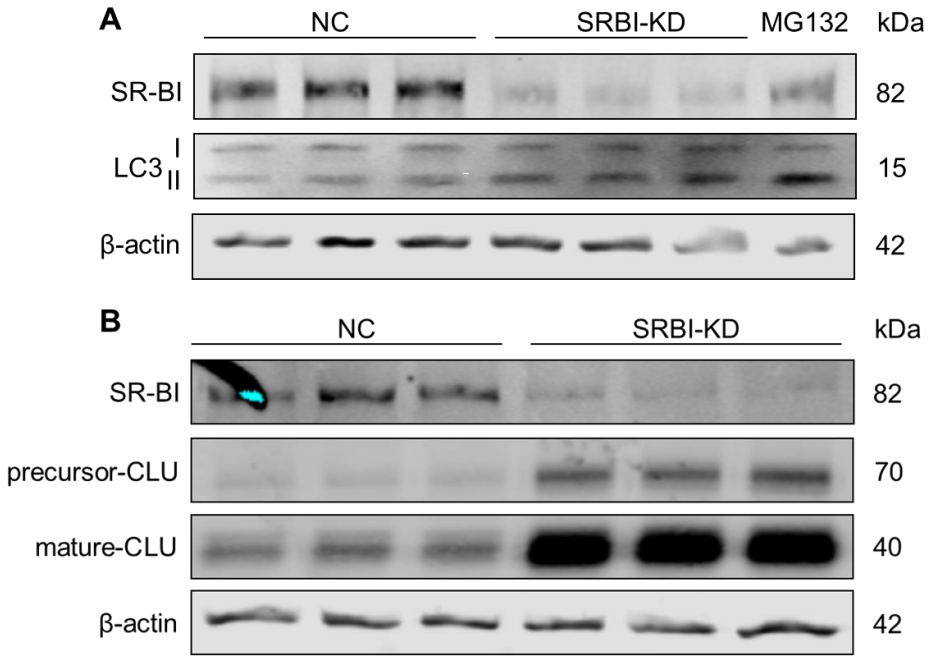

Figure 3.10: Knockdown of SR-BI induces autophagy activity and stimulates CLU expression.
C4-2 cells were cultured in CSS for 4 days following transfection with either control siRNA (NC) or siRNA targeting SR-BI (SRBI-KD) and whole cell lysates were collected for western blots as described in sections 2.4 and 2.5. In all blots, SR-BI was probed to assess siRNA silencing while β-actin was used as a loading control. (**A**) Cells were treated overnight with chloroquine (10 μM) prior to sample collection. Untransfected C4-2 cells treated overnight with chloroquine (10 μM) and the proteasome inhibitor MG132 (10 μM) was used as a positive control. Autophagy activity was determined by probing for LC3-I & LC3-II. Blot shown is representative of 4 independent experiments. (**B**) Cell stress response was determined by probing for CLU. The 70 kDa CLU bands represent the full, unprocessed form of the protein while the 40 kDa bands represent the mature form, post-processing. Blot shown is representative of 3 independent experiments.

3.6 Silencing SR-BI expression is associated with the emergence of senescent features

Anti-cancer treatments cause immense cell stress, evoking an array of cellular responses, including mitotic arrest and autophagy (102). Cell cycle arrest, mediated by elevated p53 expression and induction of pRB hypophosphorylation, is also a feature of senescence (125). While senescence has long been associated with ageing and age-related illness, more recently, it has been described as a tumor suppressor mechanism (238). Along with growth arrest, other common markers of senescence include drastic morphological transformation and increased SA-βgal activity (125). Senescent cells may increase their size more than 2-fold, and appear quite flat, relative to actively proliferating cells (132). Therefore, C4-2 cells cultured in 5% CSS and treated as described in sections 2.2 and 2.3 were examined for evidence of a senescent phenotype as described in section 2.13. Cell morphology was assessed by bright field microscopy and small molecule fluorescence staining. Furthermore, cell size changes were evaluated while simultaneously determining changes in SA-βgal by FACS analysis. Cells were incubated with the fluorogenic SA-βgal substrate, C_{12}FDG. Fluorescence intensity was measured as an estimate of SA-βgal enzyme activity and FSC parameters were collected as an indicator of cell size changes. Western blot analysis was conducted as described in section 2.5 to confirm efficiency of SR-BI targeted siRNA treatment (Figure 3.11A). Observationally, microscopy images (Figure 3.11) demonstrate morphological transformation associated with SR-BI silencing. At the 10X magnification (Figure 3.11B), SRBI-KD cells appear larger than their NC counterparts while at the 20X magnification, SRBI-KD cells appear flatter than NC cells. Both of these features are illustrated in fluorescence images in Figure 3.11C, indicating flattened and expanded cytoplasmic features as indicated by WGA staining and enlarged and often multilobed nuclei as indicated by DAPI staining. This conclusion that SR-BI targeted siRNA transfection induced

increase in cell size was further corroborated quantitatively; SRBI-KD cells have significantly higher FSC parameters compared to NC (Figure 3.11 D). Together, these results strongly indicate that knockdown of SR-BI is correlated with a senescent morphology.

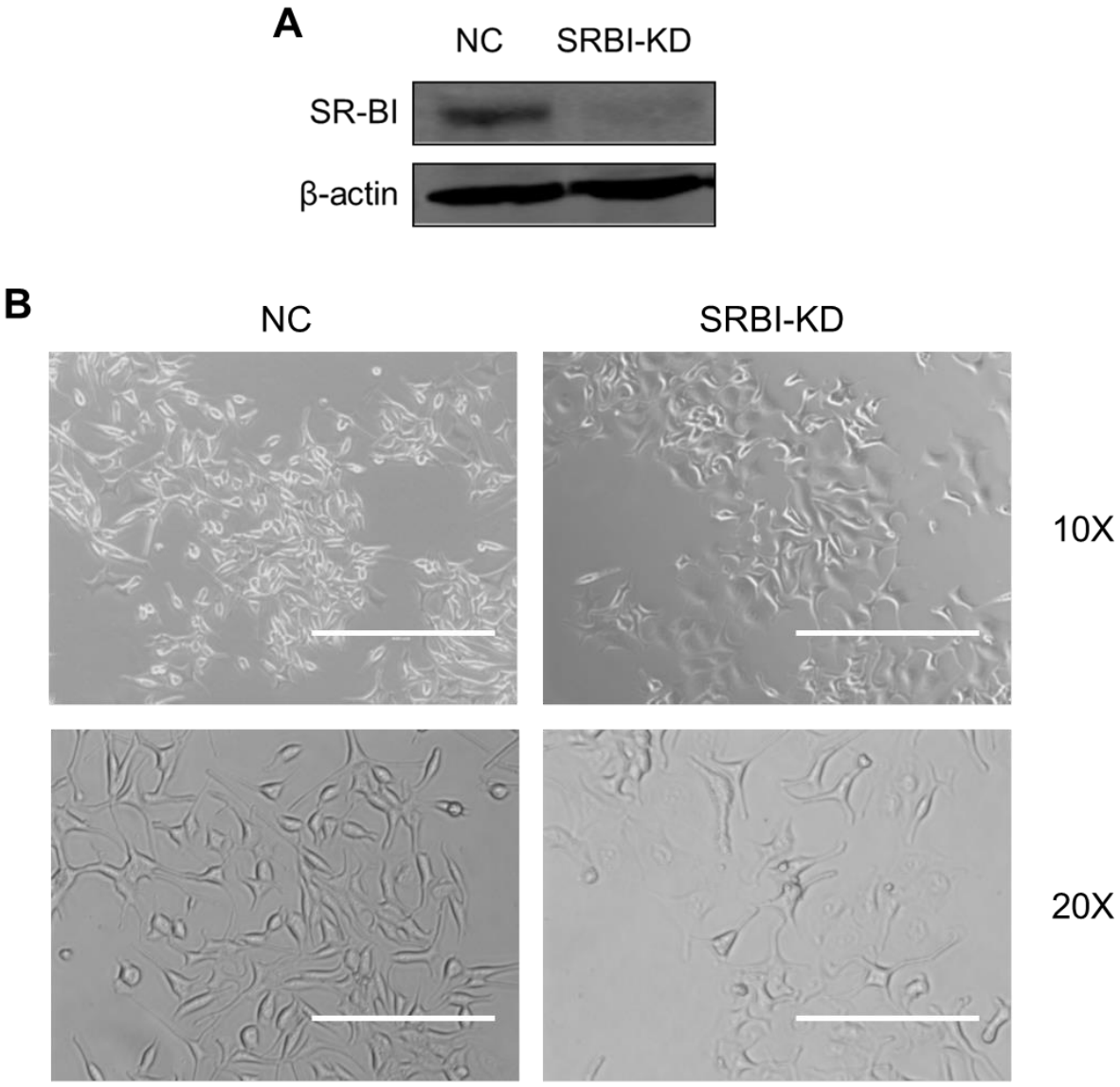

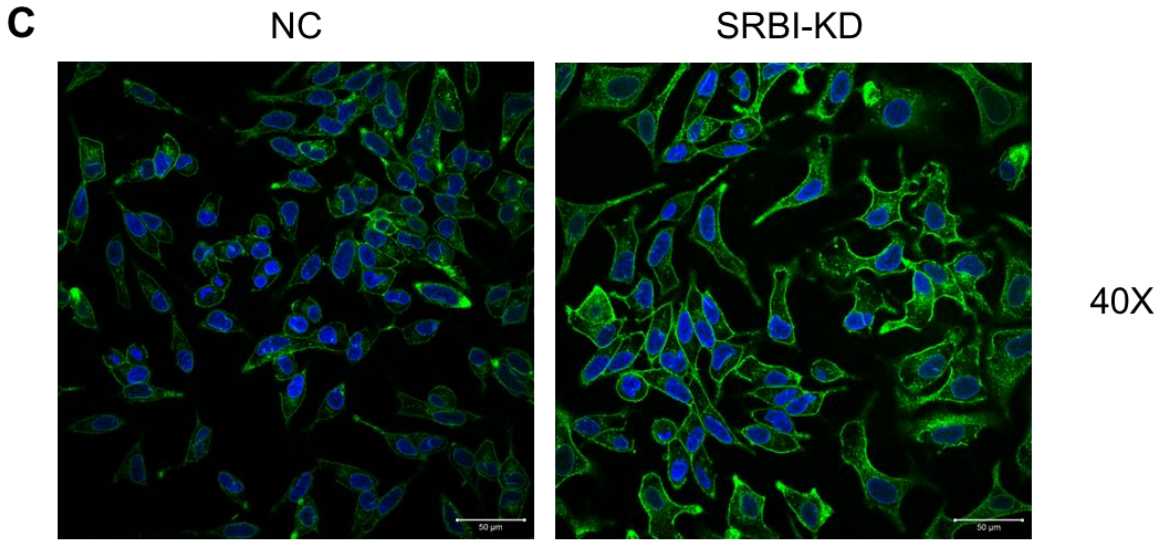

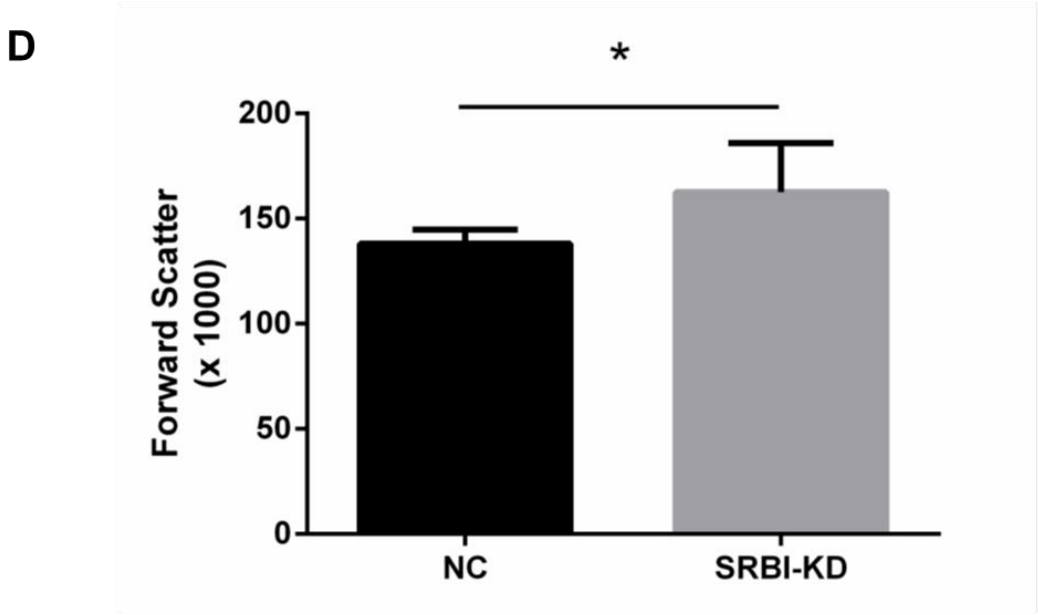

Figure 3.11: Knockdown of SR-BI is associated with a senescence-like morphological transformation.
C4-2 cells were cultured in CSS for 4 days following transfection with either control siRNA (NC) or siRNA targeting SR-BI (SRBI-KD). Senescent morphology was assessed by bright phase microscopy, fluorescent microscopy, and analysis of forward scatter (FSC) parameters. (**A**) Whole cell lysates were prepared and subjected to western blot analysis as described in sections 2.4 and 2.5 on cells subjected to SA-βgal FACS analysis as described in section 2.13 (FACS data Figure 3.12). Representative western blot: SR-BI was probed to assess siRNA silencing while β-actin was used as a loading control. (**B**) Bright field images of cells, magnification is indicated. 10X scale bar = 400 µm, 20X scale bar = 200 µm. (**C**) Cell morphology was examined using WGA-647 and DAPI staining as described in section 2.12. Magnification is indicated. Scale bar = 50 µm. (**D**) FSC parameters were recorded on cells subjected to SA-βgal FACS analysis as described in section 2.13 (FACS data Figure 3.12). Columns represent mean forward scatter (FSC) from six independent flow cytometric experiments ± SEM, *$p < 0.05$ by Student's t-test.

Histograms of event (cell) counts vs. fluorescence intensity (Figure 3.12 A&B) indicate that senescence inducing stresses, such as doxorubicin (239), result in enhanced SA-βgal activity relative to unstressed cells. A similar shift in fluorescence intensity is seen with SRBI-KD compared to NC. Median fluorescence intensity, indicative of SA-βgal activity, increased approximately 71% in SRBI-KD cells compared to NC (Figure 3.12C) which was very similar to the ~80% increase in enzyme seen in untransfected cells treated with doxorubicin compared to unstressed controls (Figure 3.12D). Faced with a loss of extracellular cholesterol sources due to SR-BI silencing, C4-2 cells induce adaptive stress responses resulting in the emergence of a senescent phenotype characterized by tumor suppressor induced growth arrest, characteristic morphological changes, and an induction of SA-βgal activity.

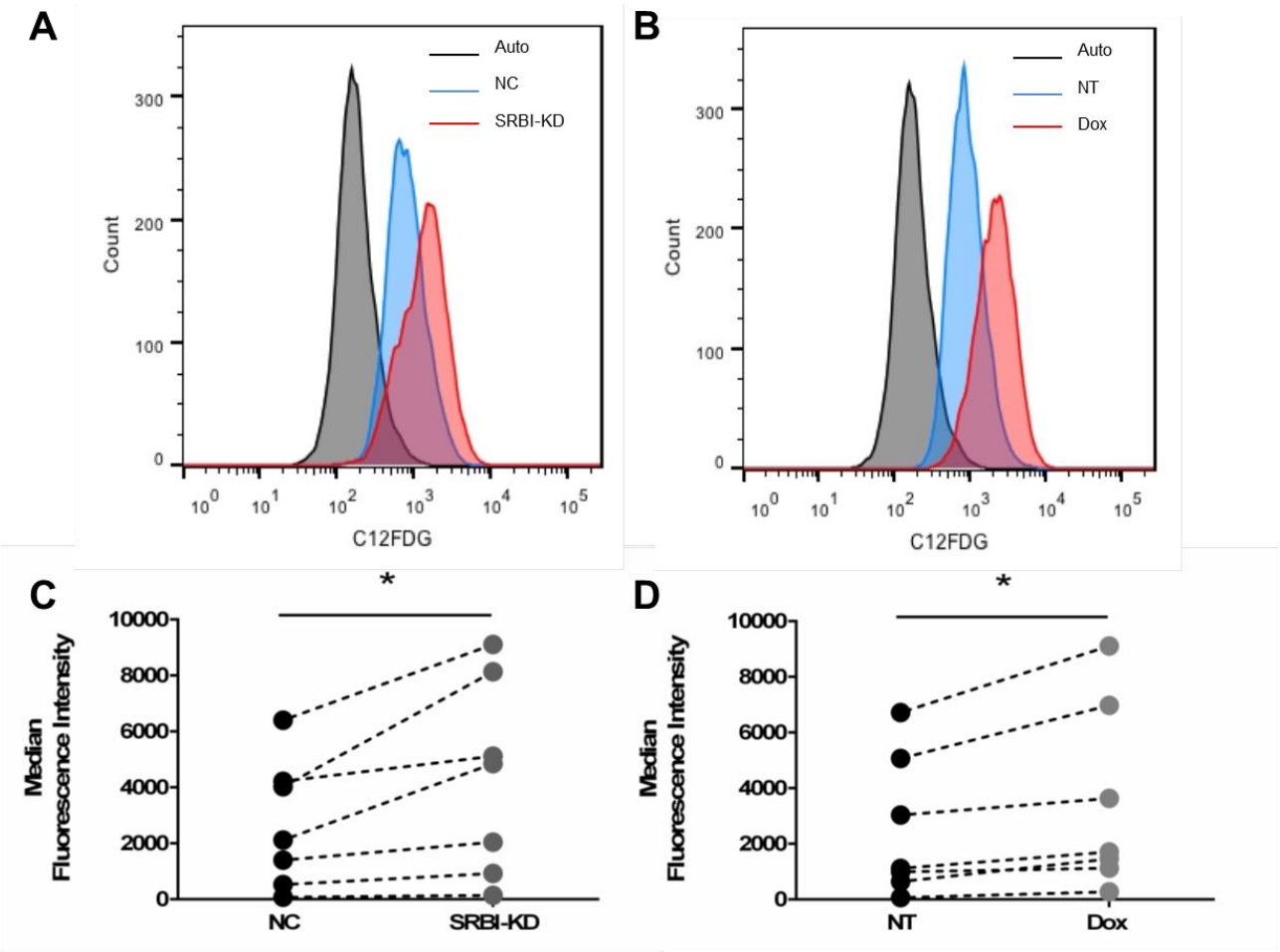

Figure 3.12: Activity of SA-βgal is enhanced by knockdown of SR-BI.
SA-βgal activity was determined in C4-2 cells treated with chloroquine (100 µM) for 2 hours followed by incubation with the fluorogenic SA-βgal substrate, C_{12}FDG (33 µM), for 1 hour prior to FACS analysis as described in section 2.13. (**A**) Representative histogram indicating relative levels of SA-βgal activity in stressed (red tracing; SRBI-KD) and unstressed (blue tracing; NC) cells; grey tracing represents autofluorescence of cells treated only with chloroquine. (**B**) Representative histogram indicating relative levels of SA-βgal activity in stressed (red tracing; Dox) and unstressed (blue tracing; NT) cells; grey tracing represents autofluorescence of cells treated only with chloroquine. (**C**) C4-2 cells were cultured in CSS for 4 days following transfection with either control siRNA (NC, black dots) or siRNA targeting SR-BI (SRBI-KD, grey dots) prior to the assay. (**D**) Untransfected cells were cultured in equivalent conditions as transfected cells then incubated overnight with (Dox [50 nM], grey dots) or without (NT, black dots) doxorubicin prior to the assay. Data points represent means of median fluorescent intensities from each of seven independent experiments, dashed lines connect data points from each experiment, respectively, *$p < 0.05$ by paired t-test for respective matched data sets.

Chapter 4: Discussion

The first reported case of prostate cancer was described over 160 years ago by John Adams, a surgeon at the London Hospital (36,240). He described the prostate of a 59 year-old man with obstructive urinary symptoms, enlarged to nearly twice its normal size, detected by rectal exam. A colleague, Dr. Copland, "remarked that scirrhus of the prostate was a very rare disease, and invited the fellows present to state their experience respecting it." In 2015, PCa will comprise roughly a quarter of new cancer cases in Canadian men leading to 10% of cancer deaths in the same cohort (1,2). As with other cancers, genomic instability leading to deregulation of several oncogenes and tumor suppressors is implicated in prostate carcinogenesis (30–33); however, ligand-activated signaling by the AR occupies a central role in the initiation and progression of prostate malignancy (241). Accordingly, androgen deprivation by surgical or chemical castration has been the foundation of PCa therapy since its advent in 1941 by Huggins and Hodges (37,71,72). ADT leads to marked treatment response characterized by apoptotic tumor regression and overall survival benefits of approximately 18 months in men with metastatic disease (73).

Despite our best efforts, current therapies are limited by transient effectiveness and disease recurrence, due to adaptive stress responses by PCa cells promoting the emergence of an incurable, castration-resistant phenotype (30). The first agent to demonstrate survival benefit in patients progressing post-ADT was docetaxel (82,83), though resistance mechanisms, such as limited cellular exposure via the drug efflux pump Pgp, limits survival benefits to approximately 3 months (105). A newer taxane, cabazitaxel, is not a substrate for Pgp and offers benefits to patients progressing after docetaxel therapy (86). Though undeniably a significant step forward, taxane drugs suffer from two major setbacks. First, as cytotoxic chemotherapeutics, patients

suffer considerable adverse drug reactions during the course of treatment (87). Moreover, taxanes do not target essential disease processes: in spite of castrate serum androgen levels, experimental and clinical evidence point to continued AR signaling as a virtually ubiquitous adaptation by CRPC cells (30).

Experimental models of disease progression exhibit impaired or delayed ability to progress to castrate-resistance when AR protein expression is suppressed by RNA-interference (242). AR transcript and protein levels are frequently elevated in clinical CRPC tissue specimens (137), as are androgen-regulated genes (243). One potential mechanism of AR re-activation is by achieving so-called ligand independence (43); however, clinical success in PCa has not been achieved by targeting these and other pro-survival and pro-proliferative pathways, as has been the case for other cancers (30). With the exception of constitutively active AR-splice variants whose clinical relevance is not clearly established (244), the detection of intratumoral androgens precludes our ability to declare truly ligand-independent AR activation by signaling cascades. As discussed in sections 1.4.3.1 and 1.4.3.2, AR hypersensitivity and AR ligand-independence are established mechanisms of AR-reactivation. Hence, efforts to antagonize the AR axis have been most successful at the receptor and pre-receptor levels (245).

Newer AR antagonists are under development, with enzalutamide the first to be approved (75). While improving survival outcomes, treatment resistance has been reported (76,147). Though its affinity for the AR is up to eight-fold greater than older AR antagonists, enzalutamide is impotent next to even the smallest concentration of DHT which binds the AR with up to 100-fold higher affinity (246,247). Deregulation of AR chaperones and co-regulators can also increase AR responsiveness and attempts to target various AR-associated proteins in combination with established AR-directed therapies are under investigation (30). The CYP17A1

inhibitor abiraterone was also recently approved and survival benefits demonstrate a clear rationale for targeting *de novo* androgen synthesis in CRPC (80,81). Hence, agents targeting different enzymes in the androgen synthesis pathway are under development (30). Though this is promising, resistance by way of a mutated AR-LBD can be predicted. Therefore, we propose an alternative approach to limiting AR-ligand availability by restricting the supply of the necessary androgen precursor, cholesterol. Sources of cellular cholesterol for steroidogenesis include synthesis from acetyl-CoA through the mevalonate pathway and uptake from circulating lipoproteins (47,233).

Here, we demonstrate for the first time that antagonizing SR-BI-mediated selective cholesterol uptake from HDL can induce a senescent growth arrest in C4-2 cells as an adaptive stress response to reduced AR activation. Previously, colleagues demonstrated that SR-BI protein levels are increased in CRPC tumors compared to pre-castration tumors in the LNCaP xenograft mouse model (180). Furthermore, *in vitro* findings indicated that SR-BI protein expression is approximately two-fold higher in C4-2 cells compared to their parental LNCaP cell line (208). When SR-BI protein expression was suppressed by siRNA treatment, Twiddy *et al*. reported a reduction in PSA secretion and cell viability in LNCaP and C4-2 cells (208). This provided the first indication that SR-BI may serve as a target in CRPC.

In this study, the mechanisms underlying previously reported decreases in PSA secretion and cell viability were assessed. First, key findings from the report by Twiddy *et al.* were validated, including: siRNA-mediated knockdown of SR-BI (Figure 3.1), reduced PSA secretion (Figure 3.6), reduced viability (Figure 3.7), and quantification of total cellular cholesterol concentration (Figure 3.4). Our results demonstrate the reproducibility of this cell culture model to study SR-BI in LNCaP derived cell lines. In order to use the model for subsequent studies,

adaptations were necessary. The study by Twiddy *et al*. was conducted using C4-2 cells cultured for up to 6 days in a low-serum environment using RPMI media 1640 supplemented with 1% FBS (208). LNCaP and their derivative cell lines grow well in medium supplemented with 2.5 to 10% serum with lesser amounts delaying doubling times (209). Serum provides cells their nutritional and growth factor requirements, thus it is essential to culture them with an amount adequate to maintain cell physiology (248). To mimic androgen-deprived conditions, cells should be cultured in CSS (249). Hence, the model was adapted by culturing cells in RPMI 1640 media supplemented with 5% CSS following transfection. Time-dependent SR-BI suppression was determined by culturing cells in CSS for up to 4 days. Maximal suppression was achieved at 4 days post-transfection (Figure 3.2B), while appreciable suppression was seen as early as 2 days post-transfection (Figure 3.2A). These findings improve experimental efficiency by defining earlier time points for subsequent experiments.

In normal physiology, cellular cholesterol levels are tightly regulated by nuclear receptors (158); SREBP transcription factors enhance lipogenesis by activating target genes involved in the synthesis and uptake of cholesterol and fatty acids (250). In particular the SREBP-2 isoform is induced by sterol-depletion, while SREBP-1c acts to increase fatty acid synthesis. SREBP-1a stimulates both transcription programs (250). LXRs are induced in response to elevated oxysterols and work to normalize cholesterol levels by inducing cholesterol efflux mechanisms such as ABCA1, and by targeted degradation of LDLR (176). Typically, most adult human tissues obtain lipids and cholesterol from circulating lipoproteins generated from dietary sources, while lipogenesis is restricted to specialized tissues, such as hepatic, adipose, and lactating breast; however, activated lipid biosynthesis is a common occurrence in cancer (251). Accumulating evidence highlights numerous disruptions in cholesterol and lipid homeostasis,

collectively termed the “lipogenic phenotype”, due in part to the perpetually heightened demand for constituents needed for membrane biogenesis (156). In the case of steroid hormone driven malignancies, the cholesterol requirement is likely exaggerated by its role as a precursor for steroid synthesis. SREBP-2 expression increases during PCa progression and is significantly higher post-castration due to a loss of feedback regulation (156,183). Interestingly, SREBP-2 expression is stimulated by androgens (49,50) resulting in accumulation of cholesterol and lipids (252). SREBP-1 appears to regulate AR expression (253), demonstrating a reciprocal relationship between lipogenesis and AR signaling, suggestive of an essential role for cholesterol in CRPC.

Studies in rodents have implicated cholesterol acquired by SR-BI from HDL as a key source of cholesterol for steroidogenesis (231). LDLR and *de novo* cholesterol synthesis are additional sources of cholesterol for steroid production, but have been deemed of secondary importance (187,196,254). Our data demonstrate the importance of SR-BI in selective lipid uptake from HDL. DiI-HDL was chosen to approximate HDL-CE uptake by SR-BI in a method adapted from other groups (216–219). DiI labeled lipoproteins have been shown to associate with cells and transfer lipids as effectively as radiolabeled-CE counterparts, thereby providing a rapid, reliable assay without the administrative and technical challenges of working with radioactivity. The small molecule inhibitor of SR-BI, BLT-1, was previously shown to inhibit SR-BI-mediated selective lipid uptake from HDL, without changing the surface expression of SR-BI (194). Our results also demonstrated SR-BI inhibitory activity by BLT-1 (Figure 3.3B), though the response was less than seen by Nieland *et al*. Using equivalent dosing and conditions (10 μM BLT for 1 h prior to incubation with DiI-HDL), we achieved a reduction in DiI uptake of approximately 26% while Nieland *et al.* reported approximately 75% inhibition. This difference

is likely due to their use of LDLR-deficient Chinese hamster ovary cells stably transfected to express high levels of murine SR-BI allowing for demonstration of maximum drug effect. In our study, comparable suppression of DiI uptake was seen with SR-BI silencing, from normal physiologic levels expressed by C4-2 cells (Figure 3.3A).

Consistent with previous findings (208), SR-BI silencing did not appear to alter total cellular cholesterol concentrations (Figure 3.4). Twiddy *et al.* reported a compensatory increase in HMGCR cholesterol synthesis activity in response to knockdown of SR-BI. Previous studies in fibroblasts report that upwards of 90% of cellular cholesterol is distributed in the plasma membrane, while approximately 10% is intracellular (255). Lange reported that intracellular cholesterol pools are generated primarily from endocytic membrane stores with very little contribution from synthesis or lipoprotein sources (157). Up to 60% of intracellular cholesterol (~6% of total) is lysosomal (256). It is estimated that newly synthesized cholesterol accounts for approximately 1% of intracellular levels (157). This distribution can change slightly in cells that accumulate CEs in lipid droplets, such as hepatocytes, which have ~80% of their cholesterol distributed to the plasma membrane (255). Remarkably, this is the lowest reported plasma membrane cholesterol disposition. CE accumulation in lipid droplets has been observed in PCa specimens and is correlated with disease severity (257). Taken together, this indicates that a very small fraction of intracellular cholesterol pools are provided by lipoproteins while the vast majority remains in the plasma membrane. Hence, total cellular cholesterol levels would not be expected to change by inhibition of SR-BI protein expression. Instead, antagonizing SR-BI is an effective means of directly targeting a large proportion of the cholesterol pool destined for the mitochondria for further conversion into androgens.

Our group has previously shown that cholesterol synthesis inhibition by simvastatin treatment of C4-2 cells is associated with reduced PSA secretion (235). More recently, using the LNCaP xenograft mouse model, we demonstrated that oral administration of simvastatin delayed tumor progression to castrate-resistant disease and resulted in reduced intratumoral testosterone levels (211). Previously, SR-BI knockdown was also associated with decreased PSA secretion (208), a result that has been reproduced here (Figure 3.6). Expanding upon these findings, we demonstrated reduced levels of both testosterone and DHT associated with knockdown of SR-BI (Figure 3.5). While these data are promising, this method was limited in three ways. First, PSA production is taken as a measure of AR activation but measurement of secreted PSA levels is a few steps removed from AR transcriptional activity. This introduces confounding factors around potential alterations to secretory processes contributing to the observed differences in secreted PSA levels. A more direct measure of AR-mediated gene transcription would be the analysis of PSA transcript levels. Second, the use of PSA without verification from an additional AR target gene is limited due to differences in the AR transcriptome between malignant and benign tissues, as well as between pre-castration and CRPC tissues (243,258,259); PSA is highly expressed in untransformed prostate cells as well as PCa cells. The altered AR-regulated transcriptome in PCa relative to untransformed prostate epithelia has been linked to enhanced binding of the receptor to chromatin in response to its over expression, leading to an increase in AR binding sites and associated target genes (260). The use of a second biomarker of AR activity such as the androgen-regulated NKX3.1 would corroborate PSA transcript findings (261). Finally, the cost of using commercially produced lipid transfection reagents coupled with our LC-MS assay was prohibitive and prevented continuing with this assay, limiting replication. This is due to the cost of transfection reagent and the sample size requirement of the LC-MS assay and could be

remedied by using tetracycline-inducible short hairpin RNA (shRNA) mediated knockdown of SR-BI instead of siRNA (242). Once a C4-2 cell line stably expressing SR-BI shRNA is developed, accumulating large samples for LC-MS analysis will be relatively affordable. This model could also be used for long-term knockdown studies when circumstances require. Knockdown of > 90% is attainable, making this system very amenable to studying SR-BI functions in PCa. Additionally, having demonstrated the efficacious HDL-lipid uptake inhibition using BLT-1, this drug could be used to determine the effect of antagonizing SR-BI on androgen synthesis. It would be most interesting to couple SR-BI inhibition with uptake of radiolabeled [^{14}C] cholesteryl oleate incorporated into HDL particles to track cholesterol from its source through to conversion to testosterone and DHT. Nevertheless, these data illustrate the potential for targeting the AR axis by reducing the supply of cholesterol precursor for androgen synthesis.

Previous work alluded to reduced proliferation of C4-2 cells in response to SR-BI protein suppression, measured by MTS assay (208). Additionally, Danilo *et al.* reported reduced proliferation by [^{3}H]-thymidine incorporation in MDA-MB-231 breast cancer cells *in vitro* in response to shRNA knockdown of SR-BI as well as to treatment with BLT-1 (262). shRNA knockdown of SR-BI also reduced tumor growth in MDA-MB-231 and MCF-7 xenograft mice. Cao *et al.* demonstrated inhibited proliferation of MCF-7 cells expressing mutant SR-BI, lacking a C-terminal tail (263). This study also described an anti-apoptotic role for SR-BI. Both of these studies did not assess selective cholesterol uptake or estrogen synthesis and instead attributed their findings to SR-BI-mediated signal transduction, activated by HDL. In agreement with these studies, we found a reduced MTS readout following SR-BI silencing (Figure 3.7).

Tetrazolium-based assays are commonly used to assess cell viability and growth rates in response to anti-cancer treatments (264), providing more accuracy and objectivity than

traditional cell counting methods such as trypan blue dye exclusion (265). The reduction of MTS to a colored formazan product is detected by absorbance measurements at 490 nm which are reported as estimates of viable cell counts (224). The output of this assay is actually a measure of mitochondrial metabolic rate, rather than overall cell viability, and formazan production is affected by numerous parameters, including: glucose content of media, cell line, culture age, pH, and mitochondrial dehydrogenase activity (264,266). Though it is argued that MTS reduction provides a count of metabolically active mitochondria, which in itself could be taken as an indirect cell count as a sample with fewer cells would likely contain fewer mitochondria, the assay does not reveal any mechanistic insights.

While the MTS findings presented herein as well as those reported by Twiddy *et al.* provide indirect evidence of reduced growth in CRPC in response to SR-BI silencing, we sought to further elucidate the underlying proliferative changes by examining cell cycle profiles of cells after transfection. Our results demonstrate that knockdown of SR-BI induces a cell cycle arrest (Figure 3.8) characterized by an accumulation of cells in the G_0-G_1 phase and a suppression of cells in S-phase and G_2M, 2 days following transfection. The Sub G_0 populations were indistinguishable between NC and SRBI-KD cells. By 4 days post-transfection, SR-BI knockdown-associated arrest persisted as determined by an arrest index and the persistent reduction of SRBI-KD cells in S-phase and G_2M; however, the G_0-G_1 populations were indistinguishable. At this point, there was an increase in the Sub G_0 population of SRBI-KD cells relative to NC, indicating an increase in cell death after 4 days of suppressed SR-BI expression. AR-targeted therapies have been linked to several stress responses by CRPC cells (30). Most notably, ADT is well documented to induce apoptosis and G_1S cell cycle arrest in surviving cells (106,107). Given the similar outcomes in our study, our cell cycle profiling suggests that

downstream consequences of SR-BI knockdown are due to attenuated AR activation. To test the basis of this correlation, future studies should involve possible rescue treatments including supplementation with LDL, DHEA, and/or DHT.

The tumor suppressive transcription factor p53 regulates numerous genes, some of which are involved in cell cycle arrest, apoptosis, and senescence (267). Protein levels of p53 are negatively regulated by the E3 ubiquitin protein ligase mouse double minute 2 (MDM2), which is itself a p53 target gene (268,269). Various stresses can trigger p53 activity by inhibiting its degradation thereby causing its accumulation, including: DNA damage, aberrant growth signals, and as a response to various chemotherapeutics and protein-kinase inhibitors. Activation of p53 is achieved by conformational changes due to various modifications by upstream regulators, leading to dissociation from MDM2. Activated p53 can then act as a transcription factor to execute its various functions (270). p53 stimulates expression of the cyclin-dependent kinase (CDK) inhibitor p21 resulting in growth arrest. p53 and p21 have been linked to both the G_1S and G_2M checkpoints to mediate growth arrest (271,272). Furthermore, p53 activation has been linked to apoptosis by various mechanisms (273). Our results are consistent with p53 mediated G_1S arrest as demonstrated by an accumulation of both p53 and p21 following SR-BI silencing (Figure 3.9B). Another tumor suppressor important in cell cycle control is pRB, active in its hypophosphorylated state in G_0 cells (274). As cells progress through G_1, pRB is increasingly phosphorylated by CDKs and thus inactivated in a hyperphosphorylated state until late mitosis (275,276). pRB contains 13 known serine and threonine sites that are phosphorylated by CDKs (277), governing different outcomes and reviewed elsewhere (276). Serine 780 (S780) is implicated in cell cycle regulation (278), while S807/S811 phosphorylation by CDK4 seems to regulate phosphorylation of other sites and hyperphosphorylation status of pRB (279–282). By

repressing transcription of genes required for transition from G_1 to S phase, pRB mediates growth arrest at the G_1S checkpoint (274). Our results suggest pRB mediates G_1S arrest in C4-2 cells following knockdown of SR-BI (Figure 3.9C); SR-BI knockdown is associated with hypophosphorylation of pRB at S780 and S807/S811. Furthermore, cell cycle profiling revealed reduced S-phase and G_2M populations in SRBI-KD cells compared to control, suggesting that cells are unable to progress through the G_1S checkpoint to enter S-phase (Figure 3.8).

Though we have shown an increase in the Sub G_0 population in response to SR-BI silencing by cell cycle profiling as well as induction of p53, additional markers for apoptosis were negative (Figure 3.9D). There was no evidence for the cleavage products of PARP or caspase 3, markers for apoptotic cell death (283). During apoptosis, energy-intensive PARP activity is inhibited by caspase 3, events which are complex and time-dependent (284). Uninhibited PARP activity can result in energy failure due to ATP depletion, inducing necrosis (285,286). It should be noted that lack of evidence of PARP cleavage alone is not indicative of a necrotic response and the relatively small increase in death rate cannot be detected by immunoblotting for cleavage events and therefore, only changes to DNA content are sensitive enough to detect death at a low rate.

Apoptosis is characterized by DNA cleavage and release of apoptotic bodies (287), which would appear as an increase in Sub 2N DNA content resulting in an accumulation in the Sub G_0 cell cycle fraction (226). This feature is supportive of an apoptotic induction in response to SR-BI knockdown. In contrast, necrotic cells maintain their DNA content in the nucleus and necrosis would not manifest as an increase in the Sub G_0 population (283). Apoptotic bodies are membrane enclosed packages of cytoplasmic and nuclear contents that are phagocytosed by

surrounding cells, including phagocytes (283,288). In necrosis, cell lysis leads to the release of cytoplasmic contents into the surrounding space (112).

Twiddy *et al*. reported indistinguishable lactase dehydrogenase (LDH) measurements in the supernatant of C4-2 cells up to 6 days post-transfection (208). LDH is a cytoplasmic enzyme whose release into cell culture media is suggestive of cell lysis due to necrotic death (289). Even if LDH had increased following SR-BI knockdown, this would not necessarily have confirmed necrotic death. Caution must be exercised when interpreting LDH release results as apoptotic cells can turn into secondary necrotic cells in the absence of phagocytosis (283), which is likely the case in our cell culture system. In response to cellular stress, p53 can promote apoptosis by inducing transcription of proteins required for intrinsic and extrinsic apoptosis pathways as well as by promoting mitochondrial outer membrane permeabilization (102). Emerging evidence has also linked p53 with necrosis, though this is not as well established and was demonstrated under classical necrotic conditions including ischemic brain injury and H_2O_2 treatment (290,291). Our results are more suggestive of apoptosis and as of yet provide no indication of necrosis. However, dual staining with PI and Alexa Fluor 488-conjugated Annexin V could be used to fully rule out necrosis (283). Annexin V binds to negatively charged phospholipids such as phosphatidylserine which is displayed on the surface of apoptotic cells while PI is impermeable across intact plasma membranes. Caution should be taken once again, as positivity for phosphatidylserine precedes positivity for PI staining, and timing could confound results as necrotic cells can stain positive for both.

Autophagy is critical for cellular homeostasis by turning over cellular contents through lysosomal digestion (292). Autophagy activity can be enhanced in response to starvation and nutrient depletion as well as anti-cancer therapies, including: radiotherapy, chemotherapy, and

hormonal therapy (293–297). During autophagy, an isolation membrane, also known as a phagophore, is generated and elongated until it closes to form the autophagosome which then fuses with lysosomes to produce autolyososomes (100). During formation of the autophagosome, lipidation of LC3 with phosphatidylethanolamine converts LC3-I to LC3-II; autophagic flux via the conversion of LC3-I to LC3-II can be monitored by immunoblotting (298). Boutin *et al.* reported enhanced autophagy activity in LNCaP cells after treatment with the AR antagonist bicalutamide, as well as by culturing cells in CSS (124). Autophagy in response to nutrient depletion has been linked to cell cycle arrest, allowing cells to survive metabolic stress instead of undergoing apoptotic death (299). The same response was not seen in DU-145 cells which lack an AR; therefore, autophagy induction was thought to be AR-mediated. When autophagy was blocked, LNCaP cells underwent apoptosis. These reports support our contention that SR-BI silencing suppressed *de novo* steroid synthesis and subsequent AR activation given the similar phenotypic response with other studies of AR-inhibition activated autophagy.

Another factor that has been linked to induction of autophagy in PCa is CLU, a multifunctional stress-activated gene which can be induced by multiple factors including hormonal, radiation, and chemotherapy in cancer (120,121). Interestingly, CLU, also known as ApoJ, was characterized as an apolipoprotein associated with ApoA-I in some classes of HDLs (300,301). CLU expression is stimulated by autophagy-inducing stresses, including androgen-deprivation, and CLU has been identified as a facilitator of autophagosome formation (98). CLU and autophagy are induced as components of an adaptive survival response, inhibiting apoptosis and inducing treatment resistance to therapies, including ADT in PCa (122–124). Our results are consistent with previous reports as both autophagy activity and CLU expression were enhanced when SR-BI was knocked down (Figure 3.10). Alternatively, autophagy can also be a precursor

for cell death, either due to self-digestion by extensive autophagy (autophagic cell death), or by triggering apoptosis or necrosis (302). The lack of evidence for necrosis coupled with persistent growth arrest suggest autophagy is largely promoting survival rather than apoptosis in C4-2 cells with suppressed SR-BI protein levels. This adaptive survival response would allow cells to maintain viable metabolic activity until being overwhelmed by sustained nutrient deprivation.

To determine if the apoptosis observed by cell cycle profiling is driven by autophagy, it is imperative to characterize the extent of autophagy. Visualization of LC3 puncta by fluorescence microscopy would allow us to assess vacuolization in response to SR-BI silencing (298,303). Consistent with our results, HDL and ApoA-I have been shown to suppress autophagy in adipocytes through SR-BI (304), though there is no indication of AR involvement in this setting; emerging evidence indicates that cholesterol depletion alone can induce autophagy. Cheng *et al.* demonstrated an induction of autophagic flux by methyl-β-cyclodextrin cholesterol depletion in fibroblasts (305). Statins have been shown to induce autophagy in PC3 cells as well as other tumor and non-tumor cells (306). This effect has been linked to depletion of geranylgeranyl pyrophosphate, a product of the mevalonate pathway needed for post-translational modifications of Rho GTPases (307). Loss of geranylgeranyl diphosphate induces AMP-activated protein kinase activity which inhibits mTOR, thereby inducing autophagy. A more direct connection between cholesterol and autophagy implicates SREBP-2 as an activator of genes involved in autophagy, including LC3, in response sterol depletion (308). In light of these findings, sterol reduction as a form of nutrient depletion by antagonizing SR-BI can induce autophagy as a protective stress response.

Cell cycle arrest, mediated by p53 and pRB activation, is also a feature of senescence (125). Along with growth arrest, other markers of senescence include drastic morphological

transformation and increased SA-βgal activity (125). Senescent growth arrest is thought to be tumor suppressive in cells at risk for oncogenic transformation (238), but can also be a response to anti-cancer therapy (131). Previous reports have shown senescent cell cycle arrest in the absence of apoptosis when LNCaP cells were cultured in CSS for up to 16 days without reseeding (212). In the same study, LAPC-4 cells showed more resistance to androgen deprivation as senescent growth arrest was delayed. As with LNCaP cells, LAPC-4 cells were obtained from a lymph node metastasis, produce PSA in response to androgen treatment, and can progression to castrate-resistance in xenograft models (309). However, LAPC-4 cells express mutant p53. These characteristics would allow study of the effects of targeting SR-BI on growth and survival under androgen-deprived conditions with respect to p53 status.

SR-BI silencing resulted in marked morphological transformation, including an increase in cell size (Figure 3.11). Furthermore, SR-BI silencing also enhanced SA-βgal activity (Figure 3.12). Our results offer further support for senescence as a response to androgen depletion. Interestingly, senescence has been linked to HDL in the context of cardiovascular disease. Endothelial progenitor cells (EPCs) from high-risk cardiovascular patients become senescent faster in culture than cells taken from low-risk patients (310). High-risk patients also had fewer EPCs than low-risk patients; EPC counts correlate with HDL levels (311). Human dermal fibroblasts exposed to HDL from elderly people undergo senescence, determined by SA-βgal staining, while HDL from young people seems to protect against senescence (312). Interestingly, HDL from elderly people also displayed enhanced cholesterol influx into macrophages compared to HDL from young people. The pro-senescent effect has been linked to glycation of ApoA-I in the elderly, and appears to be independent of cholesterol flux in this setting. This is supported by another study in which SA-βgal staining was increased in fibroblasts treated with HDL from

smokers compared to cells treated with HDL from non-smokers (313). In this study, lipoproteins from smokers were shown to be modified by glycation and oxidation. Whether SR-BI is required for glycated-ApoA-I induced senescence is unclear.

In addition to its role in autophagy, CLU has been described as a biomarker of cellular senescence (314). Petropoulou *et al.* reported a senescence-related induction of CLU in human diploid fibroblasts. This upregulation was determined to be a result of the senescent phenotype rather than a cause of it, as stable overexpression did not alter proliferative capacity. The oxidative state of senescent cells may be responsible for inducing CLU (315). These studies did not assess autophagy activity, which is also associated with the senescent phenotype (125). Although earlier studies reported a decrease in autophagy in senescent cells (316), Patschan *et al.* demonstrated an induction of autophagosomes in senescing cells treated with glycated collagen I (317). When autophagy was inhibited, senescence was prevented. Young *et al.* reported autophagy activation during senescence, which when blocked delayed the senescent phenotype (318). Similarly, Goehe *et al.* reported that doxorubicin and camptothecin treatment induced both autophagy and senescence; when autophagy was blocked, senescence was delayed (319). While not required, autophagy can accelerate the onset of senescence.

Senescent cells are described as irreversibly arrested and resistant to cell death (132); however, these relationships are unclear. Beauséjour *et al*. demonstrated that senescence is maintained by activated p53 and p16 (320). Upon inactivation of p53 alone, neonatal foreskin cells can re-enter the cell cycle but fetal lung cells cannot. Inactivation of pRB promotes fetal lung cells to enter S-phase and synthesize DNA, but from here they are unable to progress through the cell cycle and do not continue to proliferate. Fetal lung cells are maintained in a senescent state by higher expression of p16, blocking the reversal by inactivation of p53. Burton

et al. demonstrated androgen deprivation induced senescence in the absence of apoptosis in LNCaP cells cultured in CSS for 14 days (321). Senescence was characterized by G_1S arrest and increased SA-βgal activity. While proliferation declined immediately upon androgen deprivation, senescent markers emerged after 4 days. By day 7, > 50% of cells exhibited senescence markers which increased to > 80% by day 10. If cells were switched back to FBS at day 3, proliferation resumed. In comparison, a smaller population of cells continued to proliferate when switched to FBS at day 8. Proliferation was not observed in cells switched to FBS after 14 days in CSS. Expression of p16 increased with time in CSS while p53 and p21 declined over time, further underscoring the importance of p16 in maintaining a senescent state. Interestingly, senescence-resistant cell populations capable of proliferating in CSS emerged when LNCaP cells were repeatedly switched between CSS and FBS.

This study demonstrated the reversibility of androgen deprivation-induced senescence and suggests that senescence is a pro-survival mechanism in this setting. Though our data is suggestive of androgen deprivation-induced senescence, we have not assayed for p16 status. Furthermore, by probing for tumor suppressive arrest markers at one time point relatively early after the onset of senescence, we cannot determine the stability of this phenotype. Future studies using SR-BI shRNA-treated C4-2 cells cultured in CSS could determine if senescence is maintained and increased during long-term cholesterol deprivation, and if this leads to the emergence of an even more treatment-resistant subpopulation. Regarding resistance to cell death, evidence has emerged that some cell types such as fibroblasts and keratinocytes are resistant to apoptosis (322). A study by Gosselin *et al.* demonstrated that senescent keratinocytes do not display apoptotic markers but instead display extensive vacuolization and autophagy activity and undergo autophagic cell death (323). When autophagy is blocked, cells remain senescent but do

not die. In contrast, senescent endothelial cells are susceptible to apoptosis in response to certain triggers. Early-passage fetal lung cells have been shown to undergo p53-mediated apoptosis in response to various insults whereas senescent counterparts undergo necrosis (324). Taken together, there is considerable evidence that senescence is reversible and senescent cells are susceptible to death. Cell fate decisions vary by cell type and source of stress. Furthermore, these studies highlight the importance of combination therapy when the identified tumor suppressive mechanism associated with antagonizing SR-BI is senescence. While these stress-adapted cells may survive androgen deprivation, they are also likely to be sensitized to other insults and more susceptible to death.

4.1 Limitations and future directions

Unlike many other targets under investigation in cancer research, there is a relative lack of evidence from human tumor tissue samples identifying an upregulation of SR-BI. Most lines of evidence suggesting a role for this protein in CRPC arise from studies conducted in cell culture as well as in the LNCaP xenograft mouse. Also, most of our knowledge concerning the role of SR-BI in steroidogenesis has been obtained from studies in rodents. By relying heavily on rodents to study SR-BI function in steroidogenesis as well as in CRPC, we are confronted by differences in lipoprotein biology. LDL makes up the majority of circulating lipoprotein in humans, while rodents are HDL-dominant. Our group has studied the impact of inhibiting cholesterol synthesis in CRPC cells and the results indicate that synthesis is an alternative source of substrate for androgen synthesis. We should therefore also evaluate the role of LDLR in this process by conducting similar studies using siRNA against LDLR.

This study was conducted in the LNCaP-derived C4-2 cell line. To date, all of our work on SR-BI has used LNCaP and derivative cell lines. With the exception of a study using the

TRAMP model of PCa (207), SR-BI has not been identified in other model systems. This, coupled with the lack of clinical evidence for SR-BI, leave open the question of whether upregulation of and reliance on SR-BI is a phenomenon limited to the LNCaP lineage. To address this, SR-BI transcript and protein levels should be studied in various cell lines to determine if SR-BI is expressed and/or upregulated in different PCa cell types. To follow up on the previous study, cell lines derived from the TRAMP model (TRAMP-C1, TRAMP-C2, and TRAMP-C3) should be studied. To further understand the connection between SR-BI and AR activation, cell lines not expressing AR and PSA such as DU-145 and PC-3 should also be tested. VCaP can also be tested, as it expresses wild-type AR instead of a mutated AR like the LNCaP lines.

To fully characterize the impact of antagonizing SR-BI on AR activation, androgen quantification will have to be repeated. This can be done using BLT-1 or the proposed shRNA system. Furthermore, using radiolabeled CE-HDL and following the radioactivity through to testosterone and DHT would firmly establish SR-BI as a source of cholesterol for steroid production in PCa cells. This should be done alongside transcript analysis of PSA and NKX3.1, as described earlier. Additionally, "rescue" experiments with added androgen and/or alternative cholesterol sources would be of value.

Cell stress responses should be followed up by assaying for reactive oxygen species to further illustrate the stress caused by antagonizing SR-BI. Additionally, autophagy should be assessed by fluorescent microscopy for LC3 puncta and vacuolization. With respect to cell cycle arrest, use of the shRNA system would allow long-term study of various markers. The stability of senescent arrest can be monitored by SA-βgal activity at various time points as well as probing for p53, p21, pRB, and p16 over the course of 14 days in culture in CSS. Over this time

course, we could also assess for senescence-associated secretory phenotype markers. The sensitizing of cells to death as a result of adaptive stress responses should be assayed for by several combination treatments following SR-BI silencing: enzalutamide, abiraterone, simvastatin, and metformin.

4.2 Summary of findings

The research in this thesis was conducted to test the hypothesis that SR-BI contributes cholesterol as a substrate for *de novo* androgen synthesis within CRPC cells. This hypothesis was tested by studying the effects of SR-BI silencing on HDL-cholesterol uptake and the cell cycle profile in C4-2 cells. The data presented and discussed herein provide evidence in support of our stated hypothesis. SR-BI protein levels were suppressed by > 80% following siRNA treatment in C4-2 cells, impairing selective CE uptake from HDL particles. Reduced HDL-CE uptake was accompanied by decreased cellular testosterone and DHT levels. Additionally, the concentration of secreted PSA was significantly reduced after SR-BI silencing. Together, these findings suggest that HDL-derived cholesterol is an important source of precursor for androgen synthesis. Antagonizing SR-BI restricts this cholesterol pool, thereby reducing androgen synthesis and subsequent AR activation. In agreement with several aforementioned studies, this form of androgen depletion induces pro-survival adaptive stress responses characterized by enhanced autophagy activity and induction of CLU. In parallel, cells undergo senescent growth arrest characterized by G_1S arrest, tumor suppressor signaling by p53 and pRB, morphological changes including increased cell size, and enhanced SA-βgal activity. These data reveal the nuanced inter-relationship between androgen deprivation-mediated cell cycle arrest, induction of senescence and autophagy, and eventual death in this CRPC cell model upon deprivation of an

extracellular cholesterol source, thereby providing the basis for further exploring the potential of targeting SR-BI to augment existing therapies for CRPC.

References

1. **Siegel R, Ma J, Zou Z, Jemal A.** Cancer statistics, 2014: Cancer Statistics, 2014. *CA. Cancer J. Clin.* 2014;64(1):9–29.

2. **Canadian Cancer Society's Advisory Committee on Cancer Statistics.** Canadian Cancer Statistics 2015. 2015. Available at: http://www.cancer.ca/en/cancer-information/cancer-101/canadian-cancer-statistics-publication/?region=bc.

3. **Walsh, Patrick C., DeWeese, Theodore L., Eisenberger, Mario A.** Localized prostate cancer. *N. Engl. J. Med.* 2007;357(26):2696–2705.

4. **Marrett LD, De P, Airia P, Dryer D.** Cancer in Canada in 2008. *Can. Med. Assoc. J.* 2008;179(11):1163–1170.

5. **Grönberg H.** Prostate cancer epidemiology. *Lancet* 2003;361(9360):859–864.

6. **Crawford ED.** Epidemiology of prostate cancer. *Urology* 2003;62(6 Suppl 1):3–12.

7. **Zhang L, Yang B-X, Zhang H-T, Wang J-G, Wang H-L, Zhao X-J.** Prostate cancer: an emerging threat to the health of aging men in Asia. *Asian J. Androl.* 2011;13(4):574–578.

8. **Carpten JD, Trent JM.** Inherited genetic changes in prostate cancer. In: *Prostate Cancer: Signaling Networks, Genetics, and New Treatment Strategies*. Totowa, NJ: Humana Press; 2008:53–70.

9. **Bratt O.** Hereditary Prostate Cancer: Clinical Aspects. *J. Urol.* 2002;168(3):906–913.

10. **Ostrander EA, Udler MS.** The role of the BRCA2 gene in susceptibility to prostate cancer revisited. *Cancer Epidemiol. Biomark. Prev. Publ. Am. Assoc. Cancer Res. Cosponsored Am. Soc. Prev. Oncol.* 2008;17(8):1843–1848.

11. **Eeles RA, Kote-Jarai Z, Giles GG, Olama AAA, Guy M, Jugurnauth SK, Mulholland S, Leongamornlert DA, Edwards SM, Morrison J, Field HI, Southey MC, Severi G, Donovan JL, Hamdy FC, Dearnaley DP, Muir KR, Smith C, Bagnato M, Ardern-Jones AT, Hall AL, O'Brien LT, Gehr-Swain BN, Wilkinson RA, Cox A, Lewis S, Brown PM, Jhavar SG, Tymrakiewicz M, Lophatananon A, Bryant SL, UK Genetic Prostate Cancer Study Collaborators, British Association of Urological Surgeons' Section of Oncology, UK ProtecT Study Collaborators, Horwich A, Huddart RA, Khoo VS, Parker CC, Woodhouse CJ, Thompson A, Christmas T, Ogden C, Fisher C, Jamieson C, Cooper CS, English DR, Hopper JL, Neal DE, Easton DF.** Multiple newly identified loci associated with prostate cancer susceptibility. *Nat. Genet.* 2008;40(3):316–321.

12. **Lindström S, Wiklund F, Adami H-O, Bälter KA, Adolfsson J, Grönberg H.** Germ-line genetic variation in the key androgen-regulating genes androgen receptor, cytochrome

P450, and steroid-5-alpha-reductase type 2 is important for prostate cancer development. *Cancer Res.* 2006;66(22):11077–11083.

13. **Locke JA.** De novo androgen synthesis as a mechanism contributing to the progression of prostate cancer to castration resistance. 2005. Available at: https://circle.ubc.ca/bitstream/handle/2429/8731/ubc_2009_fall_locke_jennifer.pdf;jsessionid=43D241779083131B0F5347E21B5616DD.route1?sequence=1.

14. **Giovannucci E, Rimm EB, Colditz GA, Stampfer MJ, Ascherio A, Chute CG, Chute CC, Willett WC.** A prospective study of dietary fat and risk of prostate cancer. *J. Natl. Cancer Inst.* 1993;85(19):1571–1579.

15. **Wright ME, Bowen P, Virtamo J, Albanes D, Gann PH.** Estimated phytanic acid intake and prostate cancer risk: a prospective cohort study. *Int. J. Cancer J. Int. Cancer* 2012;131(6):1396–1406.

16. **Whittemore AS, Kolonel LN, Wu AH, John EM, Gallagher RP, Howe GR, Burch JD, Hankin J, Dreon DM, West DW.** Prostate cancer in relation to diet, physical activity, and body size in blacks, whites, and Asians in the United States and Canada. *J. Natl. Cancer Inst.* 1995;87(9):652–661.

17. **Kolonel LN, Hankin JH, Lee J, Chu SY, Nomura AM, Hinds MW.** Nutrient intakes in relation to cancer incidence in Hawaii. *Br. J. Cancer* 1981;44(3):332–339.

18. **Wang Y, Corr JG, Thaler HT, Tao Y, Fair WR, Heston WD.** Decreased growth of established human prostate LNCaP tumors in nude mice fed a low-fat diet. *J. Natl. Cancer Inst.* 1995;87(19):1456–1462.

19. **Farnsworth WE.** Prostate Stroma: Physiology. *Prostate* 1999;38(1):60–72.

20. **Lee CH, Akin-Olugbade O, Kirschenbaum A.** Overview of Prostate Anatomy, Histology, and Pathology. *Endocrinol. Metab. Clin. North Am.* 2011;40(3):565–575.

21. **Yeh S, Niu Y, Miyamoto H, Chang T, Chang C.** Differential Roles of Androgen Receptor in Prostate Development and Cancer Progression. In: Mohler J, Tindall D, eds. *Androgen Action in Prostate Cancer*. New York, NY: Springer; 2009:73–89.

22. **Cunha GR, Ricke W, Thomson A, Marker PC, Risbridger G, Hayward SW, Wang YZ, Donjacour AA, Kurita T.** Hormonal, cellular, and molecular regulation of normal and neoplastic prostatic development. *J. Steroid Biochem. Mol. Biol.* 2004;92(4):221–236.

23. **Matsumoto T, Sakari M, Okada M, Yokoyama A, Takahashi S, Kouzmenko A, Kato S.** The Androgen Receptor in Health and Disease. *Annu. Rev. Physiol.* 2013;75(1):201–224.

24. **Dehm SM, Tindall DJ.** Androgen Receptor Structural and Functional Elements: Role and Regulation in Prostate Cancer. *Mol. Endocrinol.* 2007;21(12):2855–2863.

25. **Veveris-Lowe TL, Kruger SJ, Walsh T, Gardiner RA, Clements JA.** Seminal fluid characterization for male fertility and prostate cancer: kallikrein-related serine proteases and whole proteome approaches. *Semin. Thromb. Hemost.* 2007;33(1):87–99.

26. **Stewart AB, Anderson W, Delves G, Lwaleed BA, Birch B, Cooper A.** Prostasomes: a role in prostatic disease? *BJU Int.* 2004;94(7):985–989.

27. **Vogelstein B, Fearon ER, Hamilton SR, Kern SE, Preisinger AC, Leppert M, Nakamura Y, White R, Smits AM, Bos JL.** Genetic alterations during colorectal-tumor development. *N. Engl. J. Med.* 1988;319(9):525–532.

28. **Hanahan D, Weinberg RA.** The hallmarks of cancer. *cell* 2000;100(1):57–70.

29. **Hanahan D, Weinberg RA.** Hallmarks of cancer: the next generation. *Cell* 2011;144(5):646–674.

30. **Wyatt AW, Gleave ME.** Targeting the adaptive molecular landscape of castration-resistant prostate cancer. *EMBO Mol. Med.* 2015;7(7):878–894.

31. **Gelmann EP.** Prostate Molecular Oncogenesis. In: *Prostate Cancer: Signaling Networks, Genetics, and New Treatment Strategies*. Totowa, NJ: Humana Press; 2008:71–97.

32. **Taylor BS, Schultz N, Hieronymus H, Gopalan A, Xiao Y, Carver BS, Arora VK, Kaushik P, Cerami E, Reva B, Antipin Y, Mitsiades N, Landers T, Dolgalev I, Major JE, Wilson M, Socci ND, Lash AE, Heguy A, Eastham JA, Scher HI, Reuter VE, Scardino PT, Sander C, Sawyers CL, Gerald WL.** Integrative Genomic Profiling of Human Prostate Cancer. *Cancer Cell* 2010;18(1):11–22.

33. **Baca SC, Prandi D, Lawrence MS, Mosquera JM, Romanel A, Drier Y, Park K, Kitabayashi N, MacDonald TY, Ghandi M, Van Allen E, Kryukov GV, Sboner A, Theurillat J-P, Soong TD, Nickerson E, Auclair D, Tewari A, Beltran H, Onofrio RC, Boysen G, Guiducci C, Barbieri CE, Cibulskis K, Sivachenko A, Carter SL, Saksena G, Voet D, Ramos AH, Winckler W, Cipicchio M, Ardlie K, Kantoff PW, Berger MF, Gabriel SB, Golub TR, Meyerson M, Lander ES, Elemento O, Getz G, Demichelis F, Rubin MA, Garraway LA.** Punctuated evolution of prostate cancer genomes. *Cell* 2013;153(3):666–677.

34. **Wyatt AW, Mo F, Wang K, McConeghy B, Brahmbhatt S, Jong L, Mitchell DM, Johnston RL, Haegert A, Li E, Liew J, Yeung J, Shrestha R, Lapuk AV, McPherson A, Shukin R, Bell RH, Anderson S, Bishop J, Hurtado-Coll A, Xiao H, Chinnaiyan AM, Mehra R, Lin D, Wang Y, Fazli L, Gleave ME, Volik SV, Collins CC.** Heterogeneity in the inter-tumor transcriptome of high risk prostate cancer. *Genome Biol.* 2014;15(8):426.

35. **Miyamoto H, Altuwaijri S, Chang C.** Androgen Receptor in Prostate Cancer Progression. In: *Prostate Cancer: Signaling Networks, Genetics, and New Treatment Strategies*. Totowa, NJ: Humana Press; 2008:129–146.

36. **Denmeade SR, Isaacs JT.** A history of prostate cancer treatment. *Nat. Rev. Cancer* 2002;2(5):389–396.

37. **Huggins C, Hodges CV.** Studies on prostatic cancer. I. The effect of castration, of estrogen and of androgen injection on serum phosphatases in metastatic carcinoma of the prostate. 1941. *J. Urol.* 2002;167(2 Pt 2):948–951; discussion 952.

38. **Rousseau GG.** Fifty years ago: The quest for steroid hormone receptors. *Mol. Cell. Endocrinol.* 2013;375(1–2):10–13.

39. **Biddie SC, John S, Hager GL.** Genome-wide mechanisms of nuclear receptor action. *Trends Endocrinol. Metab.* 2010;21(1):3–9.

40. **So AI, Hurtado-Coll A, Gleave ME.** Androgens and prostate cancer. *World J. Urol.* 2003;21(5):325–337.

41. **Sharifi N, Auchus RJ.** Steroid biosynthesis and prostate cancer. *Steroids* 2012;77(7):719–726.

42. **Auchus RJ.** The backdoor pathway to dihydrotestosterone. *Trends Endocrinol. Metab.* 2004;15(9):432–438.

43. **Feldman BJ, Feldman D.** The development of androgen-independent prostate cancer. *Nat. Rev. Cancer* 2001;1(1):34–45.

44. **Vis AN, Schröder FH.** Key targets of hormonal treatment of prostate cancer. Part 1: the androgen receptor and steroidogenic pathways. *BJU Int.* 2009;104(4):438–448.

45. **Sharifi N, Farrar WL.** Androgen receptor as a therapeutic target for androgen independent prostate cancer. *Am. J. Ther.* 2006;13(2):166–170.

46. **Wang Z, ed.** *Androgen-Responsive Genes in Prostate Cancer*. New York, NY: Springer New York; 2013.

47. **Locke JA, Guns ES, Lubik AA, Adomat HH, Hendy SC, Wood CA, Ettinger SL, Gleave ME, Nelson CC.** Androgen levels increase by intratumoral de novo steroidogenesis during progression of castration-resistant prostate cancer. *Cancer Res.* 2008;68(15):6407–6415.

48. **Lamont KR, Tindall DJ.** Androgen Regulation of Gene Expression. In: *Advances in Cancer Research*.Vol 107. Elsevier; 2010:137–162.

49. **Swinnen JV, Ulrix W, Heyns W, Verhoeven G.** Coordinate regulation of lipogenic gene expression by androgens: evidence for a cascade mechanism involving sterol regulatory element binding proteins. *Proc. Natl. Acad. Sci. U. S. A.* 1997;94(24):12975–12980.

50. **Heemers H, Maes B, Foufelle F, Heyns W, Verhoeven G, Swinnen JV.** Androgens stimulate lipogenic gene expression in prostate cancer cells by activation of the sterol regulatory element-binding protein cleavage activating protein/sterol regulatory element-binding protein pathway. *Mol. Endocrinol.* 2001;15(10):1817–1828.

51. **Heidenreich A, Bastian PJ, Bellmunt J, Bolla M, Joniau S, van der Kwast T, Mason M, Matveev V, Wiegel T, Zattoni F, Mottet N, European Association of Urology.** EAU guidelines on prostate cancer. part 1: screening, diagnosis, and local treatment with curative intent-update 2013. *Eur. Urol.* 2014;65(1):124–137.

52. **Hoffman RM.** Clinical practice. Screening for prostate cancer. *N. Engl. J. Med.* 2011;365(21):2013–2019.

53. **Smith DS, Catalona WJ.** Interexaminer variability of digital rectal examination in detecting prostate cancer. *Urology* 1995;45(1):70–74.

54. **Simmons MN, Berglund RK, Jones JS.** A practical guide to prostate cancer diagnosis and management. *Cleve. Clin. J. Med.* 2011;78(5):321–331.

55. **Balk SP.** Biology of Prostate-Specific Antigen. *J. Clin. Oncol.* 2003;21(2):383–391.

56. **Greene FL, Sobin LH.** The Staging of Cancer: A Retrospective and Prospective Appraisal. *CA. Cancer J. Clin.* 2008;58(3):180–190.

57. **Greene FL, Sobin LH.** The TNM system: Our language for cancer care. *J. Surg. Oncol.* 2002;80(3):119–120.

58. **Eggener SE, Badani K, Barocas DA, Barrisford GW, Cheng J-S, Chin AI, Corcoran A, Epstein JI, George AK, Gupta GN, Hayn MH, Kauffman EC, Lane B, Liss MA, Mirza M, Morgan TM, Moses K, Nepple KG, Preston MA, Rais-Bahrami S, Resnick MJ, Siddiqui MM, Silberstein J, Singer EA, Sonn GA, Sprenkle P, Stratton KL, Taylor J, Tomaszewski J, Tollefson M, Vickers A, White WM, Lowrance WT.** Gleason 6 Prostate Cancer: Translating Biology into Population Health. *J. Urol.* doi:10.1016/j.juro.2015.01.126.

59. **Cheuck, Lanna, Attala, Christopher, Ghiraldi, Eric.** Prostate Cancer Diagnosis and Staging: Practice Essentials, Overview, Relevant Anatomy. *Medscape* 2015. Available at: http://emedicine.medscape.com/article/458011-overview. Accessed July 4, 2015.

60. **Prognosis and survival for prostate cancer.** 2015. Available at: http://www.cancer.ca/en/cancer-information/cancer-type/prostate/prognosis-and-survival/?region=on.

61. **Markert EK, Mizuno H, Vazquez A, Levine AJ.** Molecular classification of prostate cancer using curated expression signatures. *Proc. Natl. Acad. Sci. U. S. A.* 2011;108(52):21276–21281.

62. **Ananthanarayanan V, Deaton RJ, Amatya A, Macias V, Luther E, Kajdacsy-Balla A, Gann PH.** Subcellular localization of p27 and prostate cancer recurrence: automated digital microscopy analysis of tissue microarrays. *Hum. Pathol.* 2011;42(6):873–881.

63. **Klotz L.** Active surveillance for low-risk prostate cancer. *Curr. Urol. Rep.* 2015;16(4):24.

64. **Pound CR, Partin AW, Eisenberger MA, Chan DW, Pearson JD, Walsh PC.** Natural history of progression after PSA elevation following radical prostatectomy. *JAMA* 1999;281(17):1591–1597.

65. **Antonarakis ES, Feng Z, Trock BJ, Humphreys EB, Carducci MA, Partin AW, Walsh PC, Eisenberger MA.** The natural history of metastatic progression in men with prostate-specific antigen recurrence after radical prostatectomy: long-term follow-up. *BJU Int.* 2012;109(1):32–39.

66. **Martin SK, Kyprianou N.** Exploitation of the Androgen Receptor to Overcome Taxane Resistance in Advanced Prostate Cancer. *Adv. Cancer Res.* 2015;127:123–158.

67. **Han M, Partin AW, Pound CR, Epstein JI, Walsh PC.** Long-term biochemical disease-free and cancer-specific survival following anatomic radical retropubic prostatectomy. The 15-year Johns Hopkins experience. *Urol. Clin. North Am.* 2001;28(3):555–565.

68. **Eggener SE, Scardino PT, Walsh PC, Han M, Partin AW, Trock BJ, Feng Z, Wood DP, Eastham JA, Yossepowitch O, Rabah DM, Kattan MW, Yu C, Klein EA, Stephenson AJ.** Predicting 15-year prostate cancer specific mortality after radical prostatectomy. *J. Urol.* 2011;185(3):869–875.

69. **Demanes DJ, Rodriguez RR, Schour L, Brandt D, Altieri G.** High-dose-rate intensity-modulated brachytherapy with external beam radiotherapy for prostate cancer: California endocurietherapy's 10-year results. *Int. J. Radiat. Oncol. Biol. Phys.* 2005;61(5):1306–1316.

70. **Heidenreich A, Bastian PJ, Bellmunt J, Bolla M, Joniau S, van der Kwast T, Mason M, Matveev V, Wiegel T, Zattoni F, Mottet N.** EAU Guidelines on Prostate Cancer. Part II: Treatment of Advanced, Relapsing, and Castration-Resistant Prostate Cancer. *Eur. Urol.* 2014;65(2):467–479.

71. **Sharifi N, Gulley JL, Dahut WL.** Androgen deprivation therapy for prostate cancer. *J. Am. Med. Assoc.* 2005;294(2):238–244.

72. **Connolly RM, Carducci MA, Antonarakis ES.** Use of androgen deprivation therapy in prostate cancer: indications and prevalence. *Asian J. Androl.* 2012;14(2):177–186.

73. **Labrie F.** Medical castration with LHRH agonists: 25 years later with major benefits achieved on survival in prostate cancer. *J. Androl.* 2004;25(3):305–313.

74. **Klotz L.** Maximal androgen blockade for advanced prostate cancer. *Best Pract. Res. Clin. Endocrinol. Metab.* 2008;22(2):331–340.

75. **Greasley R, Khabazhaitajer M, Rosario DJ.** A profile of enzalutamide for the treatment of advanced castration resistant prostate cancer. *Cancer Manag. Res.* 2015;7:153–164.

76. **Badrising S, van der Noort V, van Oort IM, van den Berg HP, Los M, Hamberg P, Coenen JL, van den Eertwegh AJM, de Jong IJ, Kerver ED, van Tinteren H, Bergman AM.** Clinical activity and tolerability of enzalutamide (MDV3100) in patients with metastatic, castration-resistant prostate cancer who progress after docetaxel and abiraterone treatment. *Cancer* 2014;120(7):968–975.

77. **Beer TM, Armstrong AJ, Rathkopf DE, Loriot Y, Sternberg CN, Higano CS, Iversen P, Bhattacharya S, Carles J, Chowdhury S, Davis ID, de Bono JS, Evans CP, Fizazi K, Joshua AM, Kim C-S, Kimura G, Mainwaring P, Mansbach H, Miller K, Noonberg SB, Perabo F, Phung D, Saad F, Scher HI, Taplin M-E, Venner PM, Tombal B, PREVAIL Investigators.** Enzalutamide in metastatic prostate cancer before chemotherapy. *N. Engl. J. Med.* 2014;371(5):424–433.

78. **Lorente D, Mateo J, Perez-Lopez R, de Bono JS, Attard G.** Sequencing of agents in castration-resistant prostate cancer. *Lancet Oncol.* 2015;16(6):e279–e292.

79. **Grist E, Attard G.** The development of abiraterone acetate for castration-resistant prostate cancer. *Urol. Oncol.* 2015;33(6):289–294.

80. **De Bono JS, Logothetis CJ, Molina A, Fizazi K, North S, Chu L, Chi KN, Jones RJ, Goodman OB, Saad F, Staffurth JN, Mainwaring P, Harland S, Flaig TW, Hutson TE, Cheng T, Patterson H, Hainsworth JD, Ryan CJ, Sternberg CN, Ellard SL, Fléchon A, Saleh M, Scholz M, Efstathiou E, Zivi A, Bianchini D, Loriot Y, Chieffo N, Kheoh T, Haqq CM, Scher HI.** Abiraterone and Increased Survival in Metastatic Prostate Cancer. *N. Engl. J. Med.* 2011;364(21):1995–2005.

81. **Fizazi K, Scher HI, Molina A, Logothetis CJ, Chi KN, Jones RJ, Staffurth JN, North S, Vogelzang NJ, Saad F, Mainwaring P, Harland S, Goodman Jr OB, Sternberg CN, Li JH, Kheoh T, Haqq CM, de Bono JS.** Abiraterone acetate for treatment of metastatic castration-resistant prostate cancer: final overall survival analysis of the COU-AA-301 randomised, double-blind, placebo-controlled phase 3 study. *Lancet Oncol.* 2012;13(10):983–992.

82. **Berthold DR, Pond GR, Soban F, de Wit R, Eisenberger M, Tannock IF.** Docetaxel Plus Prednisone or Mitoxantrone Plus Prednisone for Advanced Prostate Cancer: Updated Survival in the TAX 327 Study. *J. Clin. Oncol.* 2008;26(2):242–245.

83. **Petrylak DP, Tangen CM, Hussain MH, Lara Jr PN, Jones JA, Taplin ME, Burch PA, Berry D, Moinpour C, Kohli M, others.** Docetaxel and estramustine compared with mitoxantrone and prednisone for advanced refractory prostate cancer. *N. Engl. J. Med.* 2004;351(15):1513–1520.

84. **Lorente D, De Bono JS.** Molecular alterations and emerging targets in castration resistant prostate cancer. *Eur. J. Cancer* 2014;50(4):753–764.

85. **Petrioli R, Francini E, Laera L, Fiaschi AI, Ponchietti R, Roviello G.** Role of chemotherapy in the treatment of metastatic castration-resistant prostate cancer patients who have progressed after abiraterone acetate. *Cancer Chemother. Pharmacol.* 2015. doi:10.1007/s00280-015-2803-y.

86. **De Bono JS, Oudard S, Ozguroglu M, Hansen S, Machiels J-P, Kocak I, Gravis G, Bodrogi I, Mackenzie MJ, Shen L, Roessner M, Gupta S, Sartor AO, TROPIC Investigators.** Prednisone plus cabazitaxel or mitoxantrone for metastatic castration-resistant prostate cancer progressing after docetaxel treatment: a randomised open-label trial. *Lancet Lond. Engl.* 2010;376(9747):1147–1154.

87. **Francini E, Fiaschi AI, Petrioli R, Laera L, Bianco V, Ponchietti R, Roviello G.** Tolerability of cabazitaxel in patients with metastatic castration-resistant prostate cancer progressing after docetaxel and abiraterone acetate: a single-institution experience. *Anticancer. Drugs* 2015. doi:10.1097/CAD.0000000000000257.

88. **Bahl A, Masson S, Birtle A, Chowdhury S, de Bono J.** Second-line treatment options in metastatic castration-resistant prostate cancer: a comparison of key trials with recently approved agents. *Cancer Treat. Rev.* 2014;40(1):170–177.

89. **Body J-J, Casimiro S, Costa L.** Targeting bone metastases in prostate cancer: improving clinical outcome. *Nat. Rev. Urol.* 2015;12(6):340–356.

90. **El-Amm J, Freeman A, Patel N, Aragon-Ching JB.** Bone-targeted therapies in metastatic castration-resistant prostate cancer: evolving paradigms. *Prostate Cancer* 2013;2013:210686.

91. **Gartrell BA, Saad F.** Managing bone metastases and reducing skeletal related events in prostate cancer. *Nat. Rev. Clin. Oncol.* 2014;11(6):335–345.

92. **El-Amm J, Aragon-Ching JB.** Radium-223 for the treatment of castration-resistant prostate cancer. *OncoTargets Ther.* 2015;8:1103–1109.

93. **Saad F, Chi KN, Finelli A, Hotte SJ, Izawa J, Kapoor A, Kassouf W, Loblaw A, North S, Rendon R, So A, Usmani N, Vigneault E, Fleshner NE.** The 2015 CUA-CUOG Guidelines for the management of castration-resistant prostate cancer (CRPC). *Can. Urol. Assoc. J. J. Assoc. Urol. Can.* 2015;9(3-4):90–96.

94. **Dougan M, Dranoff G.** Immune therapy for cancer. *Annu. Rev. Immunol.* 2009;27:83–117.

95. **Cavallo F, De Giovanni C, Nanni P, Forni G, Lollini P-L.** 2011: the immune hallmarks of cancer. *Cancer Immunol. Immunother.* 2011;60(3):319–326.

96. **Gomella LG, Gelpi-Hammerschmidt F, Kundavram C.** Practical guide to immunotherapy in castration resistant prostate cancer: the use of sipuleucel-T immunotherapy. *Can. J. Urol.* 2014;21(2 Supp 1):48–56.

97. **Mulders PF, De Santis M, Powles T, Fizazi K.** Targeted treatment of metastatic castration-resistant prostate cancer with sipuleucel-T immunotherapy. *Cancer Immunol. Immunother.* 2015;64(6):655–663.

98. **Zhang F, Kumano M, Beraldi E, Fazli L, Du C, Moore S, Sorensen P, Zoubeidi A, Gleave ME.** Clusterin facilitates stress-induced lipidation of LC3 and autophagosome biogenesis to enhance cancer cell survival. *Nat. Commun.* 2014;5. doi:10.1038/ncomms6775.

99. **Leist M, Jäättelä M.** Four deaths and a funeral: from caspases to alternative mechanisms. *Nat. Rev. Mol. Cell Biol.* 2001;2(8):589–598.

100. **Thorburn A.** Apoptosis and autophagy: regulatory connections between two supposedly different processes. *Apoptosis Int. J. Program. Cell Death* 2008;13(1):1–9.

101. **Jin Z, El-Deiry WS.** Overview of cell death signaling pathways. *Cancer Biol. Ther.* 2005;4(2):139–163.

102. **Nikoletopoulou V, Markaki M, Palikaras K, Tavernarakis N.** Crosstalk between apoptosis, necrosis and autophagy. *Biochim. Biophys. Acta* 2013;1833(12):3448–3459.

103. **Gleave ME, Cox ME, Wang Y.** Cell Biology of Prostate Cancer and Molecular Targets. In: Figg WD, Chau CH, Small EJ, eds. *Drug Management of Prostate Cancer*. New York, NY: Springer New York; 2010:1–24.

104. **Blagosklonny MV, Schulte T, Nguyen P, Trepel J, Neckers LM.** Taxol-induced apoptosis and phosphorylation of Bcl-2 protein involves c-Raf-1 and represents a novel c-Raf-1 signal transduction pathway. *Cancer Res.* 1996;56(8):1851–1854.

105. **Hwang C.** Overcoming docetaxel resistance in prostate cancer: a perspective review. *Ther. Adv. Med. Oncol.* 2012;4(6):329–340.

106. **Agus DB, Cordon-Cardo C, Fox W, Drobnjak M, Koff A, Golde DW, Scher HI.** Prostate cancer cell cycle regulators: response to androgen withdrawal and development of androgen independence. *J. Natl. Cancer Inst.* 1999;91(21):1869–1876.

107. **Scher HI, Sawyers CL.** Biology of progressive, castration-resistant prostate cancer: directed therapies targeting the androgen-receptor signaling axis. *J. Clin. Oncol. Off. J. Am. Soc. Clin. Oncol.* 2005;23(32):8253–8261.

108. **Eisenberger MA, Blumenstein BA, Crawford ED, Miller G, McLeod DG, Loehrer PJ, Wilding G, Sears K, Culkin DJ, Thompson IM, Bueschen AJ, Lowe BA.** Bilateral orchiectomy with or without flutamide for metastatic prostate cancer. *N. Engl. J. Med.* 1998;339(15):1036–1042.

109. **Wainstein MA, He F, Robinson D, Kung HJ, Schwartz S, Giaconia JM, Edgehouse NL, Pretlow TP, Bodner DR, Kursh ED.** CWR22: androgen-dependent xenograft model derived from a primary human prostatic carcinoma. *Cancer Res.* 1994;54(23):6049–6052.

110. **Nagabhushan M, Miller CM, Pretlow TP, Giaconia JM, Edgehouse NL, Schwartz S, Kung HJ, de Vere White RW, Gumerlock PH, Resnick MI, Amini SB, Pretlow TG.** CWR22: the first human prostate cancer xenograft with strongly androgen-dependent and relapsed strains both in vivo and in soft agar. *Cancer Res.* 1996;56(13):3042–3046.

111. **Lowe SW, Lin AW.** Apoptosis in cancer. *Carcinogenesis* 2000;21(3):485–495.

112. **Vanden Berghe T, Linkermann A, Jouan-Lanhouet S, Walczak H, Vandenabeele P.** Regulated necrosis: the expanding network of non-apoptotic cell death pathways. *Nat. Rev. Mol. Cell Biol.* 2014;15(2):135–147.

113. **Holler N, Zaru R, Micheau O, Thome M, Attinger A, Valitutti S, Bodmer JL, Schneider P, Seed B, Tschopp J.** Fas triggers an alternative, caspase-8-independent cell death pathway using the kinase RIP as effector molecule. *Nat. Immunol.* 2000;1(6):489–495.

114. **Zong W-X, Ditsworth D, Bauer DE, Wang Z-Q, Thompson CB.** Alkylating DNA damage stimulates a regulated form of necrotic cell death. *Genes Dev.* 2004;18(11):1272–1282.

115. **Tse BWC, Scott KF, Russell PJ.** Paradoxical Roles of Tumour Necrosis Factor-Alpha in Prostate Cancer Biology. *Prostate Cancer* 2012;2012:e128965.

116. **Davis JS, Nastiuk KL, Krolewski JJ.** TNF is necessary for castration-induced prostate regression, whereas TRAIL and FasL are dispensable. *Mol. Endocrinol.* 2011;25(4):611–620.

117. **Harada S, Keller ET, Fujimoto N, Koshida K, Namiki M, Matsumoto T, Mizokami A.** Long-term exposure of tumor necrosis factor alpha causes hypersensitivity to androgen and anti-androgen withdrawal phenomenon in LNCaP prostate cancer cells. *Prostate* 2001;46(4):319–326.

118. **Fujimoto N, Miyamoto H, Mizokami A, Harada S, Nomura M, Ueta Y, Sasaguri T, Matsumoto T.** Prostate cancer cells increase androgen sensitivity by increase in nuclear

androgen receptor and androgen receptor coactivators; a possible mechanism of hormone-resistance of prostate cancer cells. *Cancer Invest.* 2007;25(1):32–37.

119. **Mizushima N, Yoshimori T.** How to Interpret LC3 Immunoblotting. *Autophagy* 2007;3(6):542–545.

120. **Jones SE, Jomary C.** Clusterin. *Int. J. Biochem. Cell Biol.* 2002;34(5):427–431.

121. **Wyatt AR, Yerbury JJ, Berghofer P, Greguric I, Katsifis A, Dobson CM, Wilson MR.** Clusterin facilitates in vivo clearance of extracellular misfolded proteins. *Cell. Mol. Life Sci.* 2011;68(23):3919–3931.

122. **Yom CK, Woo H-Y, Min SY, Kang SY, Kim HS.** Clusterin overexpression and relapse-free survival in breast cancer. *Anticancer Res.* 2009;29(10):3909–3912.

123. **July LV, Akbari M, Zellweger T, Jones EC, Goldenberg SL, Gleave ME.** Clusterin expression is significantly enhanced in prostate cancer cells following androgen withdrawal therapy. *Prostate* 2002;50(3):179–188.

124. **Boutin B, Tajeddine N, Vandersmissen P, Zanou N, Van Schoor M, Mondin L, Courtoy PJ, Tombal B, Gailly P.** Androgen deprivation and androgen receptor competition by bicalutamide induce autophagy of hormone-resistant prostate cancer cells and confer resistance to apoptosis. *Prostate* 2013;73(10):1090–1102.

125. **Kuilman T, Michaloglou C, Mooi WJ, Peeper DS.** The essence of senescence. *Genes Dev.* 2010;24(22):2463–2479.

126. **Hayflick L, Moorhead PS.** The serial cultivation of human diploid cell strains. *Exp. Cell Res.* 1961;25:585–621.

127. **Hayflick L.** The limited in vitro lifetime of human diploid cell strains. *Exp. Cell Res.* 1965;37:614–636.

128. **D' Adda di Fagagna F, Reaper PM, Clay-Farrace L, Fiegler H, Carr P, Von Zglinicki T, Saretzki G, Carter NP, Jackson SP.** A DNA damage checkpoint response in telomere-initiated senescence. *Nature* 2003;426(6963):194–198.

129. **Fujita K, Mondal AM, Horikawa I, Nguyen GH, Kumamoto K, Sohn JJ, Bowman ED, Mathe EA, Schetter AJ, Pine SR, Ji H, Vojtesek B, Bourdon J-C, Lane DP, Harris CC.** p53 isoforms Delta133p53 and p53beta are endogenous regulators of replicative cellular senescence. *Nat. Cell Biol.* 2009;11(9):1135–1142.

130. **Shay JW, Pereira-Smith OM, Wright WE.** A role for both RB and p53 in the regulation of human cellular senescence. *Exp. Cell Res.* 1991;196(1):33–39.

131. **Ben-Porath I, Weinberg RA.** The signals and pathways activating cellular senescence. *Int. J. Biochem. Cell Biol.* 2005;37(5):961–976.

132. **Rodier F, Campisi J.** Four faces of cellular senescence. *J. Cell Biol.* 2011;192(4):547–556.

133. **Pérez-Mancera PA, Young ARJ, Narita M.** Inside and out: the activities of senescence in cancer. *Nat. Rev. Cancer* 2014;14(8):547–558.

134. **Goldenberg SL, Gleave ME, Taylor D, Bruchovsky N.** Clinical Experience with Intermittent Androgen Suppression in Prostate Cancer: Minimum of 3 Years' Follow-Up. *Mol. Urol.* 1999;3(3):287–292.

135. **Visakorpi T, Hyytinen E, Koivisto P, Tanner M, Keinänen R, Palmberg C, Palotie A, Tammela T, Isola J, Kallioniemi OP.** In vivo amplification of the androgen receptor gene and progression of human prostate cancer. *Nat. Genet.* 1995;9(4):401–406.

136. **Koivisto P, Kononen J, Palmberg C, Tammela T, Hyytinen E, Isola J, Trapman J, Cleutjens K, Noordzij A, Visakorpi T, Kallioniemi OP.** Androgen receptor gene amplification: a possible molecular mechanism for androgen deprivation therapy failure in prostate cancer. *Cancer Res.* 1997;57(2):314–319.

137. **Holzbeierlein J, Lal P, LaTulippe E, Smith A, Satagopan J, Zhang L, Ryan C, Smith S, Scher H, Scardino P, Reuter V, Gerald WL.** Gene expression analysis of human prostate carcinoma during hormonal therapy identifies androgen-responsive genes and mechanisms of therapy resistance. *Am. J. Pathol.* 2004;164(1):217–227.

138. **Sun C, Shi Y, Xu LL, Nageswararao C, Davis LD, Segawa T, Dobi A, McLeod DG, Srivastava S.** Androgen receptor mutation (T877A) promotes prostate cancer cell growth and cell survival. *Oncogene* 2006;25(28):3905–3913.

139. **Chen EJ, Sowalsky AG, Gao S, Cai C, Voznesensky O, Schaefer R, Loda M, True LD, Ye H, Troncoso P, Lis RL, Kantoff PW, Montgomery RB, Nelson PS, Bubley GJ, Balk SP, Taplin M-E.** Abiraterone treatment in castration-resistant prostate cancer selects for progesterone responsive mutant androgen receptors. *Clin. Cancer Res.* 2015;21(6):1273–1280.

140. **Krishnan AV, Zhao X-Y, Swami S, Brive L, Peehl DM, Ely KR, Feldman D.** A glucocorticoid-responsive mutant androgen receptor exhibits unique ligand specificity: therapeutic implications for androgen-independent prostate cancer. *Endocrinology* 2002;143(5):1889–1900.

141. **Carreira S, Romanel A, Goodall J, Grist E, Ferraldeschi R, Miranda S, Prandi D, Lorente D, Frenel J-S, Pezaro C, Omlin A, Rodrigues DN, Flohr P, Tunariu N, de Bono JS, Demichelis F, Attard G.** Tumor clone dynamics in lethal prostate cancer. *Sci. Transl. Med.* 2014;6(254):254ra125.

142. **Gregory CW, He B, Johnson RT, Ford OH, Mohler JL, French FS, Wilson EM.** A mechanism for androgen receptor-mediated prostate cancer recurrence after androgen deprivation therapy. *Cancer Res.* 2001;61(11):4315–4319.

143. **Culig Z, Hobisch A, Cronauer MV, Radmayr C, Trapman J, Hittmair A, Bartsch G, Klocker H.** Androgen receptor activation in prostatic tumor cell lines by insulin-like growth factor-I, keratinocyte growth factor, and epidermal growth factor. *Cancer Res.* 1994;54(20):5474–5478.

144. **Craft N, Shostak Y, Carey M, Sawyers CL.** A mechanism for hormone-independent prostate cancer through modulation of androgen receptor signaling by the HER-2/neu tyrosine kinase. *Nat. Med.* 1999;5(3):280–285.

145. **Yeh S, Lin HK, Kang HY, Thin TH, Lin MF, Chang C.** From HER2/Neu signal cascade to androgen receptor and its coactivators: a novel pathway by induction of androgen target genes through MAP kinase in prostate cancer cells. *Proc. Natl. Acad. Sci. U. S. A.* 1999;96(10):5458–5463.

146. **Wen Y, Hu MC, Makino K, Spohn B, Bartholomeusz G, Yan DH, Hung MC.** HER-2/neu promotes androgen-independent survival and growth of prostate cancer cells through the Akt pathway. *Cancer Res.* 2000;60(24):6841–6845.

147. **Antonarakis ES, Lu C, Wang H, Luber B, Nakazawa M, Roeser JC, Chen Y, Mohammad TA, Chen Y, Fedor HL, Lotan TL, Zheng Q, De Marzo AM, Isaacs JT, Isaacs WB, Nadal R, Paller CJ, Denmeade SR, Carducci MA, Eisenberger MA, Luo J.** AR-V7 and resistance to enzalutamide and abiraterone in prostate cancer. *N. Engl. J. Med.* 2014;371(11):1028–1038.

148. **Sedelaar JPM, Isaacs JT.** Tissue culture media supplemented with 10% fetal calf serum contains a castrate level of testosterone. *Prostate* 2009;69(16):1724–1729.

149. **Geller J.** Megestrol acetate plus low-dose estrogen in the management of advanced prostatic carcinoma. *Urol. Clin. North Am.* 1991;18(1):83–91.

150. **Mohler JL, Gregory CW, Ford OH, Kim D, Weaver CM, Petrusz P, Wilson EM, French FS.** The androgen axis in recurrent prostate cancer. *Clin. Cancer Res. Off. J. Am. Assoc. Cancer Res.* 2004;10(2):440–448.

151. **Bhanalaph T, Varkarakis MJ, Murphy GP.** Current status of bilateral adrenalectomy or advanced prostatic carcinoma. *Ann. Surg.* 1974;179(1):17–23.

152. **Stanbrough M, Bubley GJ, Ross K, Golub TR, Rubin MA, Penning TM, Febbo PG, Balk SP.** Increased expression of genes converting adrenal androgens to testosterone in androgen-independent prostate cancer. *Cancer Res.* 2006;66(5):2815–2825.

153. **Hofland J, van Weerden WM, Dits NFJ, Steenbergen J, van Leenders GJLH, Jenster G, Schröder FH, de Jong FH.** Evidence of limited contributions for intratumoral steroidogenesis in prostate cancer. *Cancer Res.* 2010;70(3):1256–1264.

154. **Ikonen E.** Cellular cholesterol trafficking and compartmentalization. *Nat. Rev. Mol. Cell Biol.* 2008;9(2):125–138.

155. **Freeman MR, Solomon KR.** Cholesterol and prostate cancer. *J. Cell. Biochem.* 2004;91(1):54–69.

156. **Zadra G, Photopoulos C, Loda M.** The fat side of prostate cancer. *Biochim. Biophys. Acta* 2013;1831(10):1518–1532.

157. **Lange Y.** Disposition of intracellular cholesterol in human fibroblasts. *J. Lipid Res.* 1991;32(2):329–339.

158. **Beaven SW, Tontonoz P.** Nuclear Receptors in Lipid Metabolism: Targeting the Heart of Dyslipidemia. *Annu. Rev. Med.* 2006;57(1):313–329.

159. **Heemers HV, Verhoeven G, Swinnen JV.** Androgen Activation of the Sterol Regulatory Element-Binding Protein Pathway: Current Insights. *Mol. Endocrinol.* 2006;20(10):2265–2277.

160. **Calkin AC, Tontonoz P.** Transcriptional integration of metabolism by the nuclear sterol-activated receptors LXR and FXR. *Nat. Rev. Mol. Cell Biol.* 2012;13(4):213–224.

161. **Yeaman S.** Hormone-sensitive lipase-new roles for an old enzyme. *Biochem J* 2004;379:11–22.

162. **Miller WL.** Steroid hormone synthesis in mitochondria. *Mol. Cell. Endocrinol.* 2013;379(1-2):62–73.

163. **Locke JA, Guns EST, Lehman ML, Ettinger S, Zoubeidi A, Lubik A, Margiotti K, Fazli L, Adomat H, Wasan KM, Gleave ME, Nelson CC.** Arachidonic acid activation of intratumoral steroid synthesis during prostate cancer progression to castration resistance. *Prostate* 2010;70(3):239–251.

164. **Simons K, Ikonen E.** How Cells Handle Cholesterol. *Science* 2000;290(5497):1721–1726.

165. **Brown MS, Goldstein JL.** A proteolytic pathway that controls the cholesterol content of membranes, cells, and blood. *Proc. Natl. Acad. Sci. U. S. A.* 1999;96(20):11041–11048.

166. **Goldstein JL, DeBose-Boyd RA, Brown MS.** Protein Sensors for Membrane Sterols. *Cell* 2006;124(1):35–46.

167. **Nohturfft A, Yabe D, Goldstein JL, Brown MS, Espenshade PJ.** Regulated step in cholesterol feedback localized to budding of SCAP from ER membranes. *Cell* 2000;102(3):315–323.

168. **Radhakrishnan A, Ikeda Y, Kwon HJ, Brown MS, Goldstein JL.** Sterol-regulated transport of SREBPs from endoplasmic reticulum to Golgi: oxysterols block transport by binding to Insig. *Proc. Natl. Acad. Sci. U. S. A.* 2007;104(16):6511–6518.

169. **Adams CM, Reitz J, De Brabander JK, Feramisco JD, Li L, Brown MS, Goldstein JL.** Cholesterol and 25-hydroxycholesterol inhibit activation of SREBPs by different mechanisms, both involving SCAP and Insigs. *J. Biol. Chem.* 2004;279(50):52772–52780.

170. **Brown AJ, Sun L, Feramisco JD, Brown MS, Goldstein JL.** Cholesterol addition to ER membranes alters conformation of SCAP, the SREBP escort protein that regulates cholesterol metabolism. *Mol. Cell* 2002;10(2):237–245.

171. **DeBose-Boyd RA.** Feedback regulation of cholesterol synthesis: sterol-accelerated ubiquitination and degradation of HMG CoA reductase. *Cell Res.* 2008;18(6):609–621.

172. **Locke JA, Wasan KM, Nelson CC, Guns ES, Leon CG.** Androgen-mediated cholesterol metabolism in LNCaP and PC-3 cell lines is regulated through two different isoforms of acyl-coenzyme A:Cholesterol Acyltransferase (ACAT). *Prostate* 2008;68(1):20–33.

173. **Wasan KM, Brocks DR, Lee SD, Sachs-Barrable K, Thornton SJ.** Impact of lipoproteins on the biological activity and disposition of hydrophobic drugs: implications for drug discovery. *Nat. Rev. Drug Discov.* 2008;7(1):84–99.

174. **Acton S, Rigotti A, Landschulz KT, Xu S, Hobbs HH, Krieger M.** Identification of scavenger receptor SR-BI as a high density lipoprotein receptor. *Science* 1996;271(5248):518–520.

175. **Brown MS, Goldstein JL.** A receptor-mediated pathway for cholesterol homeostasis. *Science* 1986;232(4746):34–47.

176. **Zelcer N, Hong C, Boyadjian R, Tontonoz P.** LXR regulates cholesterol uptake through Idol-dependent ubiquitination of the LDL receptor. *Science* 2009;325(5936):100–104.

177. **Yannucci J, Manola J, Garnick MB, Bhat G, Bubley GJ.** The effect of androgen deprivation therapy on fasting serum lipid and glucose parameters. *J. Urol.* 2006;176(2):520–525.

178. **Sekine Y, Koike H, Nakano T, Nakajima K, Takahashi S, Suzuki K.** Remnant lipoproteins induced proliferation of human prostate cancer cell, PC-3 but not LNCaP, via low density lipoprotein receptor. *Cancer Epidemiol.* 2009;33(1):16–23.

179. **Sekine Y, Demosky SJ, Stonik JA, Furuya Y, Koike H, Suzuki K, Remaley AT.** High-density lipoprotein induces proliferation and migration of human prostate androgen-

independent cancer cells by an ABCA1-dependent mechanism. *Mol. Cancer Res. MCR* 2010;8(9):1284–1294.

180. **Leon CG, Locke JA, Adomat HH, Etinger SL, Twiddy AL, Neumann RD, Nelson CC, Guns ES, Wasan KM.** Alterations in cholesterol regulation contribute to the production of intratumoral androgens during progression to castration-resistant prostate cancer in a mouse xenograft model. *Prostate* 2009;70(4):390 – 400.

181. **Chen Y, Hughes-Fulford M.** Human prostate cancer cells lack feedback regulation of low-density lipoprotein receptor and its regulator, SREBP2. *Int. J. Cancer J. Int. Cancer* 2001;91(1):41–45.

182. **Krycer JR, Kristiana I, Brown AJ.** Cholesterol homeostasis in two commonly used human prostate cancer cell-lines, LNCaP and PC-3. *PloS One* 2009;4(12):e8496.

183. **Ettinger SL, Sobel R, Whitmore TG, Akbari M, Bradley DR, Gleave ME, Nelson CC.** Dysregulation of sterol response element-binding proteins and downstream effectors in prostate cancer during progression to androgen independence. *Cancer Res.* 2004;64(6):2212–2221.

184. **Parinaud J, Perret B, Ribbes H, Chap H, Pontonnier G, Douste-Blazy L.** High density lipoprotein and low density lipoprotein utilization by human granulosa cells for progesterone synthesis in serum-free culture: respective contributions of free and esterified cholesterol. *J. Clin. Endocrinol. Metab.* 1987;64(3):409–417.

185. **Enk L, Crona N, Hillensjö T.** High- and low-density lipoproteins stimulate progesterone production in cultured human granulosa cells. *Hum. Reprod.* 1987;2(4):291–295.

186. **Richardson MC, Davies DW, Watson RH, Dunsford ML, Inman CB, Masson GM.** Cultured human granulosa cells as a model for corpus luteum function: relative roles of gonadotrophin and low density lipoprotein studied under defined culture conditions. *Hum. Reprod.* 1992;7(1):12–18.

187. **Kraemer FB, Shen W-J, Patel S, Osuga J, Ishibashi S, Azhar S.** The LDL receptor is not necessary for acute adrenal steroidogenesis in mouse adrenocortical cells. *Am. J. Physiol. - Endocrinol. Metab.* 2007;292(2):E408–E412.

188. **Krieger M.** Charting the fate of the "good cholesterol": identification and characterization of the high-density lipoprotein receptor SR-BI. *Annu. Rev. Biochem.* 1999;68:523–558.

189. **Laue L, Hoeg JM, Barnes K, Loriaux DL, Chrousos GP.** The effect of mevinolin on steroidogenesis in patients with defects in the low density lipoprotein receptor pathway. *J. Clin. Endocrinol. Metab.* 1987;64(3):531–535.

190. **Illingworth DR, Kenny TA, Connor WE, Orwoll ES.** Corticosteroid production in abetalipoproteinemia: evidence for an impaired response ACTH. *J. Lab. Clin. Med.* 1982;100(1):115–126.

191. **Andersen JM, Dietschy JM.** Relative importance of high and low density lipoproteins in the regulation of cholesterol synthesis in the adrenal gland, ovary, and testis of the rat. *J. Biol. Chem.* 1978;253(24):9024–9032.

192. **Rigotti A, Miettinen HE, Krieger M.** The role of the high-density lipoprotein receptor SR-BI in the lipid metabolism of endocrine and other tissues. *Endocr. Rev.* 2003;24(3):357–387.

193. **Gu X, Trigatti B, Xu S, Acton S, Babitt J, Krieger M.** The Efficient Cellular Uptake of High Density Lipoprotein Lipids via Scavenger Receptor Class B Type I Requires Not Only Receptor-mediated Surface Binding but Also Receptor-specific Lipid Transfer Mediated by Its Extracellular Domain. *J. Biol. Chem.* 1998;273(41):26338–26348.

194. **Nieland TJ, Penman M, Dori L, Krieger M, Kirchhausen T.** Discovery of chemical inhibitors of the selective transfer of lipids mediated by the HDL receptor SR-BI. *Proc. Natl. Acad. Sci. U. S. A.* 2002;99(24):15422–15427.

195. **Landschulz KT, Pathak RK, Rigotti A, Krieger M, Hobbs HH.** Regulation of scavenger receptor, class B, type I, a high density lipoprotein receptor, in liver and steroidogenic tissues of the rat. *J. Clin. Invest.* 1996;98(4):984–995.

196. **Rigotti A, Edelman ER, Seifert P, Iqbal SN, DeMattos RB, Temel RE, Krieger M, Williams DL.** Regulation by adrenocorticotropic hormone of the in vivo expression of scavenger receptor class B type I (SR-BI), a high density lipoprotein receptor, in steroidogenic cells of the murine adrenal gland. *J. Biol. Chem.* 1996;271(52):33545–33549.

197. **Al-Jarallah A, Trigatti BL.** A role for the scavenger receptor, class B type I in high density lipoprotein dependent activation of cellular signaling pathways. *Biochim. Biophys. Acta BBA - Mol. Cell Biol. Lipids* 2010;1801(12):1239–1248.

198. **Grewal T, de Diego I, Kirchhoff MF, Tebar F, Heeren J, Rinninger F, Enrich C.** High density lipoprotein-induced signaling of the MAPK pathway involves scavenger receptor type BI-mediated activation of Ras. *J. Biol. Chem.* 2003;278(19):16478–16481.

199. **Wood P, Mulay V, Darabi M, Chan KC, Heeren J, Pol A, Lambert G, Rye K-A, Enrich C, Grewal T.** Ras/Mitogen-activated Protein Kinase (MAPK) Signaling Modulates Protein Stability and Cell Surface Expression of Scavenger Receptor SR-BI. *J. Biol. Chem.* 2011;286(26):23077–23092.

200. **Mineo C, Yuhanna IS, Quon MJ, Shaul PW.** High density lipoprotein-induced endothelial nitric-oxide synthase activation is mediated by Akt and MAP kinases. *J. Biol. Chem.* 2003;278(11):9142–9149.

201. **Cao G, Garcia CK, Wyne KL, Schultz RA, Parker KL, Hobbs HH.** Structure and Localization of the Human Gene Encoding SR-BI/CLA-1: Evidence for Transcriptional Control by Steroidogenic Factor 1. *J. Biol. Chem.* 1997;272(52):33068–33076.

202. **Gwynne JT, Mahaffee DD.** Rat adrenal uptake and metabolism of high density lipoprotein cholesteryl ester. *J. Biol. Chem.* 1989;264(14):8141–8150.

203. **Gwynne JT, Mahaffee D, Brewer HB, Ney RL.** Adrenal cholesterol uptake from plasma lipoproteins: regulation by corticotropin. *Proc. Natl. Acad. Sci. U. S. A.* 1976;73(12):4329–4333.

204. **Lopez D, McLean MP.** Estrogen regulation of the scavenger receptor class B gene: Anti-atherogenic or steroidogenic, is there a priority? *Mol. Cell. Endocrinol.* 2006;247(1-2):22–33.

205. **Chiba-Falek O, Nichols M, Suchindran S, Guyton J, Ginsburg GS, Barrett-Connor E, McCarthy JJ.** Impact of gene variants on sex-specific regulation of human Scavenger receptor class B type 1 (SR-BI) expression in liver and association with lipid levels in a population-based study. *BMC Med. Genet.* 2010;11:9.

206. **Ni J, Pang S-T, Yeh S.** Differential retention of alpha-vitamin E is correlated with its transporter gene expression and growth inhibition efficacy in prostate cancer cells. *Prostate* 2007;67(5):463–471.

207. **Llaverias G, Danilo C, Wang Y, Witkiewicz AK, Daumer K, Lisanti MP, Frank PG.** A Western-type diet accelerates tumor progression in an autochthonous mouse model of prostate cancer. *Am. J. Pathol.* 2010;177(6):3180–3191.

208. **Twiddy AL, Cox ME, Wasan KM.** Knockdown of scavenger receptor Class B Type I reduces prostate specific antigen secretion and viability of prostate cancer cells. *Prostate* 2012;72(9):955–965.

209. **Sobel RE, Sadar MD.** Cell lines used in prostate cancer research: a compendium of old and new lines--part 1. *J. Urol.* 2005;173(2):342–359.

210. **Sato N, Gleave ME, Bruchovsky N, Rennie PS, Beraldi E, Sullivan LD.** A metastatic and androgen-sensitive human prostate cancer model using intraprostatic inoculation of LNCaP cells in SCID mice. *Cancer Res.* 1997;57(8):1584–1589.

211. **Gordon JA, Midha A, Szeitz A, Ghaffari M, Adomat HH, Guo Y, Klassen TL, Guns ES, Wasan KM, Cox ME.** Oral simvastatin administration delays castration-resistant progression and reduces intratumoral steroidogenesis of LNCaP prostate cancer xenografts. *Prostate Cancer Prostatic Dis.* 2015:Online.

212. **Pernicová Z, Slabáková E, Kharaishvili G, Bouchal J, Král M, Kunická Z, Machala M, Kozubík A, Součcek K.** Androgen Depletion Induces Senescence in Prostate Cancer Cells through Down-regulation of Skp2. *Neoplasia* 2011;13(6):526–536.

213. **Gassmann M, Grenacher B, Rohde B, Vogel J.** Quantifying Western blots: Pitfalls of densitometry. *Electrophoresis* 2009;30(11):1845–1855.

214. **Degasperi A, Birtwistle MR, Volinsky N, Rauch J, Kolch W, Kholodenko BN.** Evaluating Strategies to Normalise Biological Replicates of Western Blot Data. *PLoS ONE* 2014;9(1):e87293.

215. **Taylor SC, Posch A.** The Design of a Quantitative Western Blot Experiment. *BioMed Res. Int.* 2014;2014:e361590.

216. **Yu M, Romer KA, Nieland TJF, Xu S, Saenz-Vash V, Penman M, Yesilaltay A, Carr SA, Krieger M.** Exoplasmic cysteine Cys384 of the HDL receptor SR-BI is critical for its sensitivity to a small-molecule inhibitor and normal lipid transport activity. *Proc. Natl. Acad. Sci.* 2011;108(30):12243–12248.

217. **Yen CF, Kalunta CI, Chen FS, Kaptein JS, Lin CK, Lad PM.** Flow cytometric evaluation of LDL receptors using DiI-LDL uptake and its application to B and T lymphocytic cell lines. *J. Immunol. Methods* 1994;177(1-2):55–67.

218. **Pagler TA, Rhode S, Neuhofer A, Laggner H, Strobl W, Hinterndorfer C, Volf I, Pavelka M, Eckhardt ERM, Westhuyzen DR van der, Schütz GJ, Stangl H.** SR-BI-mediated High Density Lipoprotein (HDL) Endocytosis Leads to HDL Resecretion Facilitating Cholesterol Efflux. *J. Biol. Chem.* 2006;281(16):11193–11204.

219. **Stephan ZF, Yurachek EC.** Rapid fluorometric assay of LDL receptor activity by DiI-labeled LDL. *J. Lipid Res.* 1993;34(2):325–330.

220. **Tung JW, Heydari K, Tirouvanziam R, Sahaf B, Parks DR, Herzenberg LA, Herzenberg LA.** Modern Flow Cytometry: A Practical Approach. *Clin. Lab. Med.* 2007;27(3):453–v.

221. **Amundson DM, Zhou M.** Fluorometric method for the enzymatic determination of cholesterol. *J. Biochem. Biophys. Methods* 1999;38(1):43–52.

222. **Toren PJ, Kim S, Pham S, Mangalji A, Adomat H, Guns EST, Zoubeidi A, Moore W, Gleave ME.** Anticancer activity of a novel selective CYP17A1 inhibitor in preclinical models of castrate-resistant prostate cancer. *Mol. Cancer Ther.* 2015;14(1):59–69.

223. **Schambeck CM.** Evaluation of the COBAS CORE Immunoassay for measuring prostate-specific antigen (PSA)--multi-centre study results. The PSA Study Group. *Eur. J. Clin. Chem. Clin. Biochem. J. Forum Eur. Clin. Chem. Soc.* 1995;33(8):541–547.

224. **Riss TL, Moravec RA, Niles AL, Benink HA, Worzella TJ, Minor L.** Cell Viability Assays. In: Sittampalam GS, Gal-Edd N, Arkin M, Auld D, Austin C, Bejcek B, Glicksman M, Inglese J, Lemmon V, Li Z, McGee J, McManus O, Minor L, Napper A, Riss T, Trask OJ, Weidner J, eds. *Assay Guidance Manual*. Bethesda (MD): Eli Lilly & Company and the National Center for Advancing Translational Sciences; 2004.

225. **Furukawa J, Wraight CJ, Freier SM, Peralta E, Atley LM, Monia BP, Gleave ME, Cox ME.** Antisense oligonucleotide targeting of insulin-like growth factor-1 receptor (IGF-1R) in prostate cancer. *Prostate* 2010;70(2):206–218.

226. **Riccardi C, Nicoletti I.** Analysis of apoptosis by propidium iodide staining and flow cytometry. *Nat. Protoc.* 2006;1(3):1458–1461.

227. **Nunez R.** DNA measurement and cell cycle analysis by flow cytometry. *Curr. Issues Mol. Biol.* 2001;3(3):67–70.

228. **Ormerod MG.** Investigating the relationship between the cell cycle and apoptosis using flow cytometry. *J. Immunol. Methods* 2002;265(1-2):73–80.

229. **Debacq-Chainiaux F, Erusalimsky JD, Campisi J, Toussaint O.** Protocols to detect senescence-associated beta-galactosidase (SA-betagal) activity, a biomarker of senescent cells in culture and in vivo. *Nat. Protoc.* 2009;4(12):1798–1806.

230. **Noppe G, Dekker P, de Koning-Treurniet C, Blom J, van Heemst D, Dirks RW, Tanke HJ, Westendorp RGJ, Maier AB.** Rapid flow cytometric method for measuring senescence associated beta-galactosidase activity in human fibroblasts. *Cytom. Part J. Int. Soc. Anal. Cytol.* 2009;75(11):910–916.

231. **Connelly MA, Williams DL.** SR-BI and cholesterol uptake into steroidogenic cells. *Trends Endocrinol. Metab.* 2003;14(10):467–472.

232. **Connelly MA.** SR-BI-mediated HDL cholesteryl ester delivery in the adrenal gland. *Mol. Cell. Endocrinol.* 2009;300(1-2):83–88.

233. **Azhar S, Reaven E.** Scavenger receptor class BI and selective cholesteryl ester uptake: partners in the regulation of steroidogenesis. *Mol. Cell. Endocrinol.* 2002;195(1-2):1–26.

234. **Maxfield FR, Menon AK.** Intracellular sterol transport and distribution. *Curr. Opin. Cell Biol.* 2006;18(4):379–385.

235. **Kim JH, Cox ME, Wasan KM.** Effect of simvastatin on castration-resistant prostate cancer cells. *Lipids Health Dis.* 2014;13:56.

236. **Blagosklonny MV.** P53: an ubiquitous target of anticancer drugs. *Int. J. Cancer J. Int. Cancer* 2002;98(2):161–166.

237. **Goodrich DW, Wang NP, Qian YW, Lee EY, Lee WH.** The retinoblastoma gene product regulates progression through the G1 phase of the cell cycle. *Cell* 1991;67(2):293–302.

238. **Campisi J.** Cellular senescence as a tumor-suppressor mechanism. *Trends Cell Biol.* 2001;11(11):S27–S31.

239. **Chang B-D, Broude EV, Dokmanovic M, Zhu H, Ruth A, Xuan Y, Kandel ES, Lausch E, Christov K, Roninson IB.** A senescence-like phenotype distinguishes tumor cells that undergo terminal proliferation arrest after exposure to anticancer agents. *Cancer Res.* 1999;59(15):3761–3767.

240. **Adams J.** A case of scirrhus of the prostate gland, with a corresponding affection of the lymphatic glands in the lumbar region and in the pelvis. *The Lancet* 1853;61(1547):393–394.

241. **Lonergan PE, Tindall DJ.** Androgen receptor signaling in prostate cancer development and progression. *J. Carcinog.* 2011;10:20.

242. **Cheng H, Snoek R, Ghaidi F, Cox ME, Rennie PS.** Short hairpin RNA knockdown of the androgen receptor attenuates ligand-independent activation and delays tumor progression. *Cancer Res.* 2006;66(21):10613–10620.

243. **Sharma NL, Massie CE, Ramos-Montoya A, Zecchini V, Scott HE, Lamb AD, MacArthur S, Stark R, Warren AY, Mills IG, Neal DE.** The androgen receptor induces a distinct transcriptional program in castration-resistant prostate cancer in man. *Cancer Cell* 2013;23(1):35–47.

244. **Dehm SM, Tindall DJ.** Alternatively spliced androgen receptor variants. *Endocr. Relat. Cancer* 2011;18(5):R183–R196.

245. **Heemers HV.** Targeting androgen receptor action for prostate cancer treatment: does the post-receptor level provide novel opportunities? *Int. J. Biol. Sci.* 2014;10(6):576–587.

246. **Tan ME, Li J, Xu HE, Melcher K, Yong E.** Androgen receptor: structure, role in prostate cancer and drug discovery. *Acta Pharmacol. Sin.* 2015;36(1):3–23.

247. **Balbas MD, Evans MJ, Hosfield DJ, Wongvipat J, Arora VK, Watson PA, Chen Y, Greene GL, Shen Y, Sawyers CL.** Overcoming mutation-based resistance to antiandrogens with rational drug design. *eLife* 2013;2(e00499). doi:10.7554/eLife.00499.

248. **Barnes D, Sato G.** Serum-free cell culture: a unifying approach. *Cell* 1980;22(3):649–655.

249. **Van Steenbrugge GJ, van Uffelen CJC, Bolt J, Schröder FH.** The human prostatic cancer cell line LNCaP and its derived sublines: An in vitro model for the study of androgen sensitivity. *J. Steroid Biochem. Mol. Biol.* 1991;40(1–3):207–214.

250. **Eberlé D, Hegarty B, Bossard P, Ferré P, Foufelle F.** SREBP transcription factors: master regulators of lipid homeostasis. *Biochimie* 2004;86(11):839–848.

251. **Baenke F, Peck B, Miess H, Schulze A.** Hooked on fat: the role of lipid synthesis in cancer metabolism and tumour development. *Dis. Model. Mech.* 2013;6(6):1353–1363.

252. **Swinnen JV, Van Veldhoven PP, Esquenet M, Heyns W, Verhoeven G.** Androgens markedly stimulate the accumulation of neutral lipids in the human prostatic adenocarcinoma cell line LNCaP. *Endocrinology* 1996;137(10):4468–4474.

253. **Huang W-C, Zhau HE, Chung LWK.** Androgen Receptor Survival Signaling Is Blocked by Anti-β2-microglobulin Monoclonal Antibody via a MAPK/Lipogenic Pathway in Human Prostate Cancer Cells. *J. Biol. Chem.* 2010;285(11):7947–7956.

254. **Plump AS, Erickson SK, Weng W, Partin JS, Breslow JL, Williams DL.** Apolipoprotein A-I is required for cholesteryl ester accumulation in steroidogenic cells and for normal adrenal steroid production. *J. Clin. Invest.* 1996;97(11):2660–2671.

255. **Lange Y, Ramos BV.** Analysis of the distribution of cholesterol in the intact cell. *J. Biol. Chem.* 1983;258(24):15130–15134.

256. **Lange Y, Ye J, Steck TL.** Circulation of cholesterol between lysosomes and the plasma membrane. *J. Biol. Chem.* 1998;273(30):18915–18922.

257. **Yue S, Li J, Lee S-Y, Lee HJ, Shao T, Song B, Cheng L, Masterson TA, Liu X, Ratliff TL, Cheng J-X.** Cholesteryl ester accumulation induced by PTEN loss and PI3K/AKT activation underlies human prostate cancer aggressiveness. *Cell Metab.* 2014;19(3):393–406.

258. **Mills IG.** Maintaining and reprogramming genomic androgen receptor activity in prostate cancer. *Nat. Rev. Cancer* 2014;14(3):187–198.

259. **Wang Q, Li W, Zhang Y, Yuan X, Xu K, Yu J, Chen Z, Beroukhim R, Wang H, Lupien M, Wu T, Regan MM, Meyer CA, Carroll JS, Manrai AK, Jänne OA, Balk SP, Mehra R, Han B, Chinnaiyan AM, Rubin MA, True L, Fiorentino M, Fiore C, Loda M, Kantoff PW, Liu XS, Brown M.** Androgen Receptor Regulates a Distinct Transcription Program in Androgen-Independent Prostate Cancer. *Cell* 2009;138(2):245–256.

260. **Urbanucci A, Sahu B, Seppälä J, Larjo A, Latonen LM, Waltering KK, Tammela TLJ, Vessella RL, Lähdesmäki H, Jänne OA, Visakorpi T.** Overexpression of androgen receptor enhances the binding of the receptor to the chromatin in prostate cancer. *Oncogene* 2012;31(17):2153–2163.

261. **Sharma P, Knowell AE, Chinaranagari S, Komaragiri S, Nagappan P, Patel D, Havrda MC, Chaudhary J.** Id4 deficiency attenuates prostate development and promotes PIN-like lesions by regulating androgen receptor activity and expression of NKX3.1 and PTEN. *Mol. Cancer* 2013;12:67.

262. **Danilo C, Gutierrez-Pajares JL, Mainieri MA, Mercier I, Lisanti MP, Frank PG.** Scavenger receptor class B type I regulates cellular cholesterol metabolism and cell signaling associated with breast cancer development. *Breast Cancer Res* 2013;15(5):R87.

263. **Cao WM, Murao K, Imachi H, Yu X, Abe H, Yamauchi A, Niimi M, Miyauchi A, Wong NCW, Ishida T.** A mutant high-density lipoprotein receptor inhibits proliferation of human breast cancer cells. *Cancer Res.* 2004;64(4):1515–1521.

264. **Vistica DT, Skehan P, Scudiero D, Monks A, Pittman A, Boyd MR.** Tetrazolium-based assays for cellular viability: a critical examination of selected parameters affecting formazan production. *Cancer Res.* 1991;51(10):2515–2520.

265. **Kanemura Y, Mori H, Kobayashi S, Islam O, Kodama E, Yamamoto A, Nakanishi Y, Arita N, Yamasaki M, Okano H, Hara M, Miyake J.** Evaluation of in vitro proliferative activity of human fetal neural stem/progenitor cells using indirect measurements of viable cells based on cellular metabolic activity. *J. Neurosci. Res.* 2002;69(6):869–879.

266. **Wang P, Henning SM, Heber D.** Limitations of MTT and MTS-Based Assays for Measurement of Antiproliferative Activity of Green Tea Polyphenols. *PLoS ONE* 2010;5(4):e10202.

267. **Khoo KH, Verma CS, Lane DP.** Drugging the p53 pathway: understanding the route to clinical efficacy. *Nat. Rev. Drug Discov.* 2014;13(3):217–236.

268. **Hock A, Vousden KH.** Regulation of the p53 pathway by ubiquitin and related proteins. *Int. J. Biochem. Cell Biol.* 2010;42(10):1618–1621.

269. **Huang L, Yan Z, Liao X, Li Y, Yang J, Wang Z-G, Zuo Y, Kawai H, Shadfan M, Ganapathy S, Yuan Z-M.** The p53 inhibitors MDM2/MDMX complex is required for control of p53 activity in vivo. *Proc. Natl. Acad. Sci. U. S. A.* 2011;108(29):12001–12006.

270. **el-Deiry WS.** Regulation of p53 downstream genes. *Semin. Cancer Biol.* 1998;8(5):345–357.

271. **Agarwal ML, Agarwal A, Taylor WR, Stark GR.** p53 controls both the G2/M and the G1 cell cycle checkpoints and mediates reversible growth arrest in human fibroblasts. *Proc. Natl. Acad. Sci. U. S. A.* 1995;92(18):8493–8497.

272. **Wang S, El-Deiry WS.** P53, Cell Cycle Arrest and Apoptosis. In: Hainaut P, Wiman KG, eds. *25 Years of p53 Research*. Dordrecht, Netherlands: Springer; 2007:141–163.

273. **Vogelstein B, Lane D, Levine AJ.** Surfing the p53 network. *Nature* 2000;408(6810):307–310.

274. **Giacinti C, Giordano A.** RB and cell cycle progression. *Oncogene* 2006;25(38):5220–5227.

275. **Claudio PP, De Luca A, Howard CM, Baldi A, Firpo EJ, Koff A, Paggi MG, Giordano A.** Functional analysis of pRb2/p130 interaction with cyclins. *Cancer Res.* 1996;56(9):2003–2008.

276. **Rubin SM.** Deciphering the retinoblastoma protein phosphorylation code. *Trends Biochem. Sci.* 2013;38(1):12–19.

277. **Lees JA, Buchkovich KJ, Marshak DR, Anderson CW, Harlow E.** The retinoblastoma protein is phosphorylated on multiple sites by human cdc2. *EMBO J.* 1991;10(13):4279–4290.

278. **Lee JO, Russo AA, Pavletich NP.** Structure of the retinoblastoma tumour-suppressor pocket domain bound to a peptide from HPV E7. *Nature* 1998;391(6670):859–865.

279. **Zarkowska T, Mittnacht S.** Differential phosphorylation of the retinoblastoma protein by G1/S cyclin-dependent kinases. *J. Biol. Chem.* 1997;272(19):12738–12746.

280. **Driscoll B, T'Ang A, Hu YH, Yan CL, Fu Y, Luo Y, Wu KJ, Wen S, Shi XH, Barsky L, Weinberg K, Murphree AL, Fung YK.** Discovery of a regulatory motif that controls the exposure of specific upstream cyclin-dependent kinase sites that determine both conformation and growth suppressing activity of pRb. *J. Biol. Chem.* 1999;274(14):9463–9471.

281. **Lundberg AS, Weinberg RA.** Functional inactivation of the retinoblastoma protein requires sequential modification by at least two distinct cyclin-cdk complexes. *Mol. Cell. Biol.* 1998;18(2):753–761.

282. **Ezhevsky SA, Nagahara H, Vocero-Akbani AM, Gius DR, Wei MC, Dowdy SF.** Hypo-phosphorylation of the retinoblastoma protein (pRb) by cyclin D:Cdk4/6 complexes results in active pRb. *Proc. Natl. Acad. Sci. U. S. A.* 1997;94(20):10699–10704.

283. **Krysko DV, Vanden Berghe T, Parthoens E, D'Herde K, Vandenabeele P.** Methods for distinguishing apoptotic from necrotic cells and measuring their clearance. *Methods Enzymol.* 2008;442:307–341.

284. **Boulares AH, Yakovlev AG, Ivanova V, Stoica BA, Wang G, Iyer S, Smulson M.** Role of Poly(ADP-ribose) Polymerase (PARP) Cleavage in Apoptosis. Caspase 3-resistant PARP mutant increases rates of apoptosis in transfected cells. *J. Biol. Chem.* 1999;274(33):22932–22940.

285. **Ha HC, Snyder SH.** Poly(ADP-ribose) polymerase is a mediator of necrotic cell death by ATP depletion. *Proc. Natl. Acad. Sci. U. S. A.* 1999;96(24):13978–13982.

286. **Nishimura Y, Lemasters JJ.** Glycine blocks opening of a death channel in cultured hepatic sinusoidal endothelial cells during chemical hypoxia. *Cell Death Differ.* 2001;8(8):850–858.

287. **Wyllie AH, Morris RG, Smith AL, Dunlop D.** Chromatin cleavage in apoptosis: association with condensed chromatin morphology and dependence on macromolecular synthesis. *J. Pathol.* 1984;142(1):67–77.

288. **Schweichel JU, Merker HJ.** The morphology of various types of cell death in prenatal tissues. *Teratology* 1973;7(3):253–266.

289. **Chan FK-M, Moriwaki K, De Rosa MJ.** Detection of Necrosis by Release of Lactate Dehydrogenase (LDH) Activity. *Methods Mol. Biol. Clifton NJ* 2013;979:65–70.

290. **Zong W-X, Thompson CB.** Necrotic death as a cell fate. *Genes Dev.* 2006;20(1):1–15.

291. **Vaseva AV, Marchenko ND, Ji K, Tsirka SE, Holzmann S, Moll UM.** p53 opens the mitochondrial permeability transition pore to trigger necrosis. *Cell* 2012;149(7):1536–1548.

292. **Farrow JM, Yang JC, Evans CP.** Autophagy as a modulator and target in prostate cancer. *Nat. Rev. Urol.* 2014;11(9):508–516.

293. **Chen N, Karantza V.** Autophagy as a therapeutic target in cancer. *Cancer Biol. Ther.* 2011;11(2):157–168.

294. **Gewirtz DA.** Autophagy as a mechanism of radiation sensitization in breast tumor cells. *Autophagy* 2007;3(3):249–250.

295. **Al-Ejeh F, Kumar R, Wiegmans A, Lakhani SR, Brown MP, Khanna KK.** Harnessing the complexity of DNA-damage response pathways to improve cancer treatment outcomes. *Oncogene* 2010;29(46):6085–6098.

296. **John S, Nayvelt I, Hsu H-C, Yang P, Liu W, Das GM, Thomas T, Thomas TJ.** Regulation of estrogenic effects by beclin 1 in breast cancer cells. *Cancer Res.* 2008;68(19):7855–7863.

297. **Kroemer G, Mariño G, Levine B.** Autophagy and the integrated stress response. *Mol. Cell* 2010;40(2):280–293.

298. **Mizushima N, Yoshimorim T, Levine B.** Methods in Mammalian Autophagy Research. *Cell* 2010;140(3):313–326.

299. **Liang J, Shao SH, Xu Z-X, Hennessy B, Ding Z, Larrea M, Kondo S, Dumont DJ, Gutterman JU, Walker CL, Slingerland JM, Mills GB.** The energy sensing LKB1-AMPK pathway regulates p27(kip1) phosphorylation mediating the decision to enter autophagy or apoptosis. *Nat. Cell Biol.* 2007;9(2):218–224.

300. **De Silva HV, Stuart WD, Duvic CR, Wetterau JR, Ray MJ, Ferguson DG, Albers HW, Smith WR, Harmony JA.** A 70-kDa apolipoprotein designated ApoJ is a marker for subclasses of human plasma high density lipoproteins. *J. Biol. Chem.* 1990;265(22):13240–13247.

301. **Burkey BF, Stuart WD, Harmony JA.** Hepatic apolipoprotein J is secreted as a lipoprotein. *J. Lipid Res.* 1992;33(10):1517–1526.

302. **Maiuri MC, Zalckvar E, Kimchi A, Kroemer G.** Self-eating and self-killing: crosstalk between autophagy and apoptosis. *Nat. Rev. Mol. Cell Biol.* 2007;8(9):741–752.

303. **González-Polo R-A, Boya P, Pauleau A-L, Jalil A, Larochette N, Souquère S, Eskelinen E-L, Pierron G, Saftig P, Kroemer G.** The apoptosis/autophagy paradox: autophagic vacuolization before apoptotic death. *J. Cell Sci.* 2005;118(Pt 14):3091–3102.

304. **Wang S, Peng D.** Regulation of adipocyte autophagy--the potential anti-obesity mechanism of high density lipoprotein and ApolipoproteinA-I. *Lipids Health Dis.* 2012;11:131.

305. **Cheng J, Ohsaki Y, Tauchi-Sato K, Fujita A, Fujimoto T.** Cholesterol depletion induces autophagy. *Biochem. Biophys. Res. Commun.* 2006;351(1):246–252.

306. **Zhang J, Yang Z, Xie L, Xu L, Xu D, Liu X.** Statins, autophagy and cancer metastasis. *Int. J. Biochem. Cell Biol.* 2013;45(3):745–752.

307. **Toepfer N, Childress C, Parikh A, Rukstalis D, Yang W.** Atorvastatin induces autophagy in prostate cancer PC3 cells through activation of LC3 transcription. *Cancer Biol. Ther.* 2011;12(8):691–699.

308. **Seo Y-K, Jeon T-I, Chong HK, Biesinger J, Xie X, Osborne TF.** Genome-wide Localization of SREBP-2 in Hepatic Chromatin Predicts a Role in Autophagy. *Cell Metab.* 2011;13(4):367–375.

309. **Sobel R, Sadar M.** Cell lines used in prostate cancer research: a compendium of old and new lines--part 2. *J. Urol.* 2005;173(2):360–372.

310. **Hill JM, Zalos G, Halcox JPJ, Schenke WH, Waclawiw MA, Quyyumi AA, Finkel T.** Circulating endothelial progenitor cells, vascular function, and cardiovascular risk. *N. Engl. J. Med.* 2003;348(7):593–600.

311. **Pellegatta F, Bragheri M, Grigore L, Raselli S, Maggi FM, Brambilla C, Reduzzi A, Pirillo A, Norata GD, Catapano AL.** In vitro isolation of circulating endothelial progenitor cells is related to the high density lipoprotein plasma levels. *Int. J. Mol. Med.* 2006;17(2):203–208.

312. **Park K-H, Cho K-H.** High-Density Lipoprotein (HDL) From Elderly and Reconstituted HDL Containing Glycated Apolipoproteins A-I Share Proatherosclerotic and Prosenescent Properties With Increased Cholesterol Influx. *J. Gerontol. A. Biol. Sci. Med. Sci.* 2011;66A(5):511–520.

313. **Park K-H, Shin D-G, Cho K-H.** Dysfunctional Lipoproteins from Young Smokers Exacerbate Cellular Senescence and Atherogenesis with Smaller Particle Size and Severe Oxidation and Glycation. *Toxicol. Sci.* 2014:kfu076.

314. **Petropoulou C, Trougakos IP, Kolettas E, Toussaint O, Gonos ES.** Clusterin/apolipoprotein J is a novel biomarker of cellular senescence that does not affect the proliferative capacity of human diploid fibroblasts. *FEBS Lett.* 2001;509(2):287–297.

315. **Chen QM, Prowse KR, Tu VC, Purdom S, Linskens MH.** Uncoupling the senescent phenotype from telomere shortening in hydrogen peroxide-treated fibroblasts. *Exp. Cell Res.* 2001;265(2):294–303.

316. **Cuervo AM, Dice JF.** Age-related Decline in Chaperone-mediated Autophagy. *J. Biol. Chem.* 2000;275(40):31505–31513.

317. **Patschan S, Chen J, Polotskaia A, Mendelev N, Cheng J, Patschan D, Goligorsky MS.** Lipid mediators of autophagy in stress-induced premature senescence of endothelial cells. *Am. J. Physiol. - Heart Circ. Physiol.* 2008;294(3):H1119–H1129.

318. **Young ARJ, Narita M, Ferreira M, Kirschner K, Sadaie M, Darot JFJ, Tavaré S, Arakawa S, Shimizu S, Watt FM, Narita M.** Autophagy mediates the mitotic senescence transition. *Genes Dev.* 2009;23(7):798–803.

319. **Goehe RW, Di X, Sharma K, Bristol ML, Henderson SC, Valerie K, Rodier F, Davalos AR, Gewirtz DA.** The Autophagy-Senescence Connection in Chemotherapy: Must Tumor Cells (Self) Eat Before They Sleep? *J. Pharmacol. Exp. Ther.* 2012;343(3):763–778.

320. **Beauséjour CM, Krtolica A, Galimi F, Narita M, Lowe SW, Yaswen P, Campisi J.** Reversal of human cellular senescence: roles of the p53 and p16 pathways. *EMBO J.* 2003;22(16):4212–4222.

321. **Burton DGA, Giribaldi MG, Munoz A, Halvorsen K, Patel A, Jorda M, Perez-Stable C, Rai P.** Androgen Deprivation-Induced Senescence Promotes Outgrowth of Androgen-Refractory Prostate Cancer Cells. *PLoS ONE* 2013;8(6):e68003.

322. **Childs BG, Baker DJ, Kirkland JL, Campisi J, van Deursen JM.** Senescence and apoptosis: dueling or complementary cell fates? *EMBO Rep.* 2014;15(11):1139–1153.

323. **Gosselin K, Deruy E, Martien S, Vercamer C, Bouali F, Dujardin T, Slomianny C, Houel-Renault L, Chelli F, De Launoit Y, Abbadie C.** Senescent Keratinocytes Die by Autophagic Programmed Cell Death. *Am. J. Pathol.* 2009;174(2):423–435.

324. **Seluanov A, Gorbunova V, Falcovitz A, Sigal A, Milyavsky M, Zurer I, Shohat G, Goldfinger N, Rotter V.** Change of the death pathway in senescent human fibroblasts in response to DNA damage is caused by an inability to stabilize p53. *Mol. Cell. Biol.* 2001;21(5):1552–1564.